

Towards a mechanistic understanding of the role of
TERRA in the alternative lengthening mechanism of
telomeres

Dissertation

Zur Erlangung des Grades

“Doktor der Naturwissenschaften”

am Fachbereich Biologie

der Johannes Gutenberg-Universität Mainz

Stefano Misino

geb. Am 18.09.1992 in Canosa di Puglia, Italy

Mainz, 2021

to Jesus and my grandparents

Table of contents

Summary.....	1
Zusammenfassung.....	2
Abbreviations.....	4
Introduction.....	5
History of telomeres discovery.....	5
Telomeres first evidence.....	5
The end replication problem and the Hayflick limit.....	5
The terminal repeats.....	8
The advent of telomerase and beyond.....	8
Telomere structure.....	10
Telomeric and subtelomeric DNA.....	10
Telomere proteins.....	12
Rap1.....	12
Rif1 and 2.....	13
CST complex.....	14
Ku complex.....	15
Sir complex.....	16
T-loop/telomere fold-back.....	17
Replicative senescence.....	18
Telomere maintenance.....	20
TMM via telomerase.....	20
TMM via ALT.....	21
Survivor emergence.....	23
ALT in humans.....	24
TERRA.....	27
TERRA expression regulation.....	28
TERRA function.....	29
TERRA RNA-DNA hybrids.....	30

TERRA in ALT.....	32
Rationale.....	34
Results.....	35
TERRA is upregulated in ALT-survivors.....	35
ALT-survivors display the typical TRF pattern.....	35
TERRA accumulates in ALT-survivors, similar to human ALT cells.....	39
TERRA and TERRA RNA-DNA hybrids regulation in ALT-survivors.....	41
Impaired degradation might account for TERRA upregulation in ALT-survivors	41
Telomeres in ALT-survivors are bound by less Sir2.....	42
ALT-survivors show impaired binding of RNase H2 to telomeres	
and active DDR.....	43
TERRA expression is cell cycle regulated in ALT-survivors.....	47
High levels of TERRA originate from short telomeres in survivors.....	48
ALT-survivors do have a telomere length-dependent regulation of TERRA.....	49
TMM via ALT includes elongation and shortening phases.....	49
TERRA expression gradually increases as telomeres shorten.....	53
Post-crisis senescence: replicative potential does fluctuate in ALT-survivors.....	55
PCS rate is modulated by R-loops.....	57
RNA-DNA hybrids counteract telomere shortening in ALT-survivors.....	61
Discussion.....	65
TERRA expression is upregulated in ALT-survivors.....	65
Low binding of Rat1 and Sir2.....	66
Are there really no changes in transcription?.....	69
TERRA cell cycle regulation might reveal enhanced transcription	
at ALT telomeres.....	71
Short telomeres account for the majority of TERRA.....	72
Post-crisis senescence: between R-loops and adaptation.....	74
R-loops are required for sister chromatid HDR but not extensive	
recombinational events.....	75

Double effect of R-loops.....	76
How TERRA RNA-DNA hybrids induce BIR in ALT.....	77
R-loops to promote a telomere-telomere interplay.....	79
Conclusion.....	82
Materials and Methods.....	84
Materials.....	84
Yeast strains.....	84
Plasmids.....	85
Oligonucleotides.....	86
Liquid media.....	86
Solid media.....	86
Buffers.....	89
Reagents and additional materials.....	92
Commercial assays.....	96
Electronic instrumentation.....	96
Software.....	97
Methods.....	97
Yeast and bacteria manipulation.....	97
Yeast mating, sporulation and tetrad dissection.....	97
Yeast transformation.....	98
Bacteria transformation.....	98
TERRA analysis.....	98
RNA extraction and clean-ups.....	98
Reverse transcription.....	99
RT-qPCR.....	99
Telomere analysis.....	99
Genomic DNA extraction.....	99
Southern blot.....	100
Radioactive probe generation.....	100

Summary

Telomeres are the nucleoprotein structures that shelter the chromosome ends from illegitimate repair and degradation. Due to the inability of replication to fully duplicate DNA molecules, telomeres shorten with every cell cycle, causing replicative senescence. To counteract telomere erosion, different mechanisms of telomere maintenance are adopted. The most common one is via telomerase, a reverse transcriptase that synthesizes *de novo* telomeric DNA. In the absence of telomerase, an alternative lengthening mechanism of telomeres, namely ALT, promotes telomere maintenance via homology-directed repair (HDR).

Both telomerase and ALT are used by human cancer cells to lengthen their telomeres with the former being adopted in 85-90% of the cases and the latter in the remaining portion. Because of this, the two mechanisms represent potential targets for anti-cancer therapies.

TERRA is the long non-coding RNA transcribed at telomeres by RNA pol II in a variety of organisms. The exact function of the transcript is still unknown but gathering evidence proposes its involvement in several processes, including telomere maintenance. Emerging data validate the importance of TERRA, and the RNA-DNA hybrids it forms at telomeres, especially in ALT. Indeed, the transcript is upregulated in this type of cancer cells and telomeric RNA-DNA hybrids appear to be key triggers of telomeric HDR. However, little is known about the source of the lncRNA increased abundance in ALT and how TERRA RNA-DNA hybrids promote telomere lengthening via recombination. Uncovering these hidden aspects might be relevant to further understand the alternative lengthening mechanism of telomeres and develop more efficient therapeutics against cancer.

In this study, *Saccharomyces cerevisiae* post-senescent ALT-survivors, which lengthen their telomeres in a similar manner to human ALT, were employed to address the questions: is TERRA required for ALT and why is it required? In this regard, TERRA levels were measured in survivors to see if they upregulate the transcript like their human counterpart. Following, the regulation of the lncRNA expression was characterized.

Interestingly, TERRA abundance resulted to be increased in survivors in a manner that resembled human ALT. The main source of this upregulation seemed to be impaired degradation. Moreover, TERRA expression was regulated in a cell cycle- and telomere length-dependent manner, with the transcript peaking in early S-phase and at short telomeres, respectively. The increase of the lncRNA at short telomeres is believed to trigger HDR and telomere elongation.

In pre-survivor cells, telomere erosion triggers senescence, whose rate is negatively influenced by the abundance of TERRA RNA-DNA hybrids. Since survivors likewise shorten their telomeres, they were monitored for the presence of a senescence-like phenotype and how telomeric hybrids might affect it. Surprisingly, ALT-survivors senesced in response to telomere shortening and the pace was negatively regulated by the amount of TERRA RNA-DNA hybrids. This phenomenon is named hereafter “post-crisis senescence”.

Overall, this study shows that TERRA might be relevant in ALT to promote lengthening via HDR and avert senescence. The data here presented are expected to broaden the current knowledge of telomere transcription in ALT and emphasize its relevance as target for therapeutic applications.

Zusammenfassung

Telomere sind Nukleoproteinstrukturen, welche Chromosomenenden vor unerlaubter Reparatur und Degradation schützen. Aufgrund der Unfähigkeit vollständige DNA-Moleküle zu replizieren, verkürzen sich Telomere mit jedem Zellzyklus, was zur replikativen Seneszenz führt. Im Laufe der Evolution haben sich verschiedene Mechanismen zur Erhaltung von Telomeren entwickelt, um der Verkürzung von Telomeren entgegenzuwirken. Der üblichste Mechanismus erfolgt hierbei über das Enzym Telomerase, einer reversen Transkriptase, welche neue telomerische DNA synthetisiert. In Abwesenheit der Telomerase wird die Erhaltung der Telomere über einen alternativen Elongationsmechanismus gewährleistet, namens ALT (alternate lengthening of telomeres). ALT begünstigt hierbei die Erhaltung der Telomere über Homologe Rekombination (HR).

Sowohl Telomerase als auch ALT werden von humanen Krebszellen genutzt, um ihre Telomere zu verlängern. In 85-90% der Fälle wird hierbei die Telomerase hauptsächlich als Mechanismus dafür genutzt - ALT hingegen macht hierbei den übrigen Anteil aus. Daher eignen sich beide Mechanismen als potentielle Ziele für Krebstherapien.

TERRA ist eine lange nicht-kodierende RNA, welche an Telomeren von RNA-Polymerase II transkribiert wird und in vielen verschiedenen Organismen vertreten ist. Die genaue Funktion des TERRA-Transkriptes ist noch nicht bekannt, allerdings wird dessen Beteiligung an verschiedenen Prozessen, wie u.a. der Erhaltung von Telomeren, suggeriert. Aufkommende Daten bestätigen die Wichtigkeit von TERRA und RNA-DNA-Hybride, welche es an Telomeren, insbesondere in ALT-positiven Zellen, bildet. Tatsächlich konnte gezeigt werden, dass TERRA in ALT-positiven Tumorzellen überreguliert ist und das RNA-DNA-Hybride der Schlüsselmechanismus zur Veranlassung von HR an Telomeren ist. Über die Quelle von erhöhter Abundanz an lncRNA in ALT und darüber, wie TERRA RNA-DNA-Hybride die Verlängerung von Telomeren über HR begünstigen, ist wenig bekannt. Die Erforschung dieser Aspekte könnten für das Verständnis von ALT von großer Bedeutung sein und zur Entwicklung neuer effizienter Krebstherapien beitragen.

In dieser Dissertation wurden die Fragen ob und warum TERRA für ALT notwendig ist, adressiert. Um diese Fragestellungen zu klären, wurden *Saccharomyces cerevisiae* post-seneszenten ALT-Überlebende, welche ihre Telomere in einer ähnlichen Weise zu humanen ALT-positiven Zellen verlängern, verwendet. Hierbei wurde der Gehalt an TERRA in Überlebenden gemessen, um zu sehen ob diese Zellen ihre TERRA-Transkripte wie in humanen Zellen überregulieren. Anschließend wurde die Regulation der lncRNA-Expression charakterisiert.

Interessanterweise, war der Gehalt an TERRA in Überlebenden in einer ähnlichen Art wie in humanen ALT-positiven Zellen, erhöht. Die Hauptquelle für diese Überregulation schien eine beeinträchtigte Degradation zu sein. Vielmehr war die Expression von TERRA in einer Zellzyklus- und Telomerlängen-abhängigen Weise reguliert. Hierbei wurde der höchste Gehalt an TERRA in der S-Phase und an kurzen Telomeren festgestellt. Es wird angenommen, dass die Erhöhung der lncRNA an kurzen Telomeren die HR, sowie die Verlängerung von Telomeren veranlasst.

Die Verkürzung der Telomere ist verantwortlich für Seneszenz in Prä-Überlebenden Zellen, dessen Rate durch die Abundanz von TERRA DNA-RNA-Hybriden beeinflusst wird. Da die Überlebenden ebenso ihre Telomere verkürzen, wurden diese auf einen Seneszenz-ähnlichen Phänotypen untersucht und inwiefern Telomerhybride diesen Phänotypen beeinflussen.

Überraschenderweise alterten ALT-Überlebende als Antwort auf die Verkürzung der Telomere. Die Geschwindigkeit davon war von dem Gehalt der TERRA-RNA-DNA-Hybride negativ reguliert. Dieses Phänomen wurde daher als "Post-Krisen Seneszenz" bezeichnet.

Allumfassend zeigt diese Studie, dass TERRA in ALT von Bedeutung sein könnte, um die Verlängerung der Telomere mittels HR zu begünstigen und um dadurch Seneszenz zu verhindern. Es wird erwartet, dass die hier präsentierten Daten das derzeitige Verständnis von Telomertranskription in ALT erweitern und dessen Relevanz als Ziel für z.B. Tumorthérapien hervorhebt.

Abbreviations

aa: aminoacid(s)	MET: methionine
ALT: alternative lengthening of telomeres	MMS: methyl methansulfonate
APB: ALT-associated PML bodies	MiDAS: mitotic DNA synthesis
ARS: autonomously replicating sequence	MRX: Mre11-Rad50-Xrn2
BIR: break-induced replication	NAT: nourseothricin
BITS: BIR-induced telomeric synthesis	NHEJ: non-homologous end joining
bp: base-pair(s)	nt: nucleotide(s)
CEN: centromeric	OB: oligosaccharide/oligonucleotide/ oligopeptide binding
ChIP: chromatin immunoprecipitation	PCR: polymerase chain reaction
CST: Cdc13-Stn1-Ten1	PML: promyelocytic leukemia
CTD: carboxy-terminal domain	POL: polymerase
DDR: DNA damage response	Pre-RC: pre-replication complex
ds: double-stranded	NTP: nucleoside triphosphate
DBD: DNA-binding domain	r(-): ribo-
DSB: double strand break	RD: recruitment domain
d(-): deoxyribo-	RNH1: RNase H1
EV: empty vector	RNH201: RNase H201
FACS: fluorescence-activated cell sorting	RT-qPCR: real time quantitative PCR
GAL: galactose	ss: single-stranded
G4: G-quadruplex	TAP: tandem affinity purification
HA: hemagglutinin	TAS: telomere-associated sequence(s)
HAATI: heterochromatin amplification- mediated and telomerase- independent	T-circles: telomeric circles
HDR: homology-directed repair	TERRA: telomeric repeat-containing RNA
HIS: histidine	T-loop: telomeric loop
HU: hydroxyurea	TMM: telomere maintenance mechanism
HYG: hygromycin	TPE: telomere position effect
ICF: immunodeficiency, centromeric instability and facial anomalies	TPE-OLD: telomere position effect over long distances
IgG: immunoglobulin G	TSS: transcription start site
KAN: kanamycin	SCE: sister chromatid exchanges
kb: kilobase(s)	SCR: sister chromatid recombination
kDa: kilodalton(s)	SEM: standard error of the mean
LEU: leucine	SD: standard deviation
lncRNA: long non-coding RNA	URA: uracil
	3'-OH: 3'-hydroxyl group

1. Introduction

1.1. History of telomeres discovery

1.1.1 Telomeres: first evidence

The first notice of a structure different from the rest of the genome and able to protect the chromosomes termini dates back to the late 1920s when Hermann Muller observed that, upon X-ray-mediated breakage of chromosomes, rearrangements could occur among all fragments except for the chromosome ends¹. This peculiar characteristic brought Muller to speculate that the “end” (*télos*) “part” (*méros*) was a “terminal gene” with the property to seal the chromosome ends¹.

Later, in the 30s, Barbara McClintock uncovered a phenomenon she named “chromosome healing”, which appeared to depend on the reconstitution of a functional, protective chromosome end after breakage¹. In more details, McClintock employed a genetic system developed at Cornell where *Zea mais* cells harboring a chromosome with a non-canonical terminus would undergo fusion with the sister chromatid to form a dicentric chromosome prone to break (Figure 1). The resulting chromosomes from the breakage were characterized by an insertion and truncation, distinctively. Due to the lack of the dominant alleles in the truncated chromosome, the cell was able to express the recessive alleles present on the homolog chromosome thereby displaying the recessive phenotype. Barbara McClintock noticed that this cycle of fusion and breakage was maintained during the development of the endosperm. However, the embryo and the developed plant never featured the recessive phenotype. What McClintock postulated was that in the zygote, but not in the endosperm, broken chromosomes deriving from snapping of dicentric chromatin are rescued in preventing a subsequent cycle of fusion-breakage. In McClintock’s opinion, the chromosome ends were restored as normal after the breakage within the embryo^{1,2}.

1.1.2 The end replication problem and the Hayflick limit

As the field of molecular biology advanced in the second part of the 20th century, important discoveries led to the revelation of the DNA structure along with its identification as the genetic material. In 1958, Meselson and Stahl proved with an elegant experiment based on CsCl equilibrium density gradient centrifugation the semi-conservative nature of DNA replication³. According to it, the two strands of DNA were synthesized simultaneously during each round of replication. In the first round, the parental strands were used as templates and the daughter molecules were hybrids of the parental strand and the daughter, newly synthesized strand, which then served as template for the subsequent replication round.

This discovery and the known antiparallel property of the double helix strands brought up the dilemma regarding the directionality of each strand synthesis^{4,5,6}. In particular, given that replication proceeds in the 5’-3’ direction, one strand would necessarily be generated in a 3’-5’ direction, a reaction catalyzed by no known polymerases. One possibility to solve the problem was that both strands were synthesized in a 5’-3’ direction with one of them generated in a discontinuous manner by retrograde polymerization^{4,5,6}. According to this new theory, the

discontinuous strand would result from joining of smaller units, the Okazaki fragments, while the complementary strand forms uninterrupted in a single step of elongation. In both cases, priming was carried out by RNA primers synthesized upstream of DNA that are subsequently removed and replaced with DNA.

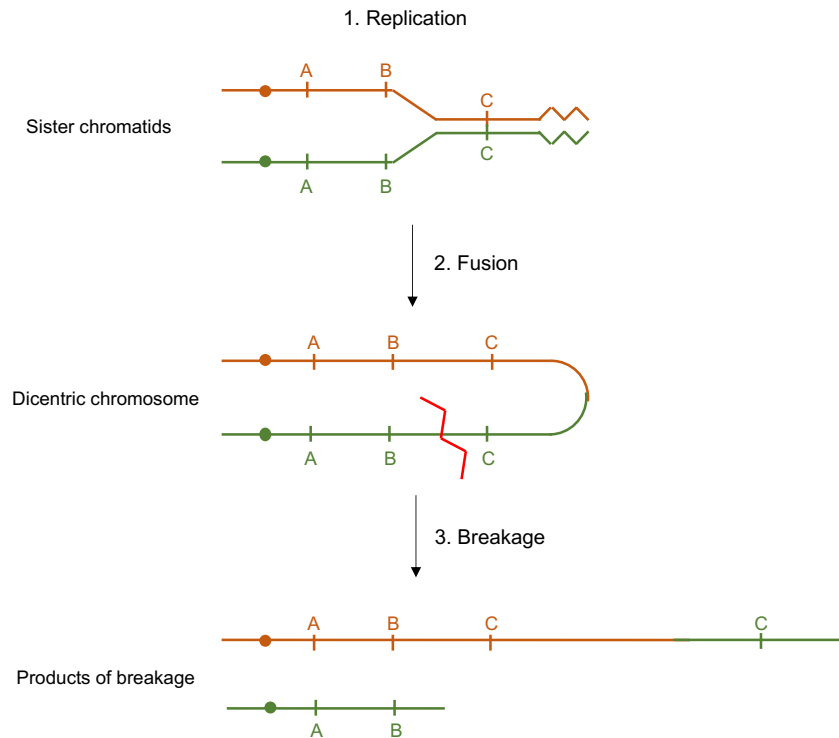


Figure 1. Schematic of the genetic system employed by Barbara McClintock to prove “chromosome healing”. Sister chromatids (orange and green line) harboring dominant alleles of three genes (A, B and C) are generated during replication (1). At their end, a non-canonical structure is present (zigzag line). Because of it, sister chromatids fuse and form a dicentric chromosome (2). During anaphase, when the centromeres (filled circles) are pulled apart, breakage occurs in the dicentric chromosome (red zigzag line). If breakage takes place between gene B and C, the breakage products will be characterized respectively by insertion of gene C and truncation of it (3). The absence of the dominant allele of gene C in cells inheriting the truncated chromosome allows the appearance of a recessive phenotype expressed by the recessive allele on the homolog chromosome.

The model of the DNA molecule replicated in a semi-conservative and discontinuous fashion carried along a new puzzle to be solved: the end replication problem. As Watson and Olovnikov correctly hypothesized, the need of an RNA primer to start replication would inevitably leave an unfillable gap at the chromosomes termini, once the RNA is removed^{7,8}. The extent of this gap would correspond to the exact length of the last RNA primer, when the RNA is synthesized at the very chromatin end, or to the length of the last RNA primer plus the length of upstream DNA left unprimed. In both cases, the impossibility to copy the terminal parts of chromosomes would lead to a progressive shortening of DNA upon each replication round (Figure 2A). This DNA “marginotomy” along with the trimming of the terminal “telogenes” might have explained, according to Olovnikov, the limit to somatic cells doubling potential⁸.

The phenomenon of finite proliferation of somatic cells, known as senescence, was already identified in 1951, when Hayflick observed that fetal fibroblasts could be cultured for the limited

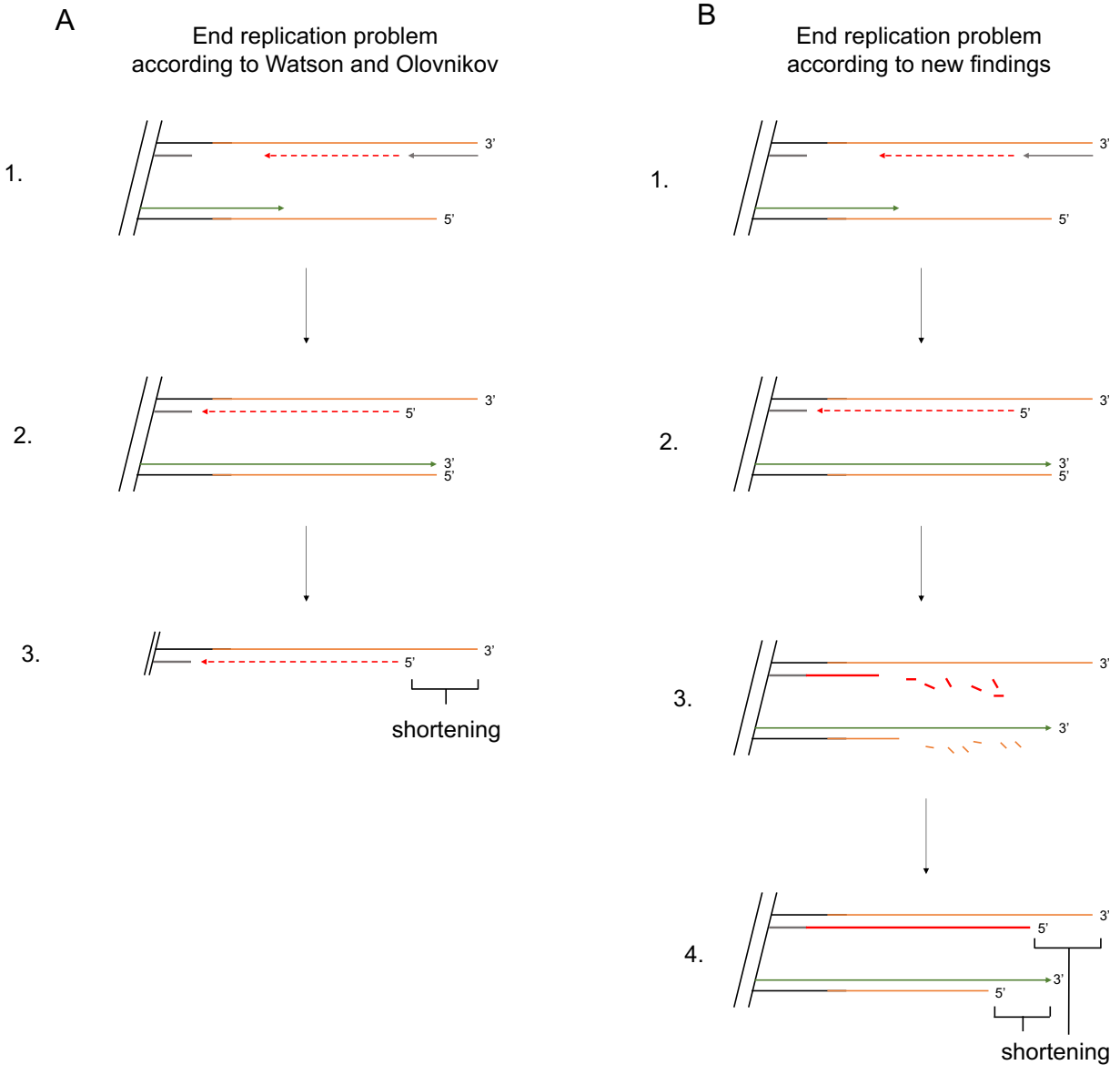


Figure 2. Schematic of the end replication problem. A) The end replication problem according to Watson and Olovnikov. The lagging strand (dashed red line) synthesis is primed by RNA (grey arrow) and proceeds in the opposite direction of the replication fork movement. The leading strand (green arrow) is synthesized in a continuous manner (1). Removal of the last primer used for the lagging strand synthesis leaves an unfillable gap whereas the leading strand synthesis generates a blunt end (2). As a consequence, telomere shortening according to this model derives from the absence of nucleotides on the lagging strand (3). B) New findings showed that, in addition to incomplete synthesis of the lagging strand (1 and 2), telomeres erode because of nucleases resecting the 5' strand of both leading and lagging strand (3). Fill-in DNA synthesis reduces the length of the 3' overhangs and defines the extent of shortening (4).

time of one year⁹. Hayflick postulated that this “degeneration” was caused by intrinsic factors rather than external influence. The “Hayflick limit” in combination with the emerging data regarding the end replication problem set the stage for the next round of explorations aimed at understanding how life is allowed in a senescence context and how the “telogenes” regulate it.

The current model of the end replication problem and telomere shortening is more elaborated than what imagined by Watson and Olovnikov. According to them, telomere shortening was caused exclusively by the incomplete synthesis of the lagging strand. Since the leading strand presented a blunt end, it did not contribute to telomere erosion (Figure 2A). Renewing this view, the Teixeira lab elegantly demonstrated that telomere shortening is also caused by the leading strand in yeast¹⁰. Accordingly, after generation of the blunt end at the end of replication, the leading strand is resected and filled in. Since the fill-in synthesis requires RNA-mediated priming, removal of the last primer determines loss of sequences at the leading strand (Figure 2B). A similar mechanism has been described in humans, where telomere processing and fill-in synthesis occur not only at the leading strand but also at the lagging strand¹¹. Overall, these new findings propose that telomere erosion depends on resection of chromosome ends and incomplete fill-in synthesis of DNA.

1.1.3 The terminal repeats

A first hint about the presence of a repetitive sequence at the chromosomes ends came from the work of MacHattie in 1967, where the DNA molecule of T2 bacteriophage was able to circularize after treatment with exonuclease III¹². According to the authors, this ability relied on the presence of identical sequences at the termini of the virus linear DNA that were prone to anneal to each other. Other studies demonstrated that this feature was shared by the bacteriophages P22, T1, T3, T4 and T7, the latter of which was employed by Watson to illustrate the end replication problem^{7,13}.

With the advent of DNA sequencing by Sanger, the terminal regions of DNA molecules were characterized in terms of their nucleotide sequence. The first one to achieve this was Elizabeth Blackburn in 1978, a then-postdoctoral fellow in Gall's lab who sought to sequence the ends of extrachromosomal ribosomal RNA genes in the ciliate *Tetrahymena*. What Blackburn observed was a hexameric sequence composed of 5'-CCCAA-3' repeated in tandem 20 to 70 times.

After her work, sequences with a similar repetitive pattern and a high content of guanosine and cytosine were identified at the end of chromosomes from different organisms. In 1984, terminal repeats were discovered in yeast and in 1988 they were observed in *Arabidopsis* and in humans¹⁴⁻¹⁶.

A key aspect that resulted from the work of Shampay et al. was the *de novo* addition of yeast telomeric sequences on *Tetrahymena* telomeres when cloned into linear plasmids and transformed in yeast cells¹⁴. The process of a "non-template-directed" synthesis of new telomeres was assumed to be relevant for telomere replication and shed light on the requirement of a non-canonical reaction for copying the chromosomes ends¹⁷. Only one year later it will become clear that the enzymatic activity of telomerase was the basis for it.

1.1.4 The advent of telomerase and beyond

One fundamental feature observed about telomeres was that they are dynamic structures¹⁷. Indeed, despite having a conserved constitution, telomeres appeared in electrophoretic gels to have a heterogeneous length. This was well in line with the concept of a continuous shortening of the DNA molecules and loss of Olovnikov's telomeres. However, one striking phenomenon

known to molecular biologists in the 80s was that telomeres length could increase in some organisms and it occurred in a controlled manner^{17,18}. This unexpected discovery, along with the observation of a non-template-directed addition of new telomeres, led Blackburn to hypothesize that telomere replication occurred via the activity of a terminal transferase^{14,17}. According to her model the enzyme would catalyze the addition of a G-rich telomeric sequence to a pre-existing one, which then would serve as a template for the synthesis of the complementary C-strand by a primase and a DNA polymerase. The removal of the primer and the inefficient ligation between the units on the C-strand would then account for the single-strand breaks observed at the telomeres of multiple organisms¹⁷.

In 1985, Greider and Blackburn detected the terminal transferase activity in the cell-free extract of *Tetrahymena*¹⁷. In their experiment, the researchers observed that the oligomer (TTGGGG)₄ and TGTGTGGGTGTGTGGGTGTGTGGG, resembling the telomeres of *Tetrahymena* and yeast, respectively, could be extended in presence of *Tetrahymena* cell extract only when dGTP and dTTP were added. The complementary sequence (CCCCAA)₄ and non-telomeric sequences were not elongated by the transferase. This showed that the activity of the putative enzyme was active exclusively on the G-rich strand of telomeres, well agreeing with the model proposed, and on telomeric repeats that presented a certain degree of similarity. Importantly, telomeres elongation occurred in absence of a template, as demonstrated by the addition of nucleotides after digestion of DNA in *Tetrahymena* extract. The unprecedented observation highlighted a novel fashion to polymerize nucleic acids, never seen before for common DNA and RNA polymerases. Finally, when Greider and Blackburn observed that the elongation reaction was prevented after heat exposure and proteinase K treatment of the cell extract, it was clear that *de novo* synthesis of telomeric sequences was dependent on a component with enzymatic properties. All together, these data corroborated the idea that an enzymatic activity was required for new telomeres formation.

The same lab in the following years discovered that the enzyme, named by them “telomerase”, contained an RNA component and both the RNA and protein part were essential for the telomere synthesis reaction¹⁹. Later, when the RNA constituting the telomerase of *Tetrahymena* was sequenced and found to harbor a telomeric sequence, it became evident that the RNA molecule within the enzyme was the template used for telomeres polymerization²⁰.

After this pioneering work, telomerase was identified and studied in several organisms. In humans, telomerase was characterized in 1989, when similar features with the enzyme described by Blackburn in *Tetrahymena* were recognized²¹. Soon after the first evidence of telomerase in humans, the correlation of the enzyme expression with tumorigenesis was proposed along with the first suggestion of employing telomerase inhibitors as anti-cancer means²². Subsequent works proved that telomerase expression is not a prerogative of malignant cells. Indeed, the enzyme was found to be expressed also in embryonic cells and, during adult life, in stem cells and germ cells²³.

In the middle of the rampant impetus for telomere research, the Blackburn lab happened to surprise the field once more with an unexpected discovery: telomeres can be maintained in a telomerase-independent manner. The finding occurred in 1993, when Lundblad and Blackburn observed that yeast lacking a functional telomerase were able to maintain their telomeres via a recombination-dependent pathway mediated by Rad52²⁴. These “*est1* survivors” escaped the senescence phenotype given by the progressive telomere shortening and, by acquiring deletion

derivatives of subtelomeric Y' elements and/or entire Y' elements, regained a cell viability similar to *EST1* wild-type cells²⁴.

After some years from its first report, the “alternative pathway” identified in yeast was observed in humans by the Reddel lab. The researchers described that some tumors and immortalized cell lines failed to display a telomerase activity and showed “very long and heterogeneous telomeres in association with immortalization”^{25,26}. The discovery immediately acquired a clinical and therapeutic relevance as potential anti-telomerase drugs used in cancer treatment might have worked poorly in ALT (alternative lengthening of telomeres)-positive tumors. Furthermore, telomerase inhibition might have induced a strong selective pressure for the emergence of telomerase-negative tumors that would have required novel counteracting means.

The recognition of two distinct pathways for *de novo* telomere synthesis, one telomerase-dependent and one -independent, has been shaping since the telomere science, which is nowadays actively attempting to decipher how the two mechanisms are triggered and regulated in normal and malignant cells.

1.2. Telomere structure

Telomeres consist of both a deoxyribonucleic acid and a protein component (Figure 3). In this section, both components will be discussed with a particular emphasis on the telomere structure of *Saccharomyces cerevisiae*.

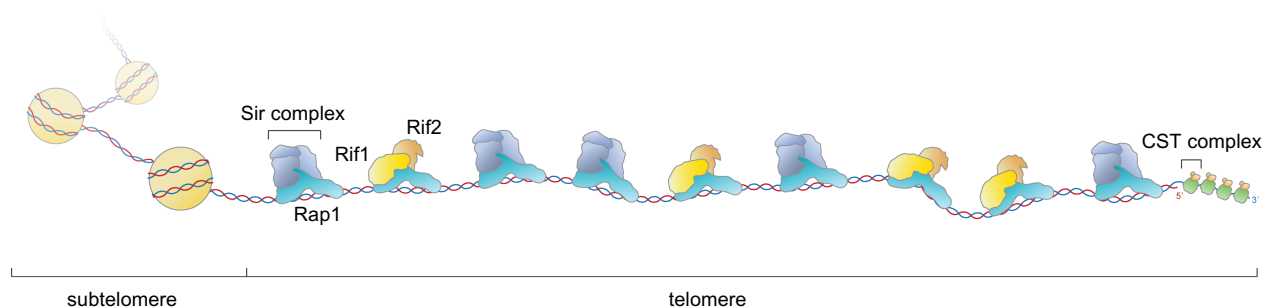


Figure 3. Schematic of a typical subtelomere and telomere in *Saccharomyces cerevisiae*. The subtelomeric region is nucleosomal whereas the telomeric one, which comprises both a DNA and a protein component, is not. Telomeric DNA is double-stranded and single-stranded at the very end. Rap1 binds the double-stranded part while the CST complex interacts with the terminal overhang. Rap1 recruits the Sir complex and the Rif1 and 2 proteins.

1.2.1 Telomeric and subtelomeric DNA

In budding yeast, the telomere sequence is degenerated, consisting of the motif TG_{1-3} repeated over a length of 300 ± 75 bp (reviewed in ²⁷). The absence of a unique motif, like the human TTAGGG, is due to the fact that telomerase uses only part of its RNA to template telomere synthesis and/or the alignment between the RNA template and the telomeric DNA is not maintained constant in every cycle of elongation²⁷. Sequencing analysis of yeast single colonies revealed that the telomere sequence is composed of two parts, one that is unchanged and one that diverges within the colony^{27,28}. Therefore, activities of telomere renewal, like degradation,

recombination and telomerase-mediated elongation, are likely to take place only on one domain of telomeres, the terminal one^{27,28}.

The most distal portion of telomeres is composed of a G-rich ssDNA overhang terminating with the 3'-hydroxyl group(3'-OH). In budding yeast, the overhang is 12-15 nt long, expanding in late S-phase up to 100 nt²⁷. This effect derives not exclusively from the telomerase reaction but also from degradation of the C-rich strand^{10,27}.

Given the high content of guanines, telomeres are prone to generate G-quadruplexes (reviewed in ²⁹). These secondary structures originate when four guanines assemble into a planar arrangement, the G-quartet, driven by Hoogsteen base-pairing contacts²⁹. Stacking of multiple quartets further stabilizes the DNA conformation²⁹.

The exact role of G-quadruplexes (G4s) at telomeres remains to be elucidated. In budding yeast, telomeric G-quadruplexes display a capping function that prevents resection of the C-strand and the following DNA damage response (DDR) activation^{29,30}. This function might be particularly important during replication, when telomeres are more exposed²⁹. Supporting this idea, G4 accumulation has been observed during late S-phase in *S. cerevisiae* and linked to active replication in humans^{29,31,32}. Another function of the G-quadruplexes is the regulation of telomeres accessibility to telomerase along with the induction of the enzyme processivity^{29,33}. Within the dsDNA portion of telomeres, G-quadruplexes, which presumably originate more frequently during the lagging strand synthesis, pose a threat for normal replication thereby requiring specialized proteins for their removal. When these factors are absent, telomere replication is slowed and a “fragile telomere” phenotype is evident^{29,34}. Further indication for the negative effect of G4s on telomere replication comes from the observation that increased telomere synthesis during ALT follows treatment with G4-stabilizing ligands, probably due to enhanced DSBs occurrence^{29,35,36}. G-quadruplexes have also been proposed to form at sites of telomere transcription (discussed in more details below), where the displaced ssDNA within an R-loop might be able to form into G4 quartets^{29,37}. Since G-quadruplexes have been seen to stabilize R-loops genome-wide, it is plausible that they exhibit this property at telomeric RNA-DNA hybrids too³⁸. TERRA, the long non-coding RNA transcribed at telomeres, itself might take part in the formation of G4s at telomeres.

Among the other functions proposed, G-quadruplexes are believed to participate in cohesion of telomeres on sister chromatids upon DNA replication or formation of the telomeres “bouquet” during meiosis²⁹.

Subtelomeres are regions composed of nucleosomal DNA that adjoin telomeres on their centromere-proximal side²⁷. They consist of repeats of heterogeneous sequences that can extend up to 500 kb in humans³⁹. Among their functions, subtelomeric regions are important for establishing heterochromatin at the chromosome ends, maintaining telomeres and regulating their localization and transcription, influencing replicative senescence and determining proper chromosomes recognition, coupling and segregation³⁹.

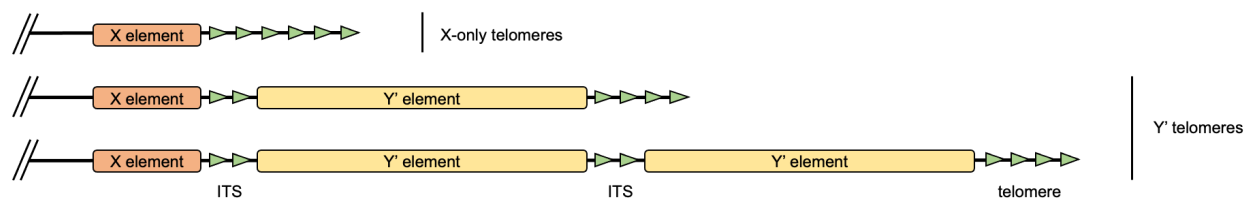
In *S. cerevisiae*, subtelomeres are 10 kb long and contain two types of the repetitive elements known as telomere-associated sequences (TAS): the X and the Y' element^{27,39,40}. The X elements are present on all chromosome ends whereas the Y' elements lie on almost half of them, ranging from 1 to 4 tandem copies within the same subtelomere^{27,40}. When an X element sits next to a Y' element (Y' telomere), the latter is always telomere-proximal (Figure 4A). Between them, it is

common to find internal telomeric sequences (also referred to as internal TG tracts), which can be present also between adjacent Y' elements^{27,40}. These sequences are used for recombination with telomeres thereby causing genome instability⁴⁰ (Figure 4B).

X elements are more heterogeneous in size and sequence than the 6.7 kb (long) or 5.2 kb (short) long Y' elements²⁷. Both elements present ARS (autonomously replicating sequences) and transcription factor-binding sites. However, removal of both units does not cause dramatic consequences like chromosome loss as observed for telomere abrogation²⁷.

Subtelomeres usually display a low gene density and, given the high number of homologous sequences, they frequently undergo rearrangements presenting an elevated polymorphism³⁹. In budding yeast, this holds true when considering that the subtelomeres containing exclusively the X-element (X-only telomeres) vary from one strain to another^{27,40}.

A



B

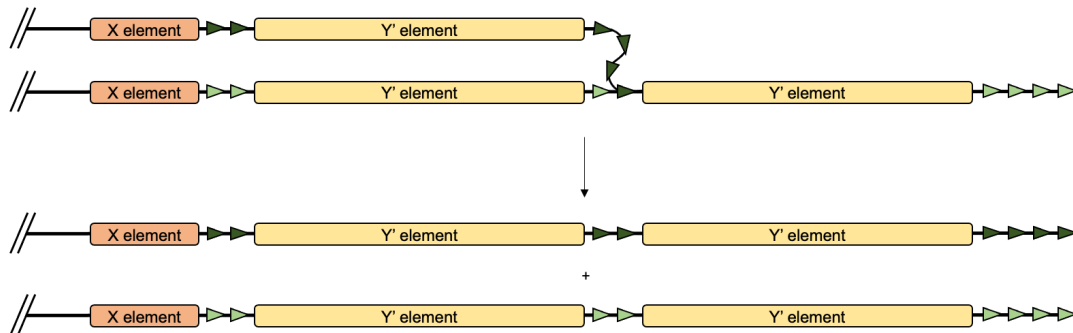


Figure 4. Chromosome ends structure in *Saccharomyces cerevisiae*. A) X-only telomeres present subtelomeric X elements upstream of telomeres (green triangles). Y' telomeres, instead, present a single or multiple copies of Y' elements adjacent to the terminal telomeric sequence. Internal TG sequences (ITS), or tracts, (green triangles) can be present between an X-element and a Y' element or between two contiguous Y' elements. B) Recombination between two Y' telomeres, a donor (light green triangles) and a recipient (dark green triangles), takes place by strand invasion of the recipient telomere into one of the internal TG tracts of the donor telomere.

1.2.2 Telomere proteins

The protein component of telomeres has paramount roles in the chromosome ends protection and homeostasis. In this part, the main features of the budding yeast telomeric proteins will be presented.

1.2.2.1 Rap1

Rap1 (repressor activator protein 1) is an abundant essential protein that acts both on telomeric and non-telomeric regions. In fact, almost 90% of the protein is not found at telomeres²⁷. At these sites, Rap1 operates as a transcription factor, regulating both transcription activation and suppression⁴¹.

At telomeres, Rap1 binds with high affinity the dsDNA portion in a non-cooperative fashion⁴². The consensus sequence recognized by Rap1 is heterogeneous and it has been reported that the protein binds the yeast telomeric sequence every 18 bp for a total of approximately 20 peptides per telomere molecule^{27,40,41}. This is accomplished via the essential DNA-binding domain (DBD) composed of two Myb-like domains, each recognizing one of the two direct repeats of the binding site^{40,43}. The N-terminal domain is dispensable and the C-terminal domain is important for establishing interactions with Rif1/2 and Sir3/4, proteins equally involved in telomere/subtelomere homeostasis.

Rap1, and bound Rif1/2, accumulation at chromosome ends is a reference for telomere length and its regulation^{40,44}. When a telomere is longer than about 120 bp, Rap1 monomers bind to a specific extent to inhibit in *cis* the activity of telomerase (telomerase-non-extendible state)^{42,45}. Below 120 bp, the amount of proteins bound is less likely to repress telomerase thus facilitating telomere elongation (telomerase-extendible state)^{42,45}.

Beside its involvement in telomere length regulation, Rap1 prevents telomere fusions by non-homologous end joining (NHEJ), protects the chromosome ends from nucleolytic attack, mediates their perinuclear positioning, promotes transcriptional silencing via telomere position effect (TPE) and prevents undesired DNA damage-dependent checkpoint activation^{40,46,47,48}. Additionally, the protein can be used to orchestrate responses to stress conditions by moving from the telomeres to specialized genes. These circumstances include glucose starvation, replicative senescence and DNA damage^{40,49,50}.

1.2.2.2 Rif1 and 2

Rif1 and 2 bind Rap1 on its C-terminal domain and work as effectors of its negative regulation on telomere length⁴⁰. This is demonstrated by the similar “very long telomeres” phenotype observed in the carboxy-terminal domain-deprived *rap1-17* mutants and the *rif1Δ rif2Δ* double mutants^{51,52}. In support of their inhibitory effect on telomere elongation, single deletions of the two genes are characterized by longer telomeres than wild-type cells⁵². Moreover, the concomitant deletion of the two exacerbates the phenotype thereby inferring two distinct roles for the Rif proteins^{51,52}.

Both Rif1 and 2 take part in the “counting” mechanism that defines the telomere length and, along with Rap1, form an interconnected capping structure that prevents telomere recognition as DSBs^{40,48,53}. In particular, the two proteins are equally involved with separate mechanisms in impeding the induction of the G2/M checkpoint at short TG tracts⁵⁴.

Rif2 and Rap1 avert the access of nucleases and NHEJ at telomeres^{40,48}. In case of the MRX complex, Rif2 blocks its accessibility in a Rap1-dependent manner while Rap1 can operate both Rif2-dependently and -independently⁵⁵. At long telomeres, Rif1 and 2 inhibit Tel1 association with the chromosome ends directly, by preventing its interaction with the MRX complex, and indirectly, by favoring Rap1-mediated reduction of MRX binding to the telomeres⁵⁶.

Among its functions, Rif1 reinforces the CST complex and impairs telomeres resection, as shown by suppression of the *cdc13-1* lethal phenotype, thus counteracting RPA accumulation and Mec1 recruitment/activation^{40,48,57}. This resection-impeding ability is however less pronounced than the one of Rap1 and Rif2⁵⁸. Additionally, Rif1 is able to regulate the checkpoint and telomerase access to telomeres independently from Rap1^{40,57}. This latter ability is mediated via the protein N-terminal domain that is used to bind directly the DNA molecule^{57,59}. Although the interaction with Rap1 appears to be important for Rif1 to localize at telomeres, its direct binding to DNA is vital to prevent telomere elongation⁵⁷.

A core function of Rif1 is the control of origin firing at telomeres⁶⁰. Telomeric origins are “late” or “dormant origins” that are fired during late S-phase or not fired at all, respectively⁶⁰. Rif1 suppresses their early firing by interacting with the PP1 phosphatase Glc7, which counteracts Mcm4, a member of the pre-replication complex (Pre-RC), phosphorylation promoted by DDK^{60,61}.

Finally, the Rif proteins interact with proteins involved in other telomere physiology-related processes, perhaps acting as a scaffold. Rat1, the RNA exonuclease responsible for TERRA degradation, is recruited to the telomeres via its interaction with both Rif1 and 2, whereas Rnh201, one of the monomers constituting the RNase H2 enzyme, telomeric localization is prompted by the binding to Rif2^{62,63,64}.

1.2.2.3 CST complex

The CST complex is a trimeric protein complex composed of Cdc13, Stn1 and Ten1⁶⁵. Due to the functional and structural similarities with the RPA complex, the CST complex is also referred to as the “telomeric RPA”²⁷. This group of proteins has crucial roles in regulating telomere resection, checkpoint activation and telomerase functionality.

Cdc13 is an essential protein that binds directly to telomeric ssDNA, either terminal or not²⁷. Its binding requires at least 11 nt *in vitro* and is mediated by the protein DBD, which sits between the N- and C-terminal regions. The N-terminal region might include two oligosaccharide/oligonucleotide/oligopeptide binding (OB1 and 2) fold domains that are used for Cdc13 dimerization and interaction with Pol1. Between them, a domain of 102 aa, the recruitment domain (RD), can recruit telomerase via Est1 binding. The C-terminal region interacts with Stn1⁶⁶.

Cdc13 regulates telomerase binding to telomeres via its interaction with Est1. This contact takes place in late S-phase and counteracts senescence, as shown by the “ever shorter telomeres” phenotype associated with the mutated RD-carrying *cdc13-2* allele^{65,67,68}. The Est1-Cdc13 interaction is facilitated by the abundance of the two proteins during S-/G2-phase and specific CDK1-mediated phosphorylation of Cdc13⁶⁷. It is also plausible that the contact established between Cdc13 and Pol1, part of the lagging strand synthesis machinery, might further restrict the protein activity at the end of replication²⁷. Cdc13 and Est1 telomeric recruitment differs between lagging and leading strand⁶⁹. Since the lagging strand can spontaneously present a G-overhang at the end of replication, Cdc13 can directly bind to the ssDNA⁵⁸. In contrast, replication of the leading strand produces a blunt end that requires nuclease-dependent processing to form a ssDNA-Cdc13 complex. This reaction is accomplished by MRX, in concert with Sae2, which

resects the C-strand on the leading strand allowing Cdc13 binding and telomerase recruitment^{58,70}. In the absence of Sae2, the pathway involving Sgs1 and Exo1 can take over^{27,58,70}. In addition to the Cdc13-Est1 pathway, the network between TLC1 and Ku and Ku and Sir4 targets telomerase to telomeric dsDNA during G1-phase (discussed in more detail below)⁶⁷.

Beside its involvement in telomerase recruitment regulation, Cdc13 presents a capping function that protects telomeres from degradation. This is particularly visible in the temperature sensitive *cdc13-1* mutants grown at non-permissive temperatures: the C-strand is resected even within the subtelomeric region and the cells are permanently arrested at the G2-/M-phase boundary via Rad9⁵⁸.

It has been shown that Cdc13 is required to cap telomeres specifically in late S- and G-phase but not in G1- and early S-phase of the cell cycle^{71,72}. This is believed to occur in order to prevent telomeres from nucleolytic attack when most vulnerable: when the passage of the replisome dismantles the protective protein shield. CDK1 or interaction of the CST complex with the lagging strand synthesis machinery might mediate this regulation. The nucleolytic processes involved in 5'-resection at *cdc13-1* uncapped telomeres are the ones that include Exo1, Sgs1 and Dna2, with Exo1 as the main nuclease⁴⁰. An additional pathway is regulated by Pif1 when Exo1 and Sgs1 are depleted⁴⁰.

Binding of Cdc13 to telomeres is also important to prevent checkpoint activation at the G-rich ssDNA via Mec1. This is accomplished by outcompeting the Mec1 recruiter and activator RPA, which transiently binds telomeric ssDNA during replication^{27,40,73,74}.

Finally, Cdc13 is important for the synchronization between leading and lagging strand synthesis and, in association with Stn1 and Ten1, promotes C-strand filling after telomerase-mediated elongation of the G-overhang via interaction with Pol α ^{10,66,75}.

The other components of the CST complex are also involved in telomere protection and telomere synthesis regulation. Both Stn1 and Ten1 are recruited to telomeres via interaction with Cdc13 despite being able to weakly bind telomeric DNA alone⁶⁵. Cdc13 capping function requires Stn1 and Ten1, which can protect uncapped telomeres in absence of Cdc13 when overexpressed^{27,65}. Overall, the three proteins are essential for capping and telomere synthesis regulation as shown by the accumulation of telomeric ssDNA and long telomeres in loss-of-function mutants for each protein^{27,65}.

In more details, Stn1 interacts with Ten1 via its N-terminal domain and with Cdc13 and Pol12, a member of the Pol α complex, via its C-terminal domain. Stn1 negatively regulates the synthesis of the G-strand by displacing telomerase, with which it overlaps in Cdc13 binding,^{65,76}

Ten1, on the other hand, promotes Cdc13 telomere-binding activity^{65,77}.

1.2.2.4 Ku complex

The Ku complex is a heterodimer composed of Ku70 and Ku80. The complex binds to dsDNA in a sequence non-specific manner and is mostly known for its role in promoting NHEJ⁶⁷. At telomeres, Ku is important for protection from degradation, telomerase recruitment, transport of telomerase TLC1 RNA into the nucleus and telomeres localization^{27,40}. Binding to the chromosome ends seems to take place via two means: the first is determined by the interaction with the Sir complex protein Sir4 and the second via a direct binding to DNA²⁷. The interaction

with Sir4 is proposed to be used by Ku, which contacts also the TLC1 RNA, to target telomerase to telomeres during G1-phase⁶⁷. This axis of associations constitutes a distinct pathway of telomerase recruitment beside the Cdc13-Est1 one, with which it collaborates and potentially reinforces⁶⁷. Contacting Sir4 is relevant also for establishing transcriptional silencing via TPE but not for mediating NHEJ or impeding telomeric resection⁶⁷.

The Ku complex prevents telomere resection mostly in G1-phase by blocking Exo1 and Sgs1, which can compensate for the lack of Mre11^{58,78}. This block is abolished during G2 and resection is mediated by MRX, Exo1 and Sgs1⁷⁸. Telomere degradation in the absence of Ku is more limited than the one caused by Cdc13 depletion and does not activate a DNA damage checkpoint, leaving the cell viability unaffected within the G1-phase^{27,79}. This indicates that Ku is more involved in impeding resection initiation rather than extensive degradation⁵⁸.

Finally, the Ku complex is essential for the late firing of telomeric origins²⁷.

1.2.2.5 Sir complex

The Sir complex is composed of the proteins Sir2, Sir3 and Sir4 and is recruited to telomeres via the interaction between Sir3 and Sir4 with the C-terminal domain of Rap1 and between Sir4 and Ku70^{27,80,81}. Sir2 is brought to the telomeres by its binding to Sir4, which enhances its catalytic activity^{82,83}.

The Sir complex is important for establishing transcriptional silencing heterochromatin at subtelomeres. In more details, Sir2, which is the only enzyme of the complex, deacetylates the tails of the histone proteins H3 and H4 within adjacent nucleosomes, generating a substrate that is more favorably bound by Sir3 and Sir4^{80,83}. The subsequent recruitment of new Sir2 determines further association of the complex to the chromatin and spreading of hypoacetylated histones up to 10-15 kb away from the telomeres^{80,83}. This telomere position effect (TPE) suppresses transcription of genes located nearby the chromosome ends and shares similarities with the transcriptional silencing observed at the mating loci^{27,80}.

Spreading of repressive chromatin can be limited by histone modifications, i.e. acetylation and methylation, transcription factors and the histone variant Htz1^{27,84}. These boundaries seem to prevent not only the silencing extension into euchromatin but also loss of the Sir proteins from their sites of action and TPE alleviation⁸³. This is evident in the activity of Sas2, which strengthens gene silencing by acetylating H4K16 and therefore limiting Sir3 escape from the chromosome ends⁸³.

Changes in the chromatin environment have important consequences on telomere recombination and replicative senescence. This was shown by Kozak et al. who observed that removal of Sas2 induced Sir3 dispersion from chromosome termini and a recombination-dependent delay of senescence⁸³. What the authors also reported is that shortening telomeres during senescence display higher levels of subtelomeric acetylation accompanied by a reduced number of Sir proteins at subtelomeres but not at telomeres⁸³. This strongly suggests that although the TPE might be lifted during senescence, the Sir proteins occupancy of shortened telomeres might not be yet favorable for recombination to take place.

The Sir proteins bind differently on X and Y' elements. X elements have been found to be poor in histones and enriched with Sir2 and Sir3 along with heterochromatic marks.^{27,85} On the other

hand, the Y' elements present low levels of Sir2 and Sir3 and a histones abundance typical of euchromatic regions^{27,85}.

Finally, Sir4 participates in telomeres tethering to the nuclear envelope and mounting evidence supports the idea that heterochromatin, and Sir2, facilitates a fold-back structure at telomeres that resembles the mammalian t-loop^{27,86}.

1.2.3 T-loop/telomere fold-back

A further level of protection at the chromosome ends is represented by a structure termed telomeric loop or t-loop. In humans and mice, telomeres have been seen by either electron- or super resolution-microscopy to loop on themselves and form a lasso-like structure, in which the terminal overhang strand invades an upstream double-stranded region of the same telomere^{86,87,88}. T-loops are believed to have provided a means for telomere maintenance in a time when telomerase had not yet evolved and might still constitute an alternative pathway of telomere elongation^{87,89}. According to Tomaska et al., the presence of a free 3'-OH terminus within the t-loop junction might be used to self-prime replication on the looped telomere generating tracts of ssDNA that are subsequently filled in by the replication machinery⁸⁷. Additionally, potential Holliday junctions (HJ) resulting from t-looping might be resolved into circles that can work as templates for rolling circle-dependent telomere extension⁸⁷. Both pathways are reasonable mechanisms by which ALT can unfold.

T-loops have been suggested to participate in end protection by sequestering the chromosome termini and therefore abolishing MRN/ATM-triggered induction of DDR and NHEJ stimulation via Ku^{88,90}. Trf2 is proposed to mediate this shielding effect as it both promotes t-loops formation and represses ATM^{86,88}. Moreover, Trf2 is required for t-loops dissolution via Rtel1 during S-phase⁸⁶.

In budding yeast, telomeres fold back on themselves establishing contacts with the subtelomeric region⁸⁶. The frequency of these interactions diminishes while moving from the telomere to the centromere suggesting a lariat or a loop structure that transiently defines single or multiple touch down points, respectively⁸⁶. A "knot-like" conformation is also plausible where stable connections are built up more inside the tangled formation than outside⁸⁶.

Similar to mammalian t-loops, yeast telomere fold-back might require strand-invasion to originate as suggested by its dependence from the HDR factors Rad51 and 52^{86,91}.

Different works suggest that a heterochromatic environment favors telomere folding in yeast. An indication of this comes from the finding that Rap1, normally sitting at telomeres, can be detected numerous kb away from the telomeres, in a region where also the Sir complex lies⁴⁰. Furthermore, the Sir complex itself and other histone modifiers that determine chromatin hypoacetylation are important for the telomere fold-back^{86,92}. Overall, these observations imply that looping structures at telomeres might exacerbate the inaccessibility provided by repressive chromatin. This "closed" state, however, is not the only one present at telomeres. Indeed, it seems to alternate with an "intermediate" and an "uncapped" state⁸⁶. In the intermediate state, telomeres lose the fold-back structure but are still resistant to telomere-telomere fusions, whereas in the uncapped state, the lack of a functional cap and a looping conformation renders the ends susceptible to processing and repair⁸⁶.

During senescence, as telomeres shorten and activate the DDR cascade, telomere folding is progressively lost⁸⁶. Since the levels of histone modifiers involved in telomere looping decrease or are modified upon senescence, it is believed that the emergence of an open state is not due to telomere shortening itself but rather to a “senescence program”⁸⁶. This might be further accentuated by the arrest in G2/M typical of senescing cells.⁸⁶

In line with the transient requirement of ATM/ATR during telomere replication to establish mammalian t-loops, yeast telomere fold-back is prompted by Rad53, whose activation depends on Mec1 (ATR) and Tel1 (ATM). However, it is likely that Rad53 shapes the fold-back independently from the two kinases as deletions of them do not affect looping⁸⁶.

Finally, given the property of the loop structure to contact regions far away from the telomeres and the link with repressive chromatin, it cannot be excluded that t-loops might take part in a transcriptional silencing program that regulates genes even >1 Mb apart from the telomeres⁹³. This form of TPE is defined as TPE-OLD since it unfolds “over-long-distances”.

1.3 Replicative senescence

Replicative senescence refers to the loss of proliferative potential that does not depend on extrinsic conditions like poor nutrition⁹. Telomere shortening causes replicative senescence in a variety of organisms and is thought to work as a potent barrier to oncogenesis (reviewed in ⁷⁵). The evidence that older organisms present shorter telomeres and accumulate senescent cells has led to the hypothesis that senescence is involved in aging as well⁹⁴. In humans, the limited proliferation is due to a permanent cell cycle arrest, mainly in G1, accompanied by changes in the cellular shape, transcription and secretion profile along with heterochromatinization⁹⁵. In budding yeast, the first indication of replicative senescence was provided by strains presenting the “ever shorter telomeres” (*est1-4*) phenotype and depletion of the TLC1 RNA gene, which lost viability after 60-80 population doublings^{75,96}. Similar to humans, yeast senescing cells are very large and display condensed DNA⁹⁷. A recent work has suggested that the enlargement of cell volume during senescence might dilute the intracellular material thereby establishing a senescence-related program of gene expression⁹⁸.

In yeast, the irreversible arrest is in G2/M and the underlying checkpoint is similar to the one adopted during DNA damage response after DSBs⁷⁵. However, at telomeres activation of the usual DDR presents further levels of regulation and complications given by the telomere structure itself and replication via telomerase. Furthermore, replication stress observed at short telomeres seems to exacerbate the DNA damage response.

In a telomerase-positive scenario, where telomeres shorten before extension by the holoenzyme, Tel1 and Mec1 are required for telomere synthesis independently from each other^{99,100}. In a first step, the MRX complex and Tel1 associate with the short telomeres and trigger 5’-3’ resection via Sae2, Sgs1, Dna2 and Exo1. As a consequence, the 3’ overhang is extended in late S-phase⁷⁵. Normally, long stretches of ssDNA are recognized and bound by the RPA protein, which initiates the DDR via Mec1 activation⁷⁴. In case of telomeres, however, the binding of Cdc13 to the overhang prevents RPA accumulation and Mec1 induction and the extended ssDNA is converted into duplex DNA presumably by Pol α and Pol δ ^{10,75}. When telomeres are sufficiently short, Cdc13 recruits telomerase to trigger new telomere synthesis, followed by C-strand filling⁶⁶.

In absence of telomerase, checkpoint activation is more multifaceted. A single short telomere is able to induce the cell cycle arrest that drives senescence by recruiting Tel1 and Mec1¹⁰¹. Although Tel1 is dispensable for the G2/M arrest, it is involved in the DDR as shown by the delayed appearance of small colonies in *tel1Δ* senescing cells. On the other hand, Mec1 is believed to commence the DDR as its absence abrogates the early onset of senescence induced by the shortest telomere.

The recruitment of Tel1 at the shortest telomere is proposed to trigger resection of the C-strand followed by the binding of RPA on the complementary G-overhang⁷⁵. This promotes Mec1 activation and phosphorylation of the downstream target Rad53 via Rad9, also phosphorylated by Mec1. Among the pathways induced by phospho-Rad53 there is the one responsible for cell cycle arrest.

Extensive resection is important for senescence to take place as demonstrated by the diminished loss of replicative potential in absence of MRX, Sae2 or Exo1 and the accumulation of telomeric/subtelomeric ssDNA¹⁰². The extent of the C-strand degradation is augmented because the anti-processing function of telomeric proteins weakens as telomeres shorten. This applies especially to Cdc13, whose reduced number of bound molecules not only does not contrast efficiently the nucleases activity but also is less able to counteract RPA binding.

Interestingly, the homologous recombination (HR) factors Rad51 and Rad52 are immediately recruited at telomeres via Tel1 in telomerase-negative cells and limit resection^{102,103}. This, along with their role in recombination, explains their effect in averting fast senescence.

Another important aspect to take into account when considering resection during senescence is the potential impairment of the C-strand filling reaction^{10,102}. Normally, when telomeres are resected in late S-phase, polymerases provide resynthesis of the C-strand to reduce the length of the 3' overhang. In case of short telomeres, however, overextension of the ssDNA G-strand seems not to be counterbalanced by a *de novo* polymerization of the complementary strand. This might be due to the presence of less Cdc13 that stimulates C-strand filling or simply to the lack of time to fully base-pair the unusually long G-overhang. A delay in the start of the reaction is also possible¹⁰².

During senescence, Rad53 can be activated at telomeres by Mec1 also via Mrc1⁷⁵. Mrc1 functions within the replication stress checkpoint by moving along the chromosomes with the replication machinery¹⁰². When replication stalls, Mrc1 participates in both signaling the stress and stabilizing the fork to prevent its collapse and promote its restart^{75,102}. Additionally, Mms1, Mms2, Pol32 and Rad5, which also take part in the repair and stabilization of stressed replication forks, contribute to counteract fast senescence¹⁰². Taken together, these data show that senescence might be provoked also by impediments to the normal replication process. Further support for this idea comes from the accumulation of X-shaped replication intermediates at short telomeres⁷⁵. This type of structure generates upon template switching, an error-free means to post-replicatively repair (PRR) stalled forks, in which Rad5 promotes fork regression and pairing with the sister chromatid^{102,104}.

Sister chromatid recombination is thought to maintain telomeres when they are short during a "pre-senescent stage"¹⁰¹. Supposedly, during this phase, Rad52 and Mms1 assure that the sequence of individual telomeres remains unchanged by aborting inter-telomeric and unequal intra-telomeric recombination¹⁰¹. Subsequently, without varying telomere length, pre-senescent cells enter senescence where Mec1 induces the cell cycle arrest¹⁰¹.

In summary, shortening telomeres trigger senescence because of their recognition as DSBs and the ongoing replication stress.

1.4. Telomere maintenance

Two main telomere maintenance mechanisms (TMM) have been described for *de novo* telomere synthesis: one mediated by telomerase and one based on HDR, the alternative lengthening of telomeres.

1.4.1 TMM via telomerase

Telomerase represents the most widespread mechanism of telomere maintenance among organisms. In humans, the holoenzyme expression is generally suppressed in most somatic tissues due to cis-acting regulatory elements and alternative splicing²³. During development, telomerase is active within the inner cell mass of the blastocyst and it is progressively downregulated in the course of differentiation to be expressed and functional in adult life solely in stem cells and germ cells²³. 85-90% cancers overcome the expression inhibition and maintain telomeres via telomerase.

In budding yeast, the telomerase holoenzyme is composed of Est2, the reverse transcriptase catalytic subunit, TLC1, the RNA used as template for telomere synthesis, and the auxiliary factors Est1 and 3, the Ku complex and the Sm proteins, which regulate telomerase binding and activity along with TLC1 localization and stability¹⁰⁵.

Telomeres are not all extended by telomerase within the same cell cycle. Short telomeres are preferentially elongated, and at a higher rate, compared to long telomeres^{40,105}. What governs this choice seems to lie in the telomere structure. Long telomeres are bound by a higher number of Rap1 and Rif proteins, which inhibit telomerase binding. Conversely, short telomeres lose space for these inhibitory proteins thus presenting an “extendible state”⁴⁵. Tel1 has an important role in triggering telomerase recruitment at short telomeres. The protein is enriched at short telomeres and interacts with Xrs2 of the MRX complex, also bound to short telomeres. This interaction is impeded at long telomeres because Rif2, and to a less extent Rif1, counteracts Tel1 in binding Xrs2. Rap1, then, might take part by dislocating MRX¹⁰⁵. Since phosphorylation of Cdc13, the recruiter of telomerase during late S-phase, prompts Est1 binding and Cdc13 is phosphorylated by Tel1, it is possible that Tel1 facilitates telomerase loading on short telomeres via this mechanism. In parallel, Tel1 might generate a more favorable environment for telomerase binding by endorsing MRX binding and the following extension of the G-overhang at short telomeres¹⁰⁵. Evidence for this comes from the accumulation of Cdc13 at short telomeres. Other factors involved in telomerase regulation are Pif1 and TERRA. Pif1 is a DNA helicase that prevents telomerase activity at long telomeres by averting its binding. On the other hand, the role of TERRA is more controversial. Studies in *rat1-1* strains, which upregulate TERRA, show that short telomeres accumulate in a telomerase-dependent fashion thus suggesting a negative regulatory function¹⁰⁵. Other works, however, have proposed that the induction of TERRA at short telomeres might be important for the generation of elongation-proficient clusters that localize on short telomeres for their extension¹⁰⁵.

Telomerase is regulated also during the cell cycle. Although Est2 and TLC1 localizes at telomeres in both G1, via Ku80, and late S-phase, via Cdc13, *de novo* synthesis occurs only in late S-phase. The discrimination between the two phases depends on the Rif proteins as *rif1* and *rif2* strains elongate telomeres in both G1 and late S-phase.

1.4.2. TMM via ALT

The alternative lengthening of telomeres is a mechanism of telomere maintenance alternative to telomerase, in which telomeres are elongated via recombinational processes using other telomeres or subtelomeres as template. Its first report dates back to 1993, when Lundblad and Blackburn observed that a subset of budding yeast cells deficient for Est1 regained viability after senescence in a Rad52-dependent manner²⁴. This led them to assume that a recombination process at telomeres mediated the survival. Later on, ALT was identified in humans too as a separate means from telomerase to maintain telomeres in cancer cells^{25,26}. Also here, a recombinational reaction underlaid telomere lengthening^{106,107}.

Since the very first pioneering study in budding yeast, it has been evident that ALT does not operate by a unique pathway. In *S. cerevisiae*, two types of ALT-performing survivors have been distinguished depending on their growth ability, genetic requirement to form and telomere organization^{24,108}. Type I survivors escape senescence by accumulating tandem arrays of Y' elements at their chromosome ends despite keeping an extremely short terminal TG tract^{24,108} (Figure 5A). This phenomenon of Y' element acquisition, also known as Y' translocation, characterizes not only Y' telomeres but also X-only telomeres thus establishing a general Y'-positive telomere state²⁴. The reaction is supposed to occur by strand invasion of one telomere into the internal TG tracts between an X element and the contiguous Y' element or between two adjacent Y' elements (Figure 4B)^{24,109,110}.

Type II survivors, on the other hand, rise by extending their telomeres without involving subtelomeric sequences (Figure 5B). The length of telomeres is heterogeneous, ranging from very short up to 12 kb or more^{108,111}. Once telomeres are extended, they gradually shorten until reaching a critical length. Abrupt lengthening occurs then again to start a new shortening cycle^{108,111}. Although the main reaction driving formation of type II telomeres involves telomere-telomere recombination, Y' translocation can occur also in type II survivors^{108,110,112}. Here, recombination would proceed according to the same dynamics described for type I survivors.

Given the differences in telomere organization, type I and type II survivors can be easily distinguished by telomere restriction fragment (TRF) analysis, a Southern blot that allows detection of telomeres after restriction enzymes-mediated genomic DNA digestion. Since restriction enzymes cut elsewhere in the genome but not at telomeres, the terminal TG tracts can be studied in their full length by this approach. An example of the two survivor types TRF profile is shown in Figure 6. Compared to a wild-type, type I survivors present two distinct bandings, one at the bottom and one at the top of the blot, with a blank zone in between. The bottom banding corresponds to extremely short telomeres attached to the 3'-terminal part of Y' elements. The top banding, instead, represents the internal and 5'-terminal part of Y' elements attached to the 3'-terminal part of other Y' elements. Moreover, the occurrence of two bands at the top implies the presence of short and long Y' elements.

The TRF profile of type II survivors is more heterogeneous, reflecting the highly diverse nature of their telomeres. There is no precise pattern beside the presence of bands or smears below the bottommost smear of wild-types and, when occurring, the Y'-corresponding banding in the upper part of the blot. In both survivor types, indication of the Y' elements expansion is given by the higher intensity, compared to wild-type telomeres, of the Y'-corresponding banding.

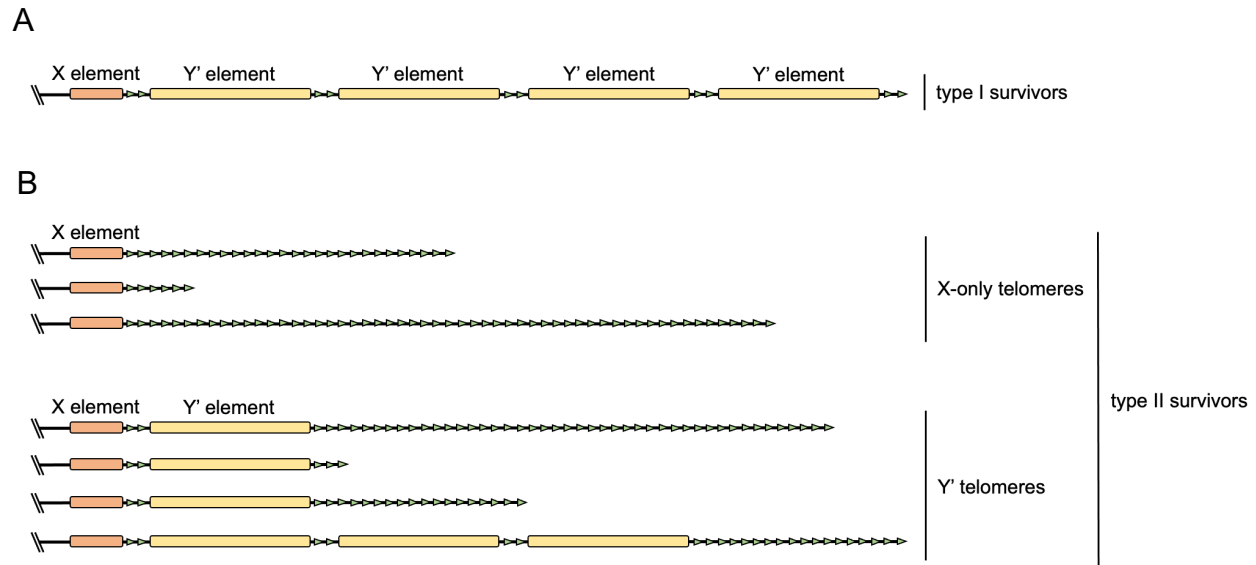


Figure 5. Telomere organization in post-senescent survivors. A) Type I survivors maintain their chromosome ends by tandem amplification of Y' elements. Telomeres are very short (green triangles at the terminus). B) Type II survivors present heterogeneously long X-only and Y' telomeres, from critically short to very extended (terminal green triangles). Y' translocation occurs also in type II survivors, as represented by the formation of a Y' elements tandem array.

Due to their different means to maintain telomeres, type I and II survivors display different growth behaviors. Because of the large availability of Y' elements, type I survivors are more favored to form, constituting approximately 90% of a survivors population. The remaining 10% is composed of the less frequent type II survivors. Although being the most likely to originate, type I survivors grow poorly, frequently showing a senescence-like viability loss and gain. This is probably due to the presence of short telomeres, which constantly induce checkpoint activation. In this respect, cells are arrested in G2/M and telomeres move repeatedly forth and back from the mother cell to the emerged bud, a phenomenon typical of senescent cells¹¹³.

Type II survivors, instead, with their long telomeres typically present growth rates similar to wild-type cells^{24,108}. For this reason, in a liquid culture type II survivors outgrow the slower proliferating type I survivors.

Different genetic requirements distinguish type I and type II survivors formation. While the former need Rad51, Rad54 and Rad57, the latter originate in presence of the MRX complex, Mec1, Tel1, Sgs1, Exo1 and Rad59 among others (reviewed in¹¹⁴). The requirement of Sgs1 and Exo1 for type II survivors to form indicates that extensive telomeric resection might be needed for type II recombination^{115,116}. Despite these differences, both survivors require Rad52 and Pol32, a non-essential subunit of Pol δ , to rise^{24,117}. This highlights that break-induced replication

(BIR) is the underlying mechanism for telomere extension after senescence. In particular, given the different requirement for Rad51 it is possible to discriminate between a Rad51-dependent BIR, which mediates type I survivors formation (type I BIR), and a Rad51-independent BIR, which underlies type II survivors rise (type II BIR). Further confirming the engagement of BIR, deletion of Pif1, a helicase required for this recombinational process, can abrogate both survivors formation¹¹⁸.

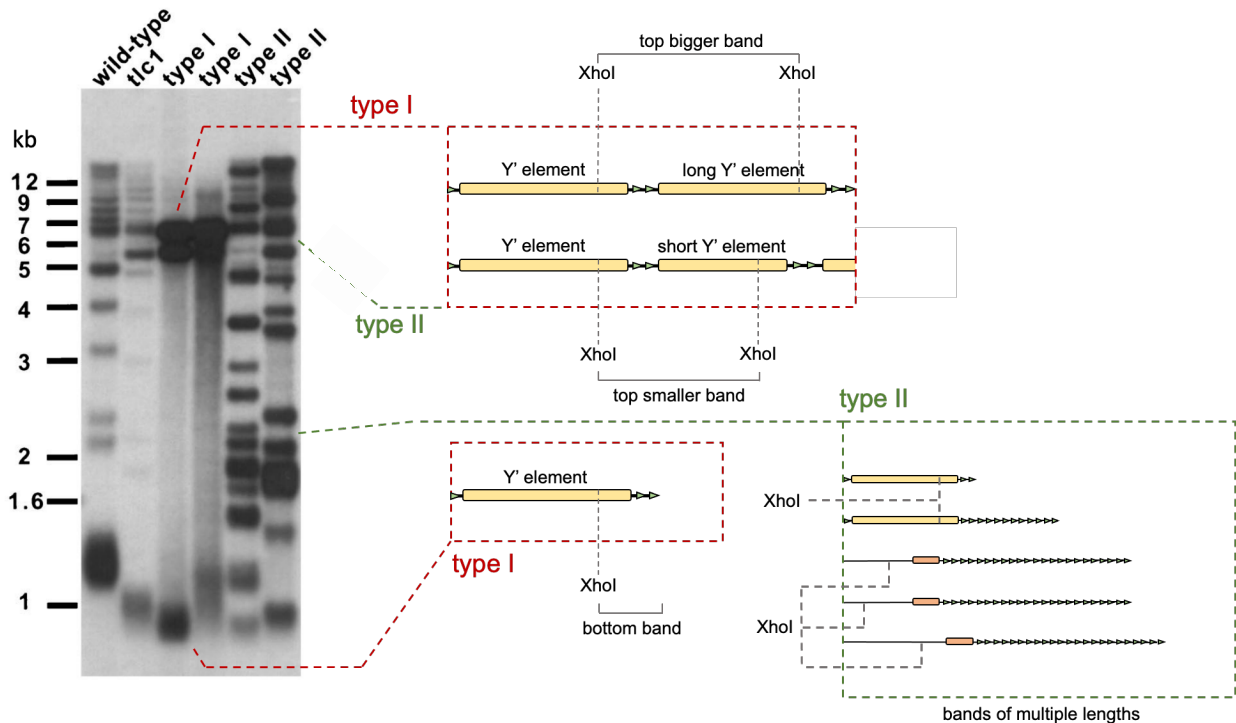


Figure 6. Representative Southern blot of type I and II survivors when genomic DNA is digested with XhoI. In type I survivors, two bandings are evident at the top and bottom of the blot. The top one corresponds to restriction fragments obtained from the internal region of the Y' elements tandem array (upper red rectangle). The bottom one results from fragments derived from the terminal part of the array (bottom red rectangle). The presence of two different bands within the top banding is caused by the presence of both long and short Y' elements. Type II survivors can also present this banding. However, the most evident feature visible in this type of cells is the heterogeneous banding profile. Since each band corresponds to a subteleromic region flanked by TG repeats, the position of the bands is determined by the length of the TG tract and the location of the XhoI cut site (green rectangle). The Southern blot is adapted from Teng et al.¹⁰⁸

1.4.2.1 Survivor emergence

It is commonly accepted that survivors rarely rise when critically short telomeres accumulate in senescing cells, presumably as part of a program aimed at repairing the damaged chromosome ends. Telomere HDR is adopted already during senescence, before survivors formation, and is believed to take place by sister chromatid exchanges⁴⁵. Similar to the BIR events that characterize post-senescence survival, this repair process depends on Rad52 and Pol32^{24,102}. The induction might derive by the progressive loss of telomere proteins, which normally inhibit HDR, as demonstrated by the increased recombination rate upon depletion of Rif1, Cdc13 and Ku.

Accumulation of RNA-DNA hybrids upon telomere shortening is also proposed to trigger HDR, potentially by inducing replication stress^{119,120}.

Emergence of survivors is defined by a two-steps process: formation of ALT-precursors and maturation of ALT-survivors¹¹². In contrast with what previously believed that type I and II survivors arise via two distinct pathways, a recent work from the Malkova lab has showed that a unified program accounts for the primary formation of ALT-telomeres¹¹². Subsequently, further recombination events take over to differentiate the two types of telomere described above (Figure 7).

In more details, when eroding telomeres reach a length between 75 and 90 bp, Rad51- and Rad52-mediated recombination induces the formation of longer telomeres, which delay the onset of senescence. This phase might coincide with the pre-senescence period described by Abdallah et al., where Rad52 and Mms1 promote telomere maintenance by equal telomeric recombination¹⁰¹. The activation of the DNA damage checkpoint within these ALT-precursors is suggested to be important for the following maturation step.

When the telomere length shrinks at 70 bp, senescence unfolds. At this point, survivor-long telomeres start appearing in a Rad51-independent but Rad59/52-dependent manner, while the majority of telomeres keeps eroding. Further dividing brings extension for more telomeres, which acquire now the typical post-senescence structure. This phase is the maturation.

Rad59 and Rad52 are suggested to direct microhomology-mediated HDR at telomeres¹¹². During maturation, if this reaction occurs between the TG tract of a short telomere (recipient) and a TG tract of a longer telomere (donor) in ALT-precursors, type II telomeres form. If the donor TG repeats, instead, lie between an X-element and a Y' element, or between two Y' elements, Y' translocation takes place^{110,112}. In type I survivors, this reaction is further prompted by Rad51, which induces the formation of Y' elements tandem arrays.

Interestingly, according to the study from the Malkova lab, type I survivors too can present long terminal TG tracts, thus generating a "hybrid" structure between type I and II telomeres. This is proposed to be the product of telomere stabilization, a process that presumably occurs at a later stage in established survivors providing indefinite proliferative capacity.

Since ALT discovery, different models try to explain the HDR mechanism underlying survivors formation (reviewed in¹¹⁴). Despite their differences, all these processes must confront the fact that ALT occurs by a one-step lengthening event¹¹¹. They include BIR via t-loops, iterative inter- and intra-telomeric BIR and rolling circle telomere extension via telomeric circles (Figure 8). Depending on the presence of Y' elements in the donor structure, both type I and II telomeres can form. Furthermore, consistent with the permanent arrest in G2 of deeply senescing cells, it is highly likely that the majority of the mechanisms acts in the attempt to overcome DNA replication impediments that accumulate at short telomeres.

1.4.2.2 ALT in humans

Similar to yeast survivors, human ALT cancers rely on HDR to maintain their telomeres in absence of telomerase¹²¹. This process requires PolD3/4, two subunits of Pol δ involved in BIR, indicating that ALT employs a break-induced replication-based mechanism^{36,122}. BIR-induced telomere synthesis (BITS) can take place during mitosis, therefore named MiDAS (mitotic DNA synthesis), or in G2^{36,123}. During this phase, telomeres cluster within specialized structures, the ALT-

associated PML bodies (APBs), which are believed to act as recombination centers due to their enrichment with recombination and replication factors (reviewed in ¹²⁴).

ALT telomeres are generally heterogeneous in length and present a structure reminiscent of that in type II survivors²⁶. For this reason, type II survivors are commonly referred to as ALT-survivors. Another similarity with the yeast system is that human BITS is mostly Rad52-dependent but Rad51-independent^{36,125}. Indeed, when Rad52 is deleted, telomeric synthesis is impaired in both G2 and mitosis, whereas absence of Rad51 disrupts clustering, promotes MiDAS and has no effect on G2 synthesis^{123,125,126}.

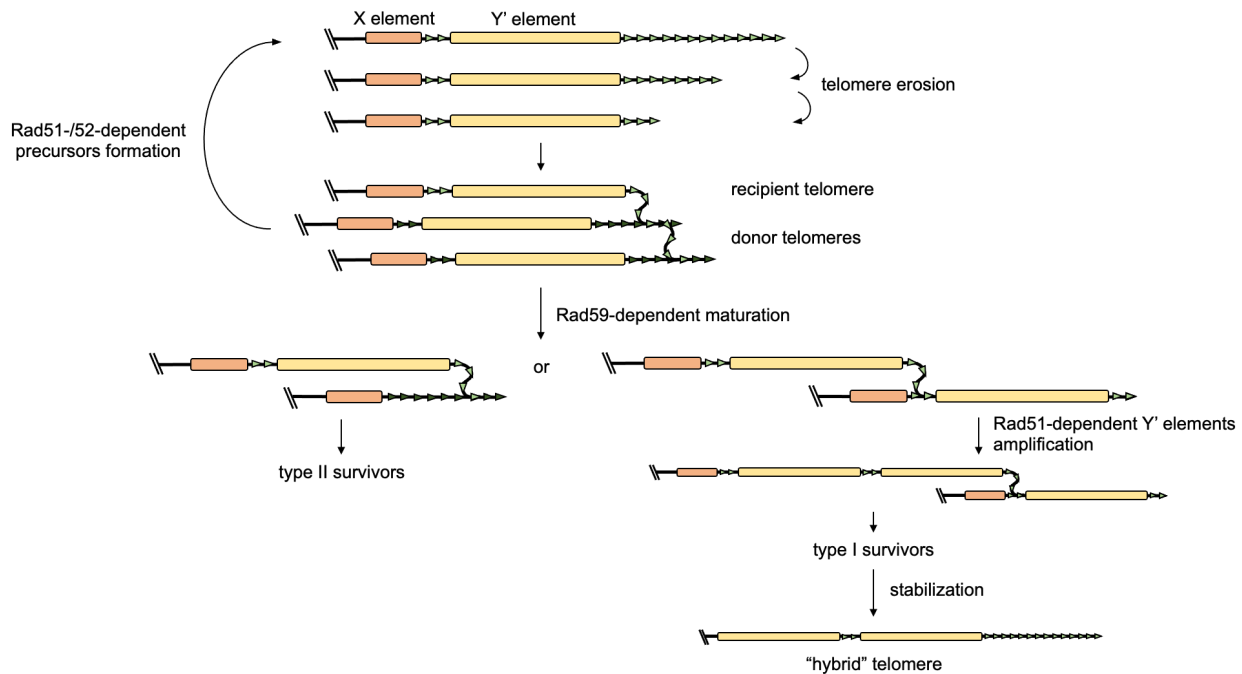


Figure 7. A unified pathway underlies type I and II survivors formation. According to Malkova et al., when telomeres reach a length between 75 and 90 bp, a Rad51-/52-dependent HDR reaction promotes telomeres lengthening and formation of survivors precursors¹¹². Subsequent maturation into the two telomere types takes place via Rad59, which mediates either strand invasion of one telomere into another telomere (left) or strand invasion of one telomere into the internal TG tracts upstream of a Y' element (right). Type I telomeres can be further stabilized by addition of long telomeric sequences at the terminus.

Despite the importance of Rad52, it is assumed that some ALT activity might yet exist in the absence of the protein¹²¹. This is particularly evident when inducing DSBs at telomeres. In this case, depletion of SLX4, a protein involved in resolving recombination intermediates, causes a growth defect in Rad52-deprived cells. Therefore, it is possible that in absence of Rad52 specific structures accumulate at telomeres that might impede BITS. Slx4 is responsible for their resolution and telomere synthesis resumption. These intermediates might be products of replication stress, which is proposed to be enhanced in ALT cells and trigger BITS¹²⁷.

Evidence for increased replication stress at ALT telomeres is broad. ALT cancer cells accumulate telomeric circles, which are bioproducts of replication stress-associated intermediates resolution, and DNA damage markers at telomeres^{127,128}. One means to alleviate replication

stress at telomeres is thought to be by fork reversal via translocases like Smarcal1 and FANCM^{127,129,130}. Accordingly, upon fork stalling at telomeres, fork regression might induce template switch of one of the two newly synthesized strands on the other and replication restart. Consistent with this, deletion of Smarcal1 or FANCM induces C-circles increase and DNA damage at telomeres, both signs of ongoing replication stress^{127,129,131}. Interestingly, the C-circles formation is dependent on Slx4 in a Smarcal1 knockout background, thus suggesting that the Rad52-independent pathway before mentioned might act in conditions where replication stress persists in absence of attenuating mechanisms¹³¹. Further proof for this comes from the observation that removal of Rad51 and Mre11, both involved in reversed forks protection and maturation, enhances C-circles levels^{125,128}.

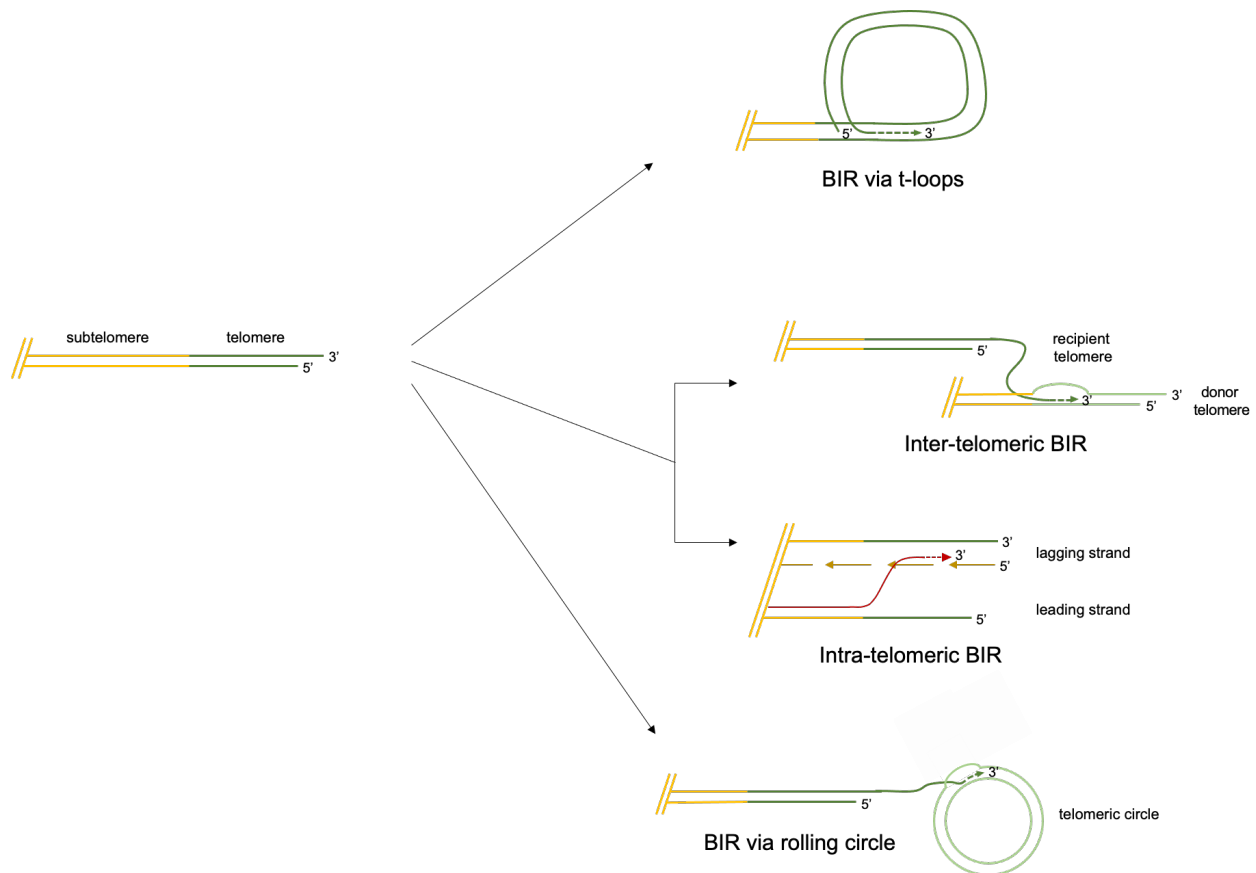


Figure 8. Different models to explain how BIR in ALT can occur. BIR can take place upon t-loops formation: the 3'-strand of one telomere invades an upstream region of the same telomere to form the loop. The 3'-OH end can be used by polymerases to extend the strand using the t-loop DNA as template. Complementary strand synthesis follows. Another possibility is BIR between two different telomeres (inter-telomeric BIR) and within the same telomere, between sister chromatids (intra-telomeric BIR). In the first case, the 3'-strand of one telomere forms a D-loop structure on another telomere, followed by extension and fill-in synthesis. In the second, template switch from the leading template strand to the newly-synthesized lagging strand of one telomere allows HDR between sister chromatids. Finally, telomeric circles can be used as template for rolling circle replication, where a telomeric 3'-strand invades the circle and is extended by polymerases. Like the other mechanisms, a fill-in reaction provides the complementary strand synthesis.

One source of replication stress at ALT telomeres is the accumulation of TERRA RNA-DNA hybrids¹³². This increase can be linked to derepressed transcription deriving from less condensed telomeric chromatin, as shown by the lower abundance of the heterochromatin marker H3K9me3¹³³. Further chromatin changes that associate with TERRA overproduction might be induced by loss of the chromatin remodeling complex ATRX-DAXX, a hallmark of ALT cancers¹³⁴. In these cells, the lack of the complex accounts not only for the transcript overexpression but also for the disruption of the cell cycle regulation¹³⁵. Absence of ATRX-DAXX is also a source of G4-quadruplexes accumulation, another trigger of replication stress¹³⁶.

In general, the alternative lengthening of telomeres is induced by replication stress but its exacerbation might be lethal¹²⁷. A clear example comes from the accumulation of TERRA RNA-DNA hybrids itself. According to Arora et al., a very specific amount of R-loops, controlled by RNase H1, is required to stimulate ALT synthesis. Deviations from it cause detrimental effects like telomere loss¹³².

Despite the growing findings about the ALT mechanism, different questions regarding in particular the origin and regulation of telomerase-independent TMMs remain still open and central in the nowadays field of telomere research.

1.5. TERRA

TERRA (telomeric repeat-containing RNA) is the long non-coding RNA transcribed at telomeres from the C-rich strand^{63,137,138}. Its presence has been observed in many organisms, including humans and yeast, which share aspects of the transcript synthesis and regulation^{63,137}. TERRA is mainly transcribed by RNA pol II starting from promoters within the subtelomeres and continuing throughout the TG repeats of telomeres^{63,137,138}. Because of this, TERRA molecules contain two parts: one corresponding to the subtelomere and one composed of the telomere-related UG pattern. Since the subtelomeric part might present distinctive sequences, it is possible to characterize TERRA from specific chromosome ends.

In humans, TERRA transcription is assumed to start from a specific class of promoters which contain CpG islands^{139,140}. They are present either in proximity of the telomeric sequence or 5 to 10 kb away from it¹⁴¹. Since promoters were identified on several subtelomeres, TERRA transcription is supposed to derive from multiple chromosomes^{139,140}. In yeast, the promoter regions are still to be recognized. However, it is proposed that both X and Y' elements hold the ability to initiate transcription^{63,142}.

The exact mechanism of TERRA transcription termination is still elusive. In yeast, almost all TERRA molecules are 3'-polyadenylated, a modification that enhances the transcript stability⁶³. The enzyme Pap1 accounts for TERRA polyadenylation, as suggested by increased turnover and absence of polyadenylation upon the protein inactivation⁶³. Unlike yeast, polyadenylation in human cells is reported only for 7% of total TERRA and determines the transcript dissociation from chromatin^{138,143,144}. Despite these observations, it is unknown whether the addition of a poly-A tail occurs immediately as the RNA detaches from DNA or requires cleavage of the nascent transcript¹⁴⁵.

Another modification described for human TERRA is the 5'-7-methylguanosine cap (m⁷G), which might protect the transcript from exonucleases¹⁴⁴. The first report of an exonuclease negatively affecting TERRA is the work from Luke et al., where the 5'-3' exonuclease Rat1 was described to

be responsible for the majority of TERRA degradation⁶³. Expectedly, Rat1 inactivation increased the levels of TERRA and extended its half-life, which is of ~ 20 min^{63,145,146}. Independently from Rat1, other factors are responsible for TERRA degradation. They include members of the PAF1 and TRAMP complex¹⁴⁷. In humans, little is known about the lncRNA degradation. In the first study about TERRA, the SMG proteins, which take part in non-sense mediated mRNA decay, negatively influence the lncRNA expression¹³⁷. Additionally, TERRA was observed to increase upon depletion of Xrn2, the orthologue of Rat1, in another primate¹⁴⁸. Further evidence of Xrn2 involvement in processing TERRA derives from a recent study, where the enzyme might negatively regulate the transcript in association with BRCA1¹⁴⁹. Like in yeast, polyadenylation might avert degradation, as suggested by the increased half-life of poly-A-positive species (8 hours) compared to the poly-A-negative ones (3 hours)^{138,144}.

Since TERRA is transcribed from subtelomeres throughout the telomeres and its termination might not occur at a specific site, the transcript length is highly heterogeneous. In humans, TERRA length ranges from ~ 100 nt to 9 kb in telomerase-positive HeLa cells whereas in yeast it is between ~ 100 nt and 1.2 kb^{63,137}. In ALT cells, the RNA can be even longer^{132,137}.

1.5.1 TERRA expression regulation

TERRA expression can be regulated at both the synthesis and degradation level. In humans, several reports address the chromatin state at telomeres/subtelomeres as a key regulator of TERRA transcription. The general idea is that the presence of a less heterochromatic state favors RNA pol II binding and RNA synthesis. Consistent with this, methylation of the CpG islands promoters via DNMT methyl transferases suppresses TERRA^{139,150}. Moreover, heterochromatin marks like H3K9me3, H4K20me3 and HP1 act negatively on the RNA expression while acetylation favors it^{138,143,149,150}. The transcription factor CTCF and the cohesin subunit Rad21 localize at CpG island promoters and trigger RNA pol II association and TERRA transcription¹⁵¹. Other transcription factors, like ATRX, and telomere proteins, like TRF1 and 2, repress TERRA transcription^{135,141,152}.

In yeast, TERRA production is regulated by the chromatin state of chromosome ends as well. In this respect, subtelomeres organization in terms of presence and absence of Y' elements has a relevant influence. TPE is reported to inhibit transcription of genes in proximity of telomeres via heterochromatin propagation¹⁵³. TERRA expression is strongly repressed by TPE, as shown by the marked transcript accumulation in *sir2Δ*, *sir3Δ* and *sir4Δ* strains^{62,146}. The effect is stronger at X-only telomeres than at Y' telomeres, in line with the observation that Y' elements are generally more euchromatic⁸⁵. Rap1 is another negative regulator of TERRA, partially due to its function in recruiting the Sir complex to telomeres¹⁴⁶. Like for the deletion of the Sir proteins, TERRA increase upon Rap1 inactivation is less evident at Y' telomeres, probably because of a lower enrichment of the protein⁸⁵. The Rif proteins negatively affect TERRA expression to different extents, with Rif1 having the bigger influence in both X-only and Y' telomeres¹⁴⁶. Interestingly, Rif1 appears to suppress TERRA transcription only at Y' telomeres¹⁴⁶.

As for the regulation of TERRA degradation, little information is provided by studies in humans. In yeast, Rat1 is shown to be recruited to telomeres by Rif1 and 2, causing TERRA suppression at both X-only and Y' telomeres^{62,146}. Rap1 indirectly participates to the negative regulation by

recruiting the Rif proteins¹⁴⁶. Therefore, those conditions that influence the binding of Rap1 and the Rif proteins to telomeres are expected to influence the activity of Rat1 and TERRA stability. By employing these circuits of regulation, cells fine tune TERRA in response to different situations. One of this is cell cycle progression. TERRA is regulated throughout the cell cycle in both humans and yeast^{62,135,144}. In humans, the lncRNA is expressed at its maximum during early G1 and progressively decreases throughout the G1 and S-phase^{144,149}. The minimum is reached between the late S-phase and G2. As reported by Flynn and colleagues, ATRX is involved in repressing TERRA in G2/M. Indeed, knocking down the protein in telomerase-positive HeLa cells determines persistence of the transcript from S-phase to G2/M. This occurs spontaneously in ALT cells, where ATRX is frequently found to be inactive (see below for further information)^{135,154,155}. Given the role of ATRX in transcription, it is likely that regulation of TERRA during the cell cycle is modulated by turning on and off the synthesis process, followed by exonuclease-mediated degradation^{149,152}. A similar mechanism has been described in yeast. Here, the expression is very low in G1, peaks in early S-phase and drops as replication approaches the chromosome ends⁶². In G2/M phase, the abundance of TERRA is also reduced. This regulation depends on transcription in S-phase and progressive degradation by Rat1. Consistent with it, the exonuclease binds to telomeres only in middle and late S-phase⁶².

In several organisms, TERRA is regulated also in a telomere length-dependent manner. In humans, a negative correlation between telomere length and the transcript abundance is reported in the work of Arnoult et al¹⁵⁰. Here, cells with longer telomeres present a higher percentage of methylation at CpG and lower levels of the RNA. Moreover, elongation of telomeres is proposed to suppress TERRA by accumulation of the heterochromatin marks H3K9me3 and HP1 α . Further proof of the negative correlation between TERRA and telomere length is given by the observation that patients with ICF (immunodeficiency, centromeric region instability, facial anomalies) syndrome present abnormally short telomeres and increased TERRA levels¹⁵⁶. In yeast, several studies report a similar regulation^{62,157,158}. Short telomeres are proposed to upregulate TERRA because of a reduced number of binding sites for negative regulators. In *S. cerevisiae*, it is suggested that short telomeres accumulate TERRA in response to a lower binding of Rap1, the Rif proteins and Rat1, which they recruit^{62,158}. This impaired degradation is particularly evident in senescent cells, where less Rat1 binds telomeres compared to telomerase-positive cells⁶². Importantly, TERRA upregulation in senescent cells appears not to be driven by enhanced transcription. In *S. pombe*, it is proposed that long telomeres are in a chromatin “closed state” that impedes TERRA transcription^{157,159}. When telomeres shorten, chromatin is more relaxed triggering the RNA synthesis.

Cellular stress and genome instability influence TERRA expression. In humans, TERRA has been reported to increase upon heat shock, etoposide treatment and oxidative stress^{138,160–162}. Similarly, in yeast, cells upregulate TERRA when adopting oxidative respiration instead of fermentation¹⁶³. All these observations suggest an involvement of the lncRNA in stress signaling and repair activities that might be not exclusively dependent on telomere homeostasis.

1.5.2 TERRA function

The exact function of TERRA is still to be determined. However, mounting evidence suggests that the transcript is involved in telomere organization and maintenance, replication, gene expression regulation and stress signaling and response (¹⁶⁴ and reviewed in¹⁶⁵).

In human cells, TERRA takes part in heterochromatin deposition, as suggested by the transcript interaction with HP1, H3K9me3 and PRC2^{166,167}. When TERRA accumulates due to TRF2 depletion, the transcript interacts with the Suv39H1 H3K9 histone methyl transferase to increase H3K9me3 at dysfunctional telomeres, presumably to sustain their repair¹⁴¹.

TERRA regulates telomere length by influencing both the lengthening and shortening processes. In mammalian cells, the lncRNA appears to negatively regulate telomerase. This is supported by the observation that TERRA hinders *in vitro* the enzyme activity in humans¹⁶⁸. A similar effect has been described *in vivo* in mouse embryonic stem cells¹⁶⁴. In yeast, instead, TERRA brings telomerase to short telomeres and may stimulate their extension^{157,158}.

Beside the involvement in telomere maintenance via telomerase, TERRA is important for telomeric HDR too. In yeast, TERRA RNA-DNA hybrids (discussed in more detail below) trigger telomere recombination to counteract shortening and fast senescence and promote type II survivors formation^{119,169}. TERRA has also been seen to induce telomeres shortening when strongly overexpressed^{120,170}. This is dependent on the lncRNA transcription stimulating Exo1 and replication stress-associated telomere loss^{120,170}. This double-edged effect implies that TERRA expression needs to be tightly controlled to favor telomere maintenance without becoming lethal.

The role of TERRA in signaling stress and promoting a response is supported by growing evidence. In yeast, cells using oxidative respiration not only accumulate the transcript but transfer it to the cytoplasm¹⁶³. This indicates that TERRA expression might be part of a regulatory pathway that senses the oxidative stress in the nucleus and induces a response outside it. Additionally, the transcript might modulate gene expression, a function that TERRA exerts physiologically, for example, in mouse cells¹⁶⁴. Further proof of the transcript being part of a stress response comes from experiments with etoposide-induced stress^{160,171}. Here, the RNA stability is augmented in response to the chemotherapeutic and telomeric replicative stress increases when TERRA is suppressed.

Overall, these data show that TERRA presents several functions, with some of them being relevant not only for telomeres physiology. When TERRA regulates telomere length, it can act both positively and negatively. Furthermore, the lncRNA appears to participate in sensing cellular stress and aiding to relieve it.

1.5.3 TERRA RNA-DNA hybrids

TERRA can anneal with DNA to form R-loops, a three-stranded structure where the RNA binds on one strand of DNA (RNA-DNA hybrid) displacing the complementary one¹⁷². TERRA can form RNA-DNA hybrids at telomeres both in *cis* and in *trans*^{119,132,173,174}. When the hybrids are generated in *cis*, the nascent RNA anneals back on the template co-transcriptionally; instead, when they form in *trans*, a strand invasion reaction is required. Evidence for the former case comes from the work of Balk et al. in yeast, where RNA-DNA hybrids were poorly detected at a transcription-deficient telomere¹¹⁹. Furthermore, Maicher et al. observed that inducing TERRA transcription at one telomere promoted replication stress and shortening in *cis*¹²⁰. In humans, a similar scenario was

observed in the osteosarcoma cell line U2OS, where induced transcription of TERRA at specific telomeres caused instability only at that class of chromosome ends¹³². No evidence is currently present in yeast for TERRA RNA-DNA hybrids forming in *trans*. In humans, the work from Lee et al. suggests that the telomeric protein TRF1 prevents TRF2 from triggering TERRA invasion into telomeres^{175,176}. In this regard, the Lingner lab recently published about the role of Rad51 in promoting exogenous TERRA strand invasion into telomeres to form RNA-DNA hybrids¹⁷⁴. Interestingly, in that paper, the subtelomeric part of TERRA influenced only marginally the hybrids formation in *trans*, supporting the idea that telomeric hybrids mainly form at the telomere side of chromosome ends. A similar outcome was obtained in another work, where removal of the telomeric part from a subset of chromosome termini *in vitro* impaired the hybrids detection via DRIP (DNA-RNA hybrids immunoprecipitation)¹⁷³.

Overall, these data affirm that TERRA forms RNA-DNA hybrids at telomeres in different organisms. They generate preferentially at the telomeric part of chromosome ends, either in *cis* or in *trans*.

The function of telomeric RNA-DNA hybrids is yet to be fully determined. In yeast, the RNA-DNA hybrids amount regulates the shortening rate of telomeres, influencing the pace of senescence¹¹⁹. When RNA-DNA hybrids accumulate, telomeres shorten slower, thus determining a delay in senescence. Oppositely, removal of R-loops increases the shortening and senescence rate. This form of telomere length regulation is dependent on Rad52-mediated recombination, thus suggesting that R-loops trigger HDR at telomeres to prevent erosion and senescence^{62,119}. The involvement of RNA-DNA hybrids in telomere recombination is also sustained by the work of Yu et al., where removal of R-loops impeded type II survivors formation¹⁶⁹. It is believed that telomeric HDR is induced by the replicative stress that RNA-DNA hybrids cause^{119,127,132,140,172}. This is particularly evident in the ALT scenario, where RNA-DNA hybrids accumulate at telomeres causing simultaneously DNA damage and BIR (further discussed below and in the Discussion session)^{127,132,140}.

If the stress induced by R-loops cannot be relieved, it becomes detrimental for the cells. In yeast deficient for recombination, the replication stress induced by RNA-DNA hybrids cannot be attenuated, leading to telomere loss, presumably via DSBs, and premature senescence^{119,120}. It is also possible that, in the attempt of resolving R-loops-induced stress, recombination becomes lethal for the cells. This is the case of the excessive activity of Mph1, the homolog of human FANCM, that generates toxic recombination intermediates in the effort to alleviate the R-loops-dependent damage¹⁷⁷. In humans, since recombination¹⁷⁷ is normally repressed, R-loops accumulation at telomeres is expected to be mostly deleterious. This is the case of patients with ICF syndrome, where the abnormally high levels of TERRA RNA-DNA hybrids cause telomere instability¹⁷³.

The abundance of RNA-DNA hybrids requires to be tightly controlled to prevent deleterious effects. In yeast, telomeric R-loops are regulated in a cell cycle- and telomere length-dependent manner, similar to what described before for total TERRA⁶². This regulation depends on the recruitment of RNase H2 to telomeres⁶². In humans, the only study addressing TERRA RNA-DNA hybrids during the cell cycle is from Sagie and colleagues, where no change of the R-loops abundance was observed throughout the different phases¹⁷³. However, a very recent work shows that BRCA1 interacts with TERRA specifically during early S-phase and G2¹⁴⁹. Since this interaction

depends on TERRA RNA-DNA hybrids, it can be assumed that R-loops peak at these two moments of the cell cycle¹⁴⁹.

Beside RNase H2, which degrades the RNA moiety within R-loops, other enzymes negatively affect the levels of telomeric RNA-DNA hybrids. RNase H1, equally able to digest the RNA component of an R-loop, removes RNA-DNA hybrids at telomeres in both yeast and humans^{119,132}. Helicases that unwind the RNA within the R-loop play also a role. FANCM (Mph1 in yeast) resolves telomeric R-loops *in vitro* and *in vivo* in ALT cells while Pif1 has been shown to unwind hybrids only *in vitro*^{127,178}. At telomeres, this ability is proposed to facilitate the detachment of telomerase RNA from the chromosome ends¹⁷⁷. Another helicase potentially involved in telomeric R-loops removal is SETX. This enzyme was recently found to interact with telomeric RNA-DNA hybrids and its depletion caused enhanced expression of TERRA¹⁴⁹. Finally, the THO complex, required for RNA export from the nucleus, suppresses TERRA RNA-DNA hybrids in yeast¹¹⁹.

1.5.4 TERRA in ALT

TERRA and TERRA RNA-DNA hybrids play an important role in the alternative lengthening mechanism of telomeres. The transcript and the hybrids it forms are more abundant in ALT cancer cells than in telomerase-positive cells, thus constituting a hallmark of this cancers type^{132,133,137,154,179}. The source of TERRA upregulation is unknown. Different works suggest that increased transcription rather than impaired degradation account for the upregulation^{132,133}. Supporting this idea, Episkopou and colleagues reported that the less condensed chromatin of ALT telomeres might facilitate the lncRNA transcription¹³³. Interestingly, that study showed that short telomeres in ALT, equally characterized by open chromatin, contribute to the overall high levels of TERRA.

ALT cancer cells are characterized in 90% of the cases by loss of ATRX¹⁵⁴. ATRX is a chromatin remodeler that, along with DAXX, places the histone variant H3.3 at telomeres¹⁵⁴. The absence of the protein is proposed to be an important step in the establishment of ALT, mainly due to the chromatin decompaction and replication impairment it causes¹⁸⁰. Since ATRX inhibits both TERRA and TERRA RNA-DNA hybrids, the protein loss associated with ALT might contribute to the transcript upregulation.^{135,181} This seems to hold true at least for TERRA persistence throughout the cell cycle in ALT cells¹³⁵.

The overexpression of TERRA and the increased formation of RNA-DNA hybrids trigger telomere recombination in ALT¹⁴⁰. This is supported by the observation that repression of TERRA transcription and exposure to RNase H1 impair the ALT phenotype^{132,140}. Since replicative stress was relieved in these conditions, the hybrids might sustain ALT by inducing DNA damage at telomeres^{127,132,140}. Interestingly, accumulation of RNA-DNA hybrids upon RNase H1 depletion did not potentiate ALT but rather weakened it¹³². This dual nature of telomeric RNA-DNA hybrids, both beneficial and detrimental for ALT, was observed also when deleting FANCM¹²⁷. Here, removal of the helicase caused acute R-loops-dependent replicative stress at telomeres while increasing BIR-induced telomere synthesis¹²⁷.

Taken together, these data indicate that although R-loops are important to trigger ALT via replicative stress, they need to be present in a specific amount to prevent cell death¹²⁷. Given the

importance of TERRA and telomeric R-loops for this type of telomere maintenance mechanism, it is reasonable that new anti-ALT therapies will be based on targeting telomere transcription.

2. Rationale

The alternative lengthening of telomeres sustains telomere maintenance in absence of telomerase in 10-15% human cancers¹⁸². The molecular mechanisms underlying its origin as well as perseverance are currently unknown. Changes in the chromatin that impair normal DNA replication at telomeres are believed to represent an important trigger for ALT¹⁸⁰. One of the effects derived from the altered state of chromatin might be the increased TERRA expression and telomeric R-loops formation, frequently associated with the ALT phenotype^{133,154,179}. Despite the increasing amount of data linking the alternative lengthening of telomeres to the abnormal expression of TERRA, several questions remain still open. The main ones are: what is the source of TERRA upregulation in ALT? Is TERRA upregulation a restricted event in time or does it characterize ALT cells indefinitely? If the transcript expression varies in time, what are the factors responsible for it?

In yeast senescent cells, TERRA RNA-DNA hybrids trigger telomere recombination at short telomeres via induction of replicative stress⁶². In human ALT, telomeric R-loops equally promote HDR by causing telomere instability^{127,132,140}. However, it is unknown whether R-loops in ALT trigger HDR at all telomeres or only at a specific subset of them. More importantly, it is yet to be determined whether R-loops in ALT promote all types of HDR at telomeres or a restricted category.

Cells that shorten their telomeres activate DDR and senesce⁷⁵. In ALT, this seems not to apply as yeast survivors keep a proliferative potential comparable to the one of telomerase-positive cells^{24,108}. The reason why ALT cells do not senesce despite telomere shortening is another unsolved puzzle.

In the present study, type II survivors, the yeast equivalent of ALT human cancer cells, were employed to address these interrogatives. This type of survivors is frequently used to study telomere biology in ALT. The evident advantage is the possibility to investigate telomere-related aspects in cell populations derived from single cellular clones, which are less heterogeneous than non-clonal populations. Furthermore, in yeast, the dynamics of single telomeres can be monitored by Southern blot and Telo-PCR with relative ease.

The findings of this study are hoped to contribute to a better understanding of the ALT mechanism, elucidating aspects that might be technically difficult to address in human cells. With a clearer view of how telomeric transcription is involved in ALT, it is expected that more precise therapies will be developed to fight this type of cancer.

3. Results

3.1. TERRA is upregulated in ALT-survivors

TERRA and related RNA-DNA hybrids have been seen to accumulate in ALT-positive cancer cell lines but not in the telomerase-positive HeLa cells^{132,133,137,138}. When TERRA expression is further enhanced in ALT, indications of telomere instability and increased recombination suggest that elevated transcription is detrimental and requires repair for the potential damage caused¹³². Furthermore, telomeric RNA-DNA hybrids seem to be maintained in a precise amount to avoid toxicity¹³².

Indication of the role of RNA-DNA hybrids in ALT-survivors formation in yeast comes from the work of Yu et al., where R-loop accumulation has been seen to anticipate senescence and trigger the onset of survivors¹⁶⁹. Strikingly, removal of RNA-DNA hybrids by RNH1 overexpression completely abolished type II survivors formation¹⁶⁹. Taken together, these data imply that, in spite of a tight control over TERRA R-loops, the genotoxic effect determined by their accumulation may be crucial for survivors escape from senescence and telomere maintenance in ALT. However, both the mechanism and regulation of how TERRA promotes homology-directed repair (HDR) in an established ALT scenario remain elusive.

To dissect in more detail these processes, budding yeast type II survivors were employed. The first task to accomplish was to validate this type of post-senescent cells as a model to study TERRA function in ALT. In particular, survivors were examined to see if they demonstrated the same TERRA upregulation observed in their human counterpart.

3.1.1 ALT-survivors display the typical TRF pattern

Four *tlc1Δ* survivors (A, B, C and D) were independently generated from four different tetrads by cell passaging in liquid culture. After streaking for single colonies, three different colonies from the four survivors were exponentially grown in liquid and their RNA and DNA were isolated for TERRA and telomere profiling, respectively.

As shown in Figure 9A, telomere restriction fragment (TRF) analysis using a radio-labeled CA-probe confirmed that all the survivors used were type II survivors. Indeed, compared to wild-type cells, survivors telomeres presented the typical length heterogeneity characterized by interspersed banding²⁴. A further feature was the presence of critically short telomeres that were positioned below the Y' band of wild-type cells, ranging from around 100 bp to almost no detectable TG-repeats. These telomeres were Y' telomeres, both original and newly formed upon HDR, as validated by a Y' element-detecting probe (Figure 9B). Interestingly, all survivors maintained the same wild-type position of the long Y' element, whose band intensity enhancement in some cases indicated events of Y' translocation (see also the junction PCR later). The short Y' element, instead, did not always appear at the same location as in wild-type cells, thereby suggesting that either modification or loss of it had occurred.

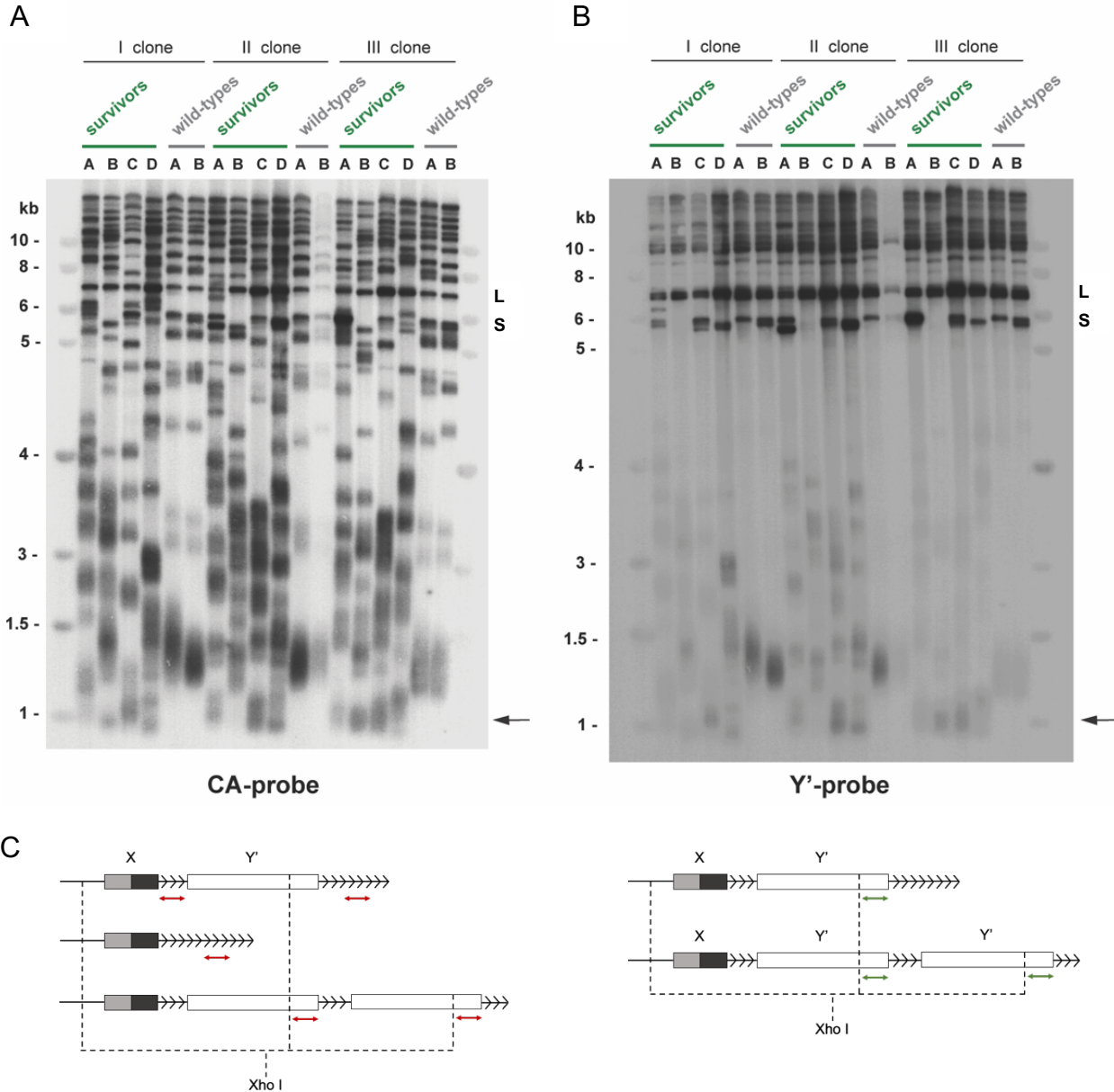


Figure 9. The *tlc1Δ* survivors are type II survivors. A) Southern blot with DNA from three different colonies (clone I, II and III) of four survivors (A, B, C and D) and two wild-types (A and B), which was digested with *Xho*I and separated by agarose gel electrophoresis. Detection was carried out with a CA-probe, which recognizes all TG-repeats. Figure adjusted from Misino et al¹⁸³. B) The CA-probe was stripped from the blot in A) and a Y'-probe detecting all Y' elements was used. "L" and "S" indicate long and short Y' elements, respectively. The arrow at the bottom of each blot points to extremely short Y' telomeres, long less than ~ 300 bp. C) Schematic of the regions recognized by the CA-probe (left panel) and Y'-probe (right panel). "X" stands for X element whereas "Y'" stands for Y' element. The CA-probe (red double arrowhead) recognizes both terminal (black arrowheads at the end of each chromosome) and internal (black arrowheads between an X element and a Y' element or between two Y' elements) TG-repeats. The Y'-probe (green double arrowhead), instead, recognizes the terminal part of Y' elements. The enzyme *Xho*I cuts within Y' elements and other subtelomeric regions. Therefore, the length of each band in the blot is defined by the site where *Xho*I cuts and the extension of telomeres. For more information see also Figure 6.

Single telomere Southern blots for telomere 1L and 15L, two X-only telomeres, revealed that each clone behaved differently when elongating telomeres via HDR, even when deriving from the

same survivor (Figure 10). Confirming the notion that type II survivors present critically short telomeres, some clones showed telomeres 1L and 15L with less than 100 bp. The source of these critically short telomeres is unknown. They can derive from eroding telomeres of previously senescing cells and/or from telomeres that were only slightly elongated during the transition into survivors. In samples with short telomeres, it was frequent to observe HDR products too, from both type II BIR and Y' translocation, suggesting that short telomeres undergo recombinational events (Figure 10A and B).

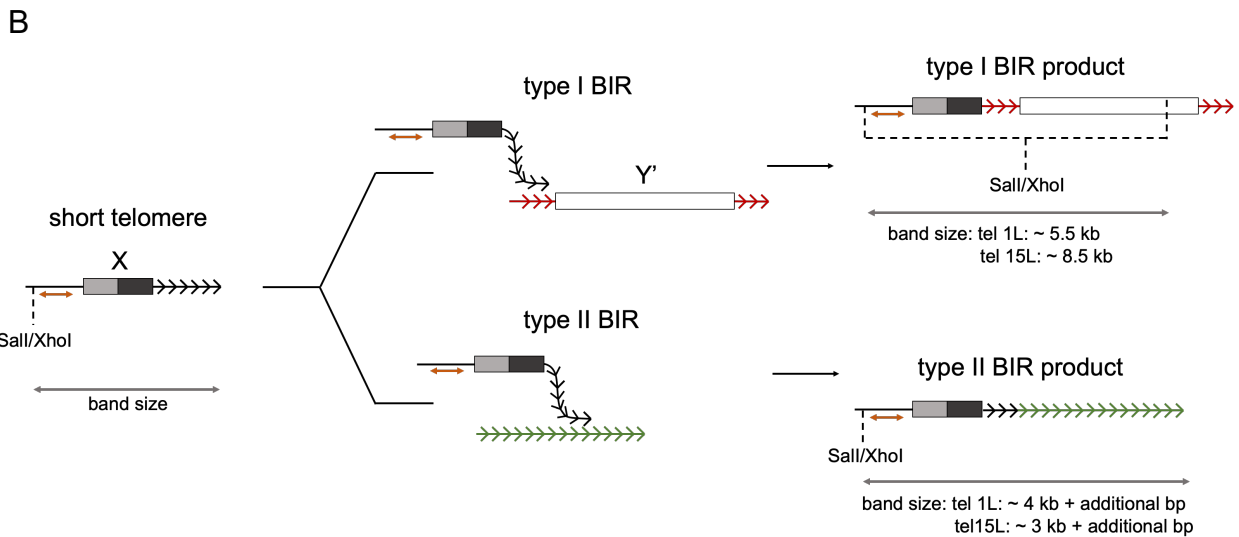
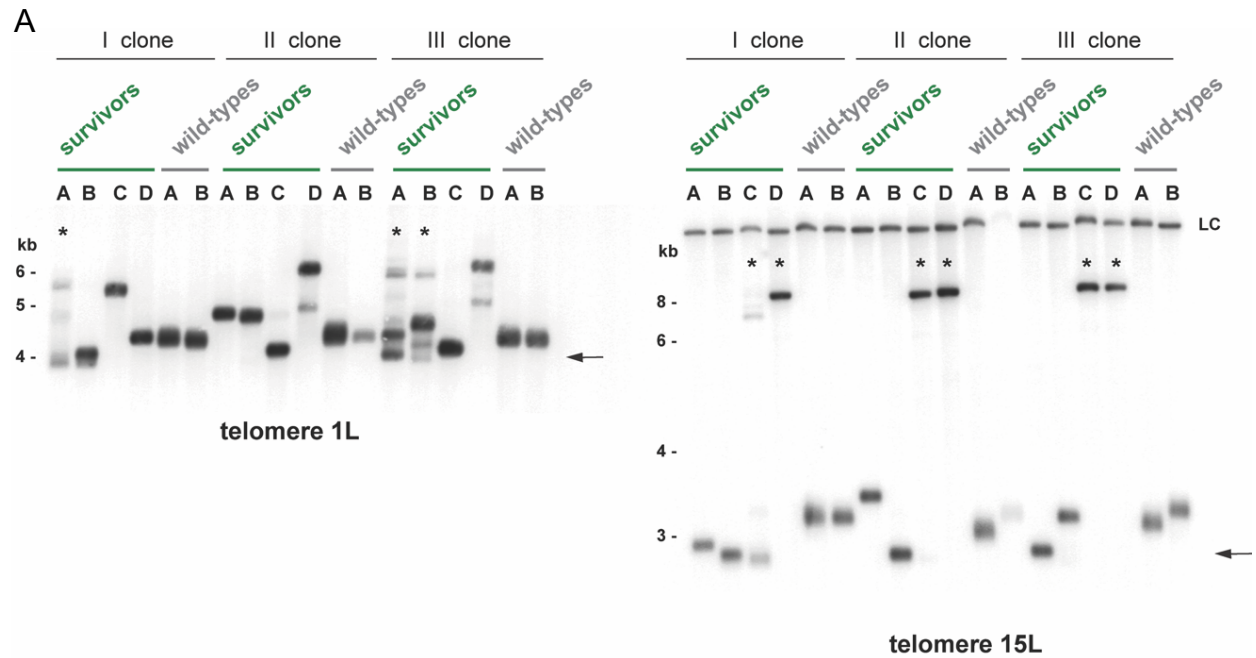


Figure 10. Each survivor presents a different TRF profile for telomere 1L and 15L. A) Single telomere Southern blots for telomere 1L (left) and 15L (right) with the same DNA as used in Figure 9. Genomic DNA was digested with Sall or XhoI to study telomere 1L and 15L, respectively. Each blot was hybridized with a subtelomere-specific probe. The asterisks in the upper part of the blots indicate events of Y' translocation, whereas the arrows at the bottom point to telomeres shorter than 100 bp. "LC" stands for loading control. B) Schematic that represents how 1L/15L short telomeres (black arrowheads) undergo type I (top) or type II (bottom) BIR. In the first case, the short telomere strand invades the internal TG-tracts (red arrowheads) upstream of a Y' element ("Y"). The result of the Y' translocation is a product that contains the X element ("X") from the recipient telomere and the Y' element of the donor telomere. In case of type II BIR, the short telomere strand invades another telomere (green arrowheads) without acquiring a Y' element. The subtelomere-specific probes for 1L and 15L telomeres are indicated as an orange double arrowhead that recognizes the region between Sall/XhoI cut site and the X element. The bands in the Southern blot correspond to the restriction fragments detected by the probes. When no Y' element is acquired, the size of the restriction fragment spans from Sall/XhoI cut site to the terminal TG repeat (short telomere and type II BIR product). For telomere 1L the subtelomeric region from the TG-repeats to Sall cut site is ~ 4 kb long, whereas for 15L the region from the TG-repeats to the XhoI cut site is ~ 3 kb long. Upon acquisition of a Y' element, the restriction fragment recognized by the probes is from the cut site in the region upstream of the X element to the cut site within the Y' element (type I BIR product). In case of telomere 1L, this fragment is ~ 5.5 kb long while for telomere 15L it extends for ~ 8.5 kb.

The presence of multiple bands within the same clone can provide information about the timing of HDR. The presence of HDR products along with the shortest telomere (e.g., survivor A, clone III for 1L and survivor C, clone I for 15L in Figure 10) indicates a recent HDR event, with some cells within the colony elongating the telomere and others still presenting a short one. Conversely, the appearance of HDR products without the shortest telomere (e.g., survivor D, clone II for 1L in Figure 10) suggests a less recent recombinational reaction that probably took place during the first cell divisions of the colony. Here, it is likely that the initial single cell already presented a critically short telomere that was elongated in the next few cell cycles.

Long telomeres were the result of elongation via both type I and type II BIR. During type I BIR, Y' translocation takes place providing telomere 1L and 15L with a single or multiple Y' elements. These Y' elements can be acquired via iterative template switching from one Y' telomere to another or in a single step by using a Y' telomere with an array of Y' elements as substrate (Figure 4B and 7). A combination of the two mechanisms is also possible. Due to the fact that Sall and XhoI, the two enzymes used for detecting telomere 1L and 15L, respectively, cut within the Y' element, it is impossible to discriminate between a single or a multiple acquisition of Y' elements. Indeed, the restriction fragment will always be ~ 5.5-5.7 kb long for 1L and ~ 8.1-8.8 kb long for 15L (Figure 6 and 10B). These fragments are visible in survivor A, clone I, survivor A and B, clone III for 1L and survivor C and D, clone I, survivor C and D, clone II, survivor C and D, clone III for 15L in Figure 10.

When telomeres were elongated by type II BIR, they extended up to >1.5 kb in some cases (e.g., telomere 1L in survivor D, clone II in Figure 10). Different elongation profiles were visible, even within the same clone, suggesting that telomere lengthening via type II BIR can occur to various extents, probably determined by stochastic events, rather than a defined pathway.

Further validation of the Y' translocation on telomere 1L and 15L was obtained by junction PCR with primers recognizing the subtelomeric part of the X-only telomeres and the centromere-proximal part of Y' elements (Figure 11A and B)¹¹⁰.

Taken together, these data indicate that type II survivors can adopt different BIR mechanisms to elongate their telomeres. Y' translocation is one of them and can occur via acquisition of at least one Y' element.

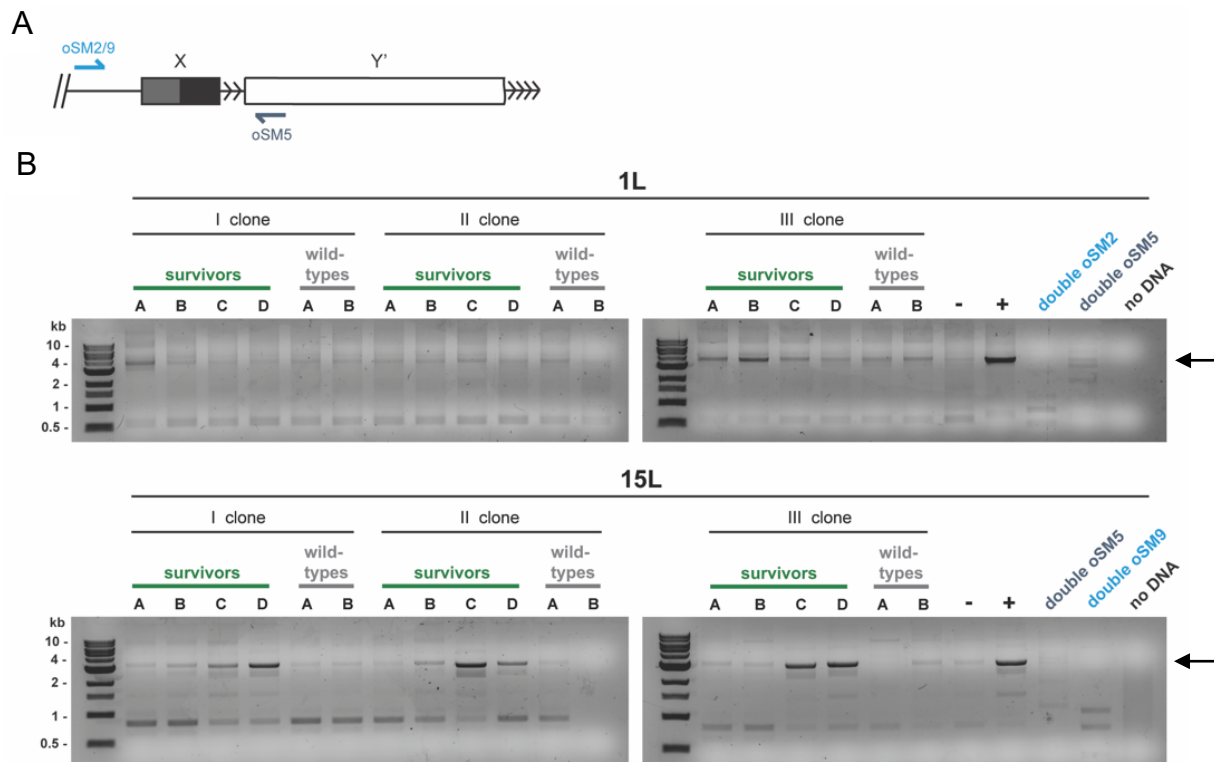


Figure 11. Y' translocation occurs at the X-only telomeres 1L and 15L. A) Schematic of the region recognized by the junction PCR primers. The two grey rectangles indicate the X element while the white one corresponds to the Y' element. The arrowheads represent TG tracts. The primers oSM2 and 9 (blue) recognize respectively the 1L- and 15L-specific subtelomere, whereas oSM5 (grey) binds to the centromere-proximal region of Y' elements. B) Junction PCR was performed with the DNA of Figure 9. In case of Y' translocation, the products size is expected to be ~ 4.5 kb for telomere 1L and ~ 3.5 kb for telomere 15L (arrows on the right). The reaction was carried out also for a negative (-) and positive (+) control, where Y' translocation was expected to be absent or present, respectively. To rule out primer dimers, the PCR reaction was conducted with the DNA from the positive control and only one of the two primers, in a double amount, or two different primers but without DNA. Figure adjusted from Misino et al¹⁸³.

3.1.2 TERRA accumulates in ALT-survivors, similar to human ALT cells

TERRA transcribed from telomere 1L, 15L and 6Y' telomeres was measured in every clone from each survivor and compared to two isogenic wild-type clones (A and B) (Figure 12A)¹⁴⁶. Each survivor displayed a different expression profile, suggesting the presence of multiple regulatory states. However, TERRA levels from all survivors were significantly higher than those from wild-type cells, especially when the transcript was produced from X-only telomeres. On average, this corresponded to a ~ 5 fold increase for telomere 1L and 15L and a ~ 3 fold increase for the 6Y' telomeres over wild-types. A similar phenotype was obtained by Episkopou et al. in human ALT-positive cells when compared to telomerase-positive cells¹³³. Here, the authors reported that the

upregulation of TERRA in ALT varies from one telomere to the other, ranging from a ~ 1- to a 4.5-fold enrichment over telomerase-positive cells.

Since long telomeres produce long TERRA transcripts and human ALT cancer cells present these elongated species, the high levels of TERRA in type II survivors might be due to an increased number of UG₁₋₃ repeats within the RNA^{132,133,150,184}. To rule this out, reverse transcription was carried out by using primers specific for the 1L subtelomere, whose binding is not influenced by the transcript length (Figure 12B). TERRA levels slightly decreased under these conditions but were still significantly higher over wild-type cells. This suggests that type II survivors might accumulate long TERRA molecules and their presence might contribute to the enhanced expression registered (Figure 12C).

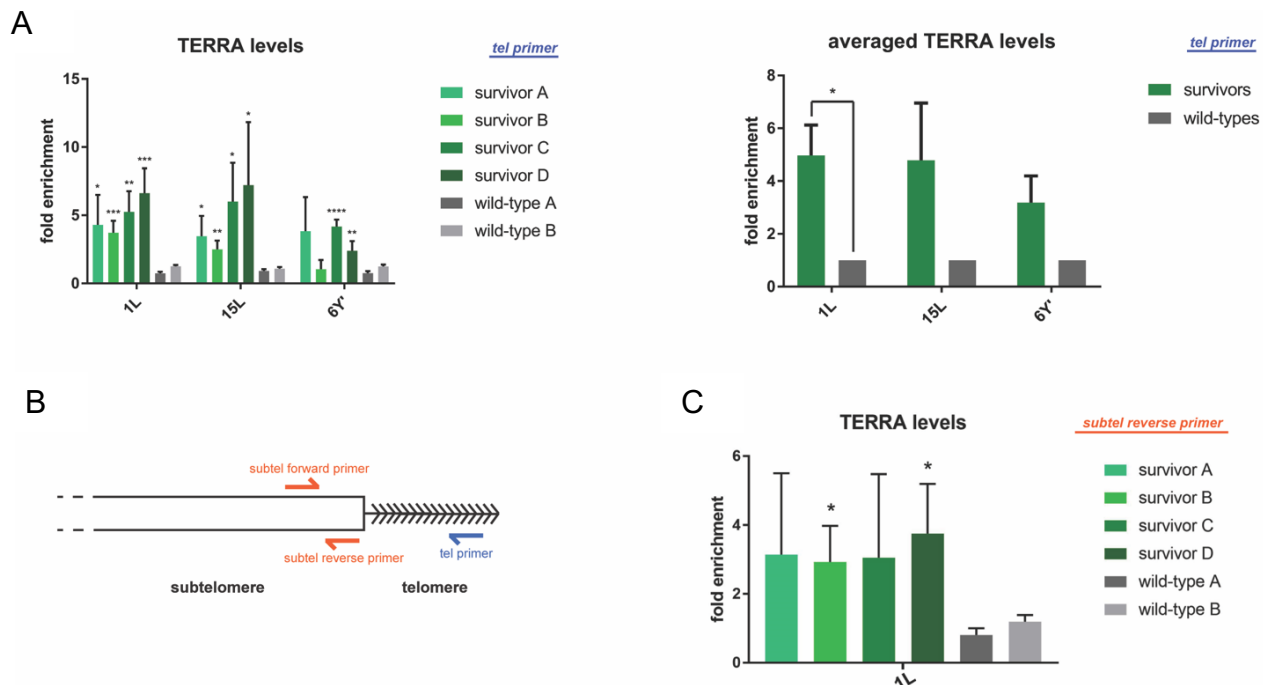


Figure 12. TERRA is upregulated in type II survivors. A) TERRA from telomere 1L, 15L and 6Y telomeres was measured in the same survivors and wild-type cells from Figure 9. Reverse transcription was performed by using a “tel primer” (B), which recognizes the TG tract (arrowheads) of the transcript. On the left, TERRA levels of each survivor were divided by the average amount from wild-type cells to give a fold enrichment over wild-types. On the right, TERRA levels are displayed as the average of the fold change over wild-types calculated in A (right). B) Schematic of the region recognized by primers during reverse transcription and RT-qPCR. In addition to the “tel primer”, a “subtel reverse primer”, which recognizes a specific subtelomere (rectangle), was used for reverse transcription. A pair of “subtel forward primer” and “subtel reverse primer”, specific for 1L, 15L and 6Y subtelomeres, was used in the qPCR reaction to measure TERRA specifically from these telomeres. C) TERRA levels from telomere 1L were measured after reverse transcription was carried out with the 1L-specific “subtel reverse primer” instead of the “tel primer”. The results are presented as mean + SD (n=3). The p values were calculated by using a one-way ANOVA test in A (left) and C. Instead, a Welch’s corrected two-tailed Student’s t test was employed in A (right) (*p<0.05; **p<0.01; ***p<0.001; ****p<0.0001). Figure adjusted from Misino et al¹⁸³.

The fact that Y’ telomeres produced a lower amount of TERRA compared to X-only telomeres is visible not only in survivors but also in wild-type cells and might indicate the existence of two distinct regulatory mechanisms¹⁴⁶. The different chromatin organization of Y’ elements and X elements might be involved in this regulation⁸⁵.

Since TERRA measurements were performed in the same samples used for TRF analysis and junction PCR, it was possible to assess whether the Y' translocation had an effect on X-only telomeres transcription. Analysis of TERRA profiles revealed that acquisition of at least one Y' element did not affect the upregulation over wild-types. This was surprising as Y' telomeres are usually associated with lower amounts of the lncRNA¹³⁸.

In summary, the data here presented show that TERRA is overexpressed in ALT-survivors in a similar manner to human ALT cells. Moreover, X-only telomeres accumulate the lncRNA regardless of Y' translocation.

3.2. TERRA and TERRA-DNA hybrids regulation in ALT-survivors

The previous results indicated that type II survivors replicate ALT human cancer cells in upregulating TERRA and therefore can be further utilized as a model to unravel the underlying mechanism of this dysregulation.

Precedent work highlighted the link between TERRA increase in ALT and the hypomethylation of telomeres¹³¹. This led to the hypothesis that sequence variants within the telomeres might contribute to the lncRNA high levels via loss of heterochromatinization. However, a study that directly tackles the source of TERRA upregulation in ALT is still missing.

3.2.1 Impaired degradation might account for TERRA upregulation in ALT-survivors

Studies in humans showed that ALT telomeres accumulate RNA pol II, suggesting that TERRA accumulation is due to increased synthesis¹³². This fits well with the decondensed chromatin of ALT telomeres, which might facilitate the enzyme loading and processivity¹³³.

As for the potential increased stability of the lncRNA in ALT, the Decottignies lab demonstrated that, upon RNA pol II inhibition, TERRA turnover in ALT is similar to telomerase-positive cells, thus excluding this possibility as a source for upregulation¹³³.

To address if increased transcription and/or compromised degradation of TERRA is responsible for the overexpression during post-senescence, RNA pol II and Rat1 telomeric enrichment was assessed in survivors and compared to wild-type cells. Clones from independently generated ALT-survivors were exponentially grown, crosslinked and processed for ChIP in parallel to wild-types. Both ChIP of RNA pol II, the enzyme form recruited at promoters, and pS2-RNA pol II, the elongating form, revealed that the enzyme is similarly enriched in survivors and wild-type cells at X-only and Y' telomeres (Figure 13). This argues against what observed in humans and suggests the absence of enhanced telomeric transcription in yeast survivors.

Conversely, Rat1 recruitment at telomeres resulted to be slightly lower in survivors compared to wild-types, with a bigger effect at Y' telomeres (Figure 14A and B). The equal recruitment of the protein at the Actin locus indicates that the phenotype was telomere-specific. Overall, both results propose a model where post-senescent survivors accumulate TERRA due to impaired turnover.

Interestingly, wild-type cells seemed to have more Rat1 at Y' telomeres than at X-only telomeres (Figure 14B). Although different from what reported in the literature, this observation might contribute to explain the general low abundance of Y' TERRA⁶³. In survivors, the exacerbated reduction of Rat1 at Y' telomeres might be due to a different telomere and chromatin

composition, unfavorable for the protein binding, and/or to a technical issue. This might originate from the disproportion between the number of Y' elements that can be bound by Rat1 and the Y' translocation-derived increased amount of Y' elements in the input.

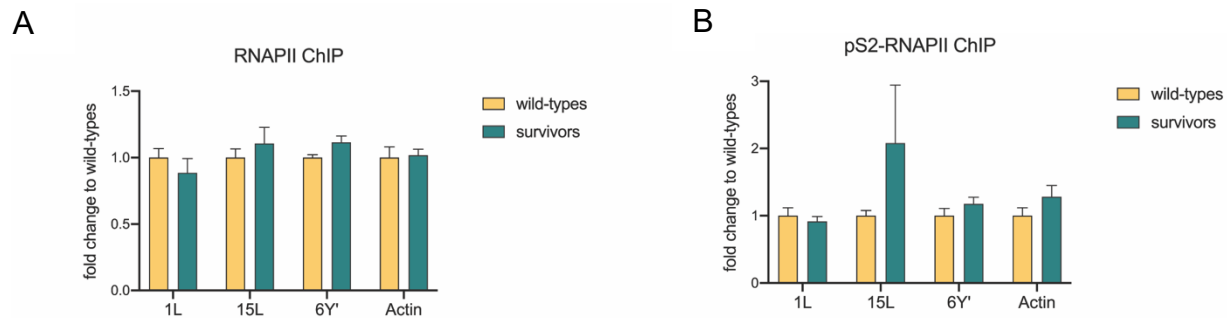


Figure 13. Survivors and wild-type cells present a similar enrichment of RNA pol II at telomeres. A) ChIP for the unphosphorylated version of RNA pol II was carried out in isolates from two different *tlc1Δ* survivors and two isogenic wild-types. The enrichment was detected at 1L, 15L and 6 Y' telomeres and the Actin locus served as positive control. The values are expressed as fold change to wild-type cells and are derived by dividing the “% input” values of each survivor and wild-type clone by the average of the “% input” values of wild-types. B) The same ChIP procedure, as described in A), was applied to detect pS2-RNA pol II, the elongating form of RNA pol II phosphorylated on Ser2 of the CTD repeat. The results are presented as mean + SEM (n=6).

By Western blot, it was possible to monitor the protein levels of both RNA pol II and Rat1. As shown in Figure 14C, the two proteins were synthesized to equal extent in survivors and wild-types. Therefore, the differences in the telomeric enrichment cannot be explained by a dissimilar protein production.

3.2.2 Telomeres in ALT-survivors are bound by less Sir2

Sir2, the enzymatic component of the Sir complex, is responsible along with Sir3 and 4 for histone deacetylation and establishment of telomere heterochromatin⁸³. When the telomeric enrichment of Sir2 was assessed in type II survivors and wild-type cells, the binding of the enzyme was reduced by ~ 50% in post-senescent cells at both X-only and Y' telomeres (Figure 15A). As expected, due to the euchromatic environment of Y' elements, the lowest binding was detected at Y' telomeres regardless of the cell type (data not shown)⁸⁵.

This result suggests that type II survivors, similar to their human counterpart, might present a loss of heterochromatin at telomeres, contributing to TERRA upregulation. However, the absence of enhanced transcription indicates that reduced heterochromatinization in survivors might positively act on TERRA by alternative means to transcription derepression. Equally possible is that survivors, despite the reduction of Sir2, are still able to form a condensed chromatin at telomeres that suppresses transcription.

The phenomenon was restricted exclusively to the chromosome ends as demonstrated by the unchanged recruitment of Sir2 at the mating locus HML. Furthermore, an unequal protein synthesis cannot account for the discrepancies in telomere recruitment as wild-types and survivors presented the same amount of Sir2 (Figure 15B).

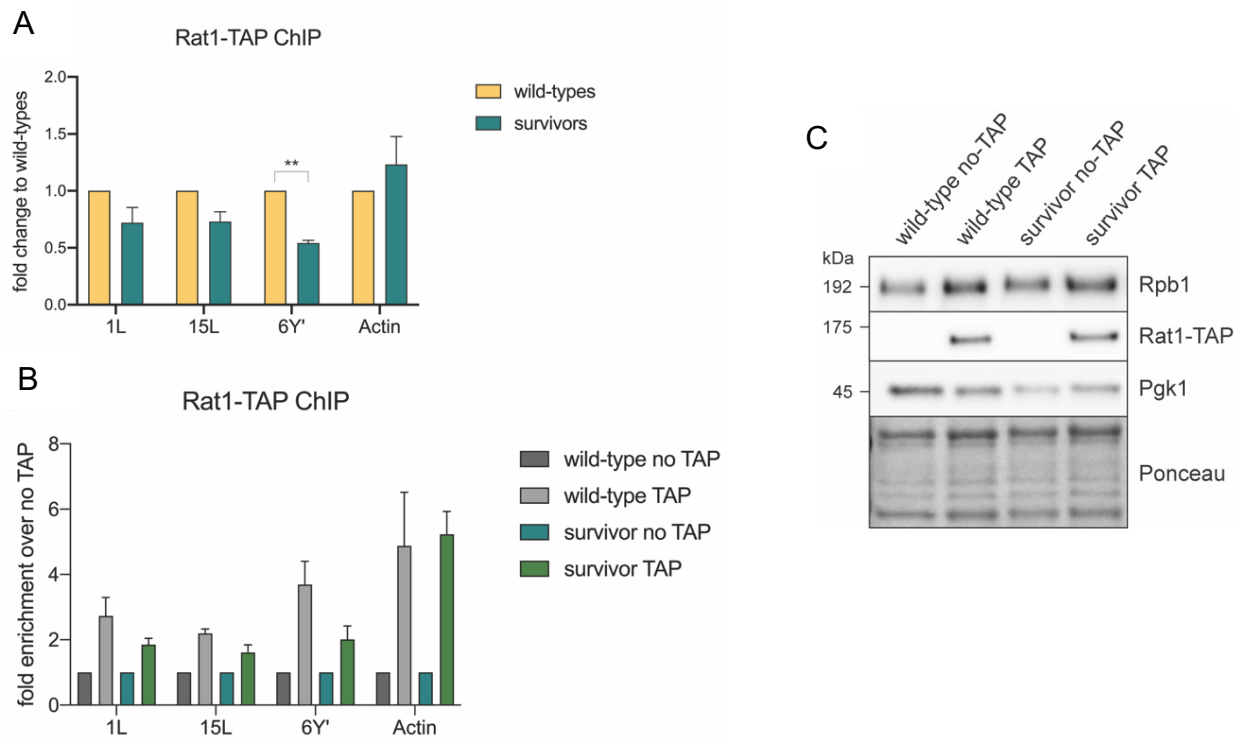


Figure 14. Survivors accumulate less Rat1 at telomeres than wild-type cells. A) ChIP for TAP-tagged Rat1 was conducted in different isolates from tagged and untagged *tlc1Δ* survivors and wild-types. The protein enrichment was detected at 1L, 15L and 6 Y' telomeres and at the Actin locus, used as positive control. The “% input” values of TAP-tagged survivors and wild-type cells were divided by the ones of the untagged survivors and wild-types. The resulting “fold enrichment over no TAP” values (B) were divided by the “fold enrichment over no TAP” of wild-type cells to obtain the displayed “fold change to wild-types”. B) The “fold enrichment over no TAP” is shown. The values were obtained as described in A. C) Western blot for Rpb1, one subunit of RNA pol II, and Rat1 in survivors and wild-type cells with or without the Rat1-TAP tag. Pgk1 levels and Ponceau staining were used as loading controls. The results are presented as mean + SEM (n=3). The p values were calculated by using a Welch’s corrected two-tailed Student’s t test (**p<0.01).

3.2.3 ALT-survivors show impaired binding of RNase H2 to telomeres and active DDR

RNA-DNA hybrids are important triggers of HDR at telomeres^{119,120}. Their repression results in impaired BIR in human ALT and abrogation of type II survivors formation in yeast^{132,169}.

In order to investigate in more detail the role of TERRA R-loops in survivors, a DRIP-qPCR procedure was adopted to measure and compare their levels to wild-type cells. Unfortunately, this approach provided inconclusive results as a general failure in detecting RNA-DNA hybrids was observed in survivors. Alternatively, since RNA-DNA hybrids are removed by RNase H2 at telomeres, the recruitment of the enzyme to these loci was utilized to estimate the R-loops status.

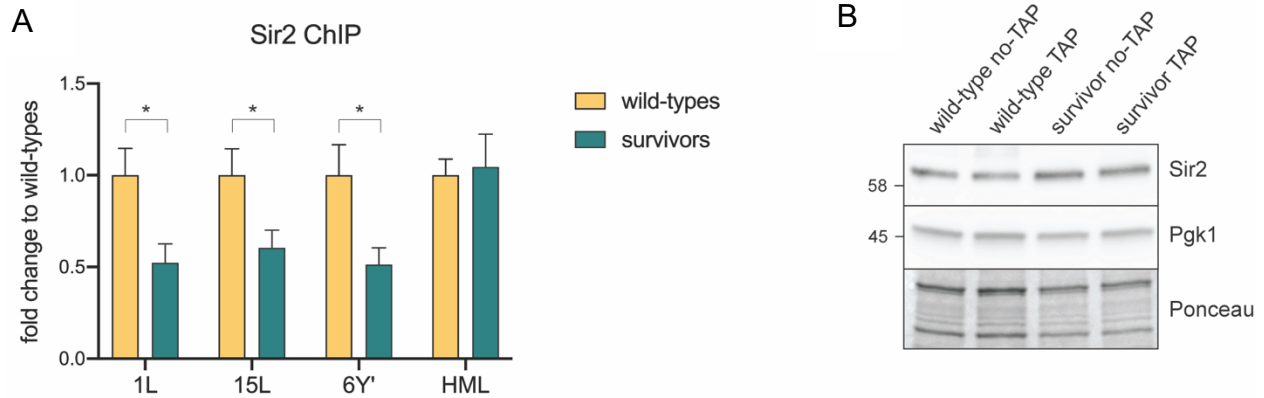


Figure 15. Survivors telomeres are bound by less Sir2 than wild-type telomeres. A) ChIP for Sir2 was carried out in isolates from three different *tlc1Δ* survivors and wild-types. The enrichment was detected at 1L, 15L and 6 Y' telomeres and the mating locus HML served as positive control. The calculation of the fold change over wild-types was conducted as described in Figure 13. B) Western blot to detect the levels of the Sir2 protein in the same Rat1-tagged and -untagged strains of Figure 14C. Pgk1 levels and Ponceau staining were used as loading controls. The results are presented as mean + SEM (n=6). The p values were calculated by using an unpaired two-tailed Student's t test (*p<0.05).

Interestingly, the recruitment of Rnh201, one subunit of RNase H2, to telomeres in survivors was below the background signal of control samples with the untagged protein (Figure 16A). On the contrary, wild-type cells showed an accumulation of Rnh201 at their telomeres. This scenario was not telomere-specific as a general lack of RNase H2 recruitment to non-telomeric loci was detected in survivors, despite the protein levels remained unchanged (Figure 16B).

Together, these data suggest that type II survivors, unlike telomerase-positive cells, might be enriched with R-loops on their telomeres, and genome-wide, due to the lack of binding of RNase H2. However, it cannot be ruled out that other enzymes responsible for the hybrids removal take over.

The potential accumulation of TERRA-DNA hybrids in survivors is reminiscent of human ALT cancer cells, where it can cause HDR as a response to replication stress and/or DSBs^{36,119,120,132}. The fact that type II survivors might activate a broad retention of RNAs onto DNA could indicate that a generalized recombinational status is required, where telomeres can exploit other genomic sequences for maintenance. This mechanism might be similar to the one described in *S. pombe* HAATI survivors or in *D. melanogaster*, in which non-canonical telomere chromatin assembles at the ends¹⁸⁵.

R-loops increase at short telomeres contributes to DDR activation, which delays the onset of senescence via HDR⁶². This was shown by the accumulation of Rad51 at an induced critically short telomere in parallel to the expression of the checkpoint reductase Rnr3 during senescence. In both cases, overexpression of RNH1 diminished the phenotype.

In order to assess if ALT-survivors present an active DDR and if RNA-DNA hybrids participate to it, the cell cycle profile was assessed in conjunction with Rnr3 expression in the presence and absence of R-loops. As expected, survivors, but not telomerase-positive cells, displayed a mild arrest in the G2-phase of the cell cycle, suggesting an ongoing checkpoint activation (Figure 17A). In support of this, Rnr3 expression was only detected in post-senescent cells (Figure 17B). Interestingly, no reduction of the protein expression was observed upon R-loops removal

indicating that either RNA-DNA hybrids are not the cause of checkpoint induction or adaptation to R-loops-mediated DNA damage took place in survivors. A similar result was obtained when detecting Mrc1 phosphorylation, an indicator of replication stress. ALT-survivors showed a mild activation of the replication stress checkpoint but no change was visible when RNH1 was overexpressed (Figure 17C). Overall, these data demonstrate that type II survivors in unchallenged conditions activate a DNA damage checkpoint that is insensitive to the amount of R-loops.

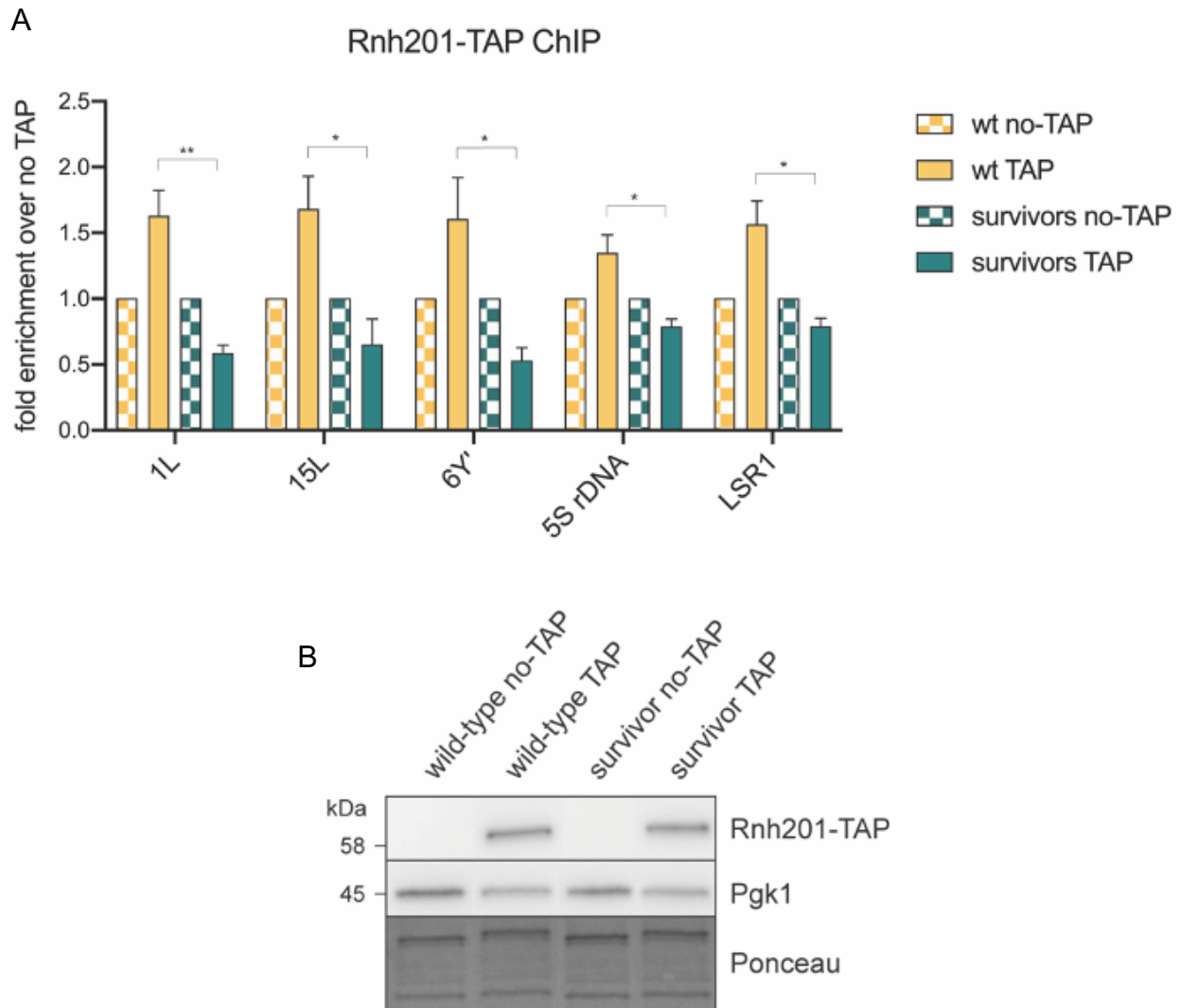


Figure 16. Rnh201 binding in survivors is impaired at telomeres and other loci. A) Two different ChIP approaches were used to measure Rnh201-TAP enrichment in three isolates (here represented) from two different tagged and untagged *est2Δ* survivors and wild-types. The protein binding was detected at 1L, 15L and 6 Y' telomeres while the 5S rDNA locus and the LSR1 gene were used as positive control. The calculation of the “fold enrichment over no TAP” was conducted as described in Figure 14. B) “The fold enrichment over no TAP” values were obtained as described in Figure 14. C) Western blot for Rnh201-TAP in tagged and untagged survivors and wild-type cells. Pgk1 levels and Ponceau staining were used as loading controls. The results are presented as mean + SEM (n=3). The p values were calculated by using an unpaired two-tailed Student’s t test (*p<0.05; **p<0.01).

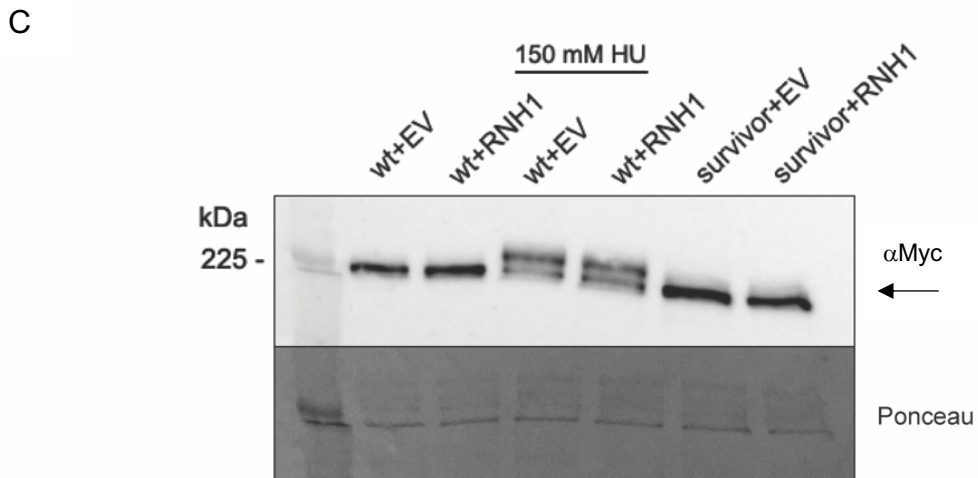
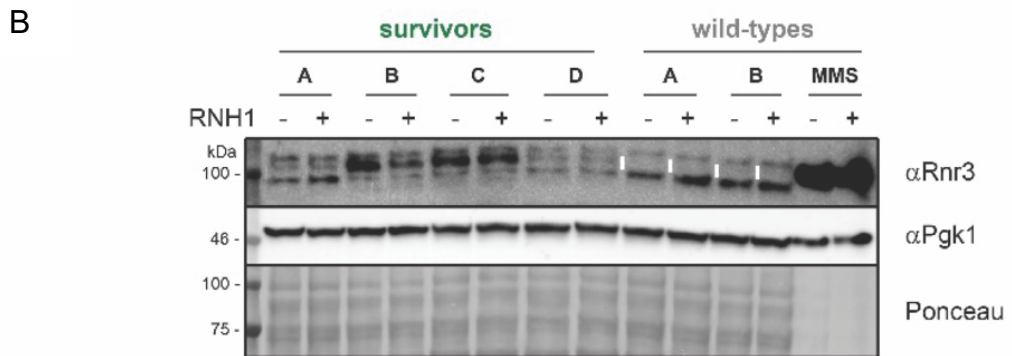
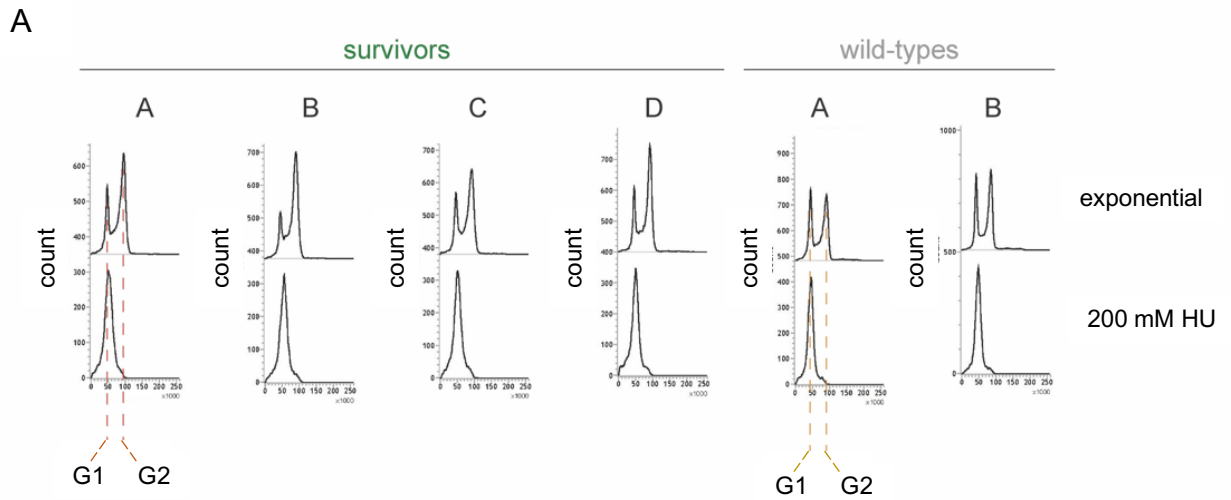


Figure 17. Survivors present a mild checkpoint activation. A) DNA content was measured by FACS in four *tlc1Δ* survivor clones and two wild-type clones in exponentially growing cultures. To validate the efficiency of the approach, DNA content was also measured in cells arrested in early S-phase with 200 mM HU. The two peaks of the FACS profile of exponential cells represent the DNA content of cells in G1 and G2 phase. B) Western blot for Rnr3 in 4 survivors and 2 wild-types, in the absence (RNH1+) or presence (RNH1-) of RNA-DNA hybrids. A wild-type strain treated with MMS was used as positive control. The white small rectangles within the blot represent the place where Rnr3 bands were expected to be in wild-type cells. Pgk1 levels and Ponceau staining were used as loading controls. C) Western blot for Mrc1-myc in survivors and wild-type cells in the absence (RNH1) and presence (EV) of RNA-DNA hybrids. Wild-type cells treated with 150 mM HU were used as positive control. The arrow points to phosphorylated species of Mrc1. Ponceau staining was used as loading control. In B) and C) RNH1 indicates the presence of a plasmid overexpressing RNase H1. EV stands for empty vector.

3.2.4 TERRA expression is cell cycle regulated in ALT-survivors

TERRA and TERRA RNA-DNA hybrids display a cell cycle-dependent regulation in both yeast and human telomerase-positive cells^{62,135}. In *S. cerevisiae*, the transcript is poorly enriched in G1 and peaks in early S-phase. As replication approaches the chromosome ends, TERRA expression progressively declines, being almost halved compared to the beginning of S-phase⁶². This regulation is mediated by Rat1 recruitment at telomeres. In ALT human cells, the cell cycle regulation of TERRA is abrogated, as shown by the absence of changes in the RNA levels between S- and G2-phase¹³⁵. The lack of TERRA reduction at the end of replication is due to ATRX loss.

To see if TERRA overexpression in type II survivors derives from an impairment of the cell cycle regulation, survivors were arrested in different cell cycle phases followed by the lncRNA measurement. α -factor was employed to arrest the cells in G1, whereas 200 mM and 75 mM hydroxyurea were used to block the cells in early and late S-phase, respectively. As expected, wild-type cells recapitulated the cell cycle-dependent fluctuations of the transcript previously published: TERRA was low in G1, peaked in early S-phase and diminished by 38% at telomere 1L and 20% at telomere 15L at the end of replication (Figure 18). Surprisingly, survivors displayed the same profile, indicating that TERRA expression is cell cycle regulated in post-senescent cells. In this case, TERRA dropped by 34% and 33% at telomere 1L and 15L, respectively, when passing from early S-phase to late S-phase. Despite having the same regulation, type II survivors presented higher TERRA levels than wild-types in every cell cycle phase.

These observations point out that an impaired control of the RNA expression during the cell cycle is not the source of increased TERRA levels in ALT-survivors. Rather, a trigger taking place throughout the entirety of survivors cells life or happening in one specific moment with long-lasting effects might be more likely the cause. This would fit with the lower recruitment of Rat1 at survivors telomeres. The protein binding during late S-phase determines TERRA decline but is insufficient for a reduction to wild-type levels. With the transcript persisting, it is plausible that it perseveres within another cell cycle, being abundant in G1 and adding up to the newly formed molecules of the next early S-phase.

Alternatively, TERRA might be overtranscribed in survivors during early S-phase and last throughout the following phases and the next cycle because of impaired degradation. To fit this with the missing increase of RNA pol II ChIP signal in survivors, it is possible that, since S-phase cells represent a small portion of the asynchronous cultures used for immunoprecipitation, the enrichment was simply undetectable.

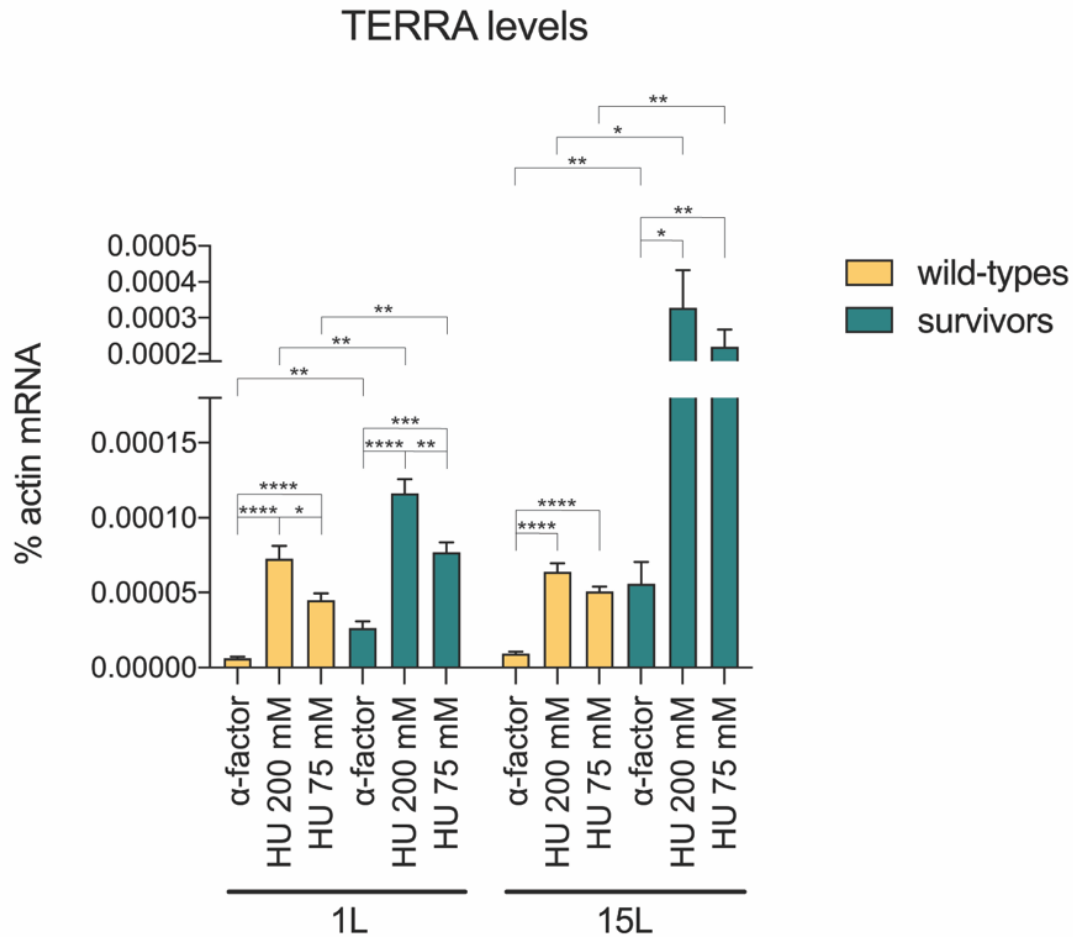


Figure 18. TERRA is cell cycle regulated in survivors. TERRA was measured in isolates from two different *tlc1Δ* survivors and wild-types when arrested in different cell cycle phases. α -factor was used to arrest the cells in G1, whereas different concentrations of hydroxyurea (HU) were employed to arrest the cells in different parts of the S-phase. 200 mM HU arrested the cells in early S-phase and 75 mM HU blocked them in late S-phase. The amount of TERRA is expressed as percentage of the actin mRNA. The results are presented as mean + SEM (n=6). The p values were calculated by using an unpaired two-tailed Student's t test (*p<0.05; **p<0.01; ***p<0.001; ****p<0.0001).

3.2.5 High levels of TERRA originate from short telomeres in survivors

TERRA expression is shaped by the telomere length in both humans and yeast. In humans, long telomeres repress transcription by enhanced H3K9 trimethylation and HP1 α recruitment, which contribute to the formation of heterochromatin¹⁵⁰. Short telomeres, on the other hand, upregulate TERRA due to a more decondensed state. This regulation seems to apply to ALT cells too as short telomeres have been seen to contribute to the transcript overall increase. However, because of a general lack of chromatin compaction it is plausible that short telomeres are not the sole source of high TERRA¹³³.

Similar to humans, yeast TERRA expression inversely correlates with telomere length. This is particularly evident in senescent cells, where the transcript and R-loops accumulate in response to telomere erosion⁶². It was proposed that TERRA upregulation depends on diminished

degradation rather than enhanced transcription. This is due to the progressive loss of telomeric repeats and proteins by which Rat1 is recruited⁶².

Due to the similarities with TERRA regulation in survivors, it was tempting to speculate that the transcript increase in post-senescent cells is caused by restricted degradation at critically short telomeres, which frequently appear in TRF blots.

To test this hypothesis, the telomerase RNA component TLC1 was reintroduced in *tlc1Δ* type II survivors to allow elongation of short telomeres, followed by TERRA quantification. As control, cells were transformed with an empty vector (EV). The efficiency of telomerase reintegration was monitored by measuring TLC1 RNA levels. The procedure worked, as demonstrated by the presence of TLC1 levels comparable to wild-types and by elimination of the short telomeres (Figure 19A and B, respectively).

When checking TERRA, wild-type cells showed expectedly no changes in the expression profile upon introduction of exogenous TLC1 (Figure 19C). Conversely, ALT-survivors presented a ~ 50% drop in some cases, suggesting that the presence of short telomeres contributes to the post-senescence-related TERRA upregulation (Figure 19C). Like in humans, the extent of reduction varied among telomeres, being the lowest at Y' telomeres, and survivors isolates¹³³. The observation that some survivors kept displaying higher levels of the transcript than wild-type cells after telomerase restoration indicates that additional mechanisms participate to the upregulation, regardless of the telomere length (Figure 19C).

Generally, these data repropose what observed in human ALT cancer cells: short telomeres take part in TERRA upregulation.

3.2.6. ALT-survivors do have a telomere length-dependent regulation of TERRA

3.2.6.1 TMM via ALT includes elongation and shortening phases

To further confirm the possibility that post-senescent cells accumulate TERRA at short telomeres, single telomeres were followed in conjunction with the lncRNA as they shortened over several population doublings (PDs). After the first restreak, single survivor clones were propagated in liquid medium by daily dilutions. A wild-type clone was passaged in parallel.

In one of the survivors tested, the initial length of telomere 1L and 15L was ~ 1 kb and ~ 0.6 kb, respectively (Figure 20). In both cases, the shortest extension detected was after 352 cell divisions and corresponded to almost no telomeric repeats detected. Similar to what is reported in literature, shortening was gradual, with no abrupt events, and proceeded at an average rate of ~ 2.6 bp/PD for telomere 1L and ~ 3 bp/PD for telomere 15L¹¹¹. Although a steady decline characterized longer TG tracts, telomeres shorter than the wild-type length appeared to reduce their shortening rate.

At this stage, both type I and type II BIR took place, thus confirming the notion that short telomeres in survivors undergo HDR^{111,186}. In either case, elongation was a one-step process, as described by Teng et al¹¹¹. While type I BIR was evident as the typical banding of Y' translocation at the top of the blot (PD 352 for telomere 1L and PD 238-464 for telomere 15L in Figure 20), type II elongation produced smears of various sizes, ranging from ~ 0.1 kb to ~ 1 kb, and only occasionally single bands (PD 352 for telomere 1L and PD 238-464 for telomere 15L in Figure 20). As expected, due to the cut of XhoI within the Y' elements, telomere shortening was undetectable

after Y' translocation (Figure 6 and 10B). In contrast, when telomeres were elongated by type II BIR, they progressively shortened. This indicated that TMM in ALT-survivors comprises cyclic periods of elongation and shortening.

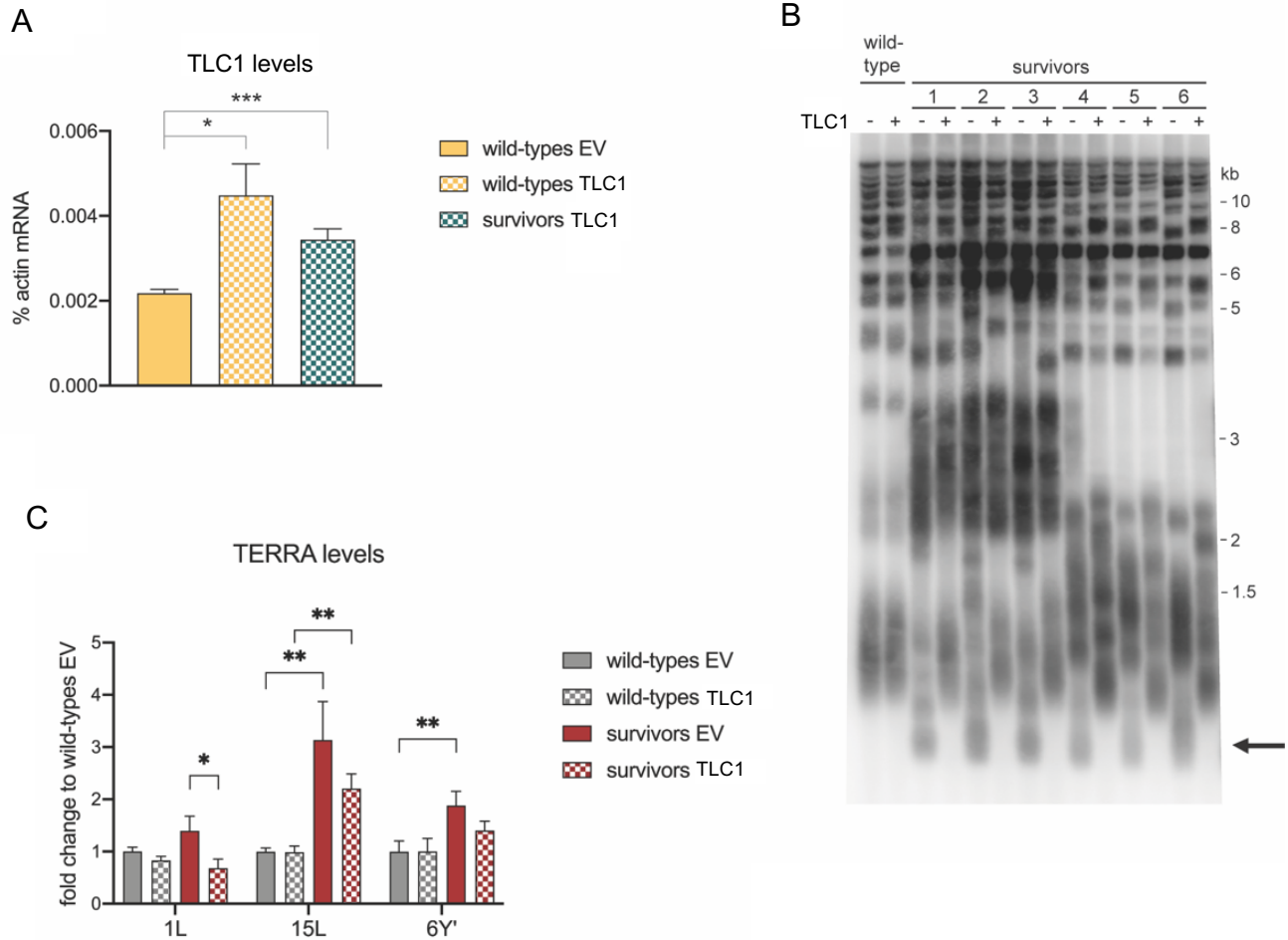


Figure 19. High levels of TERRA originate from short telomeres in survivors. A) TLC1 levels were measured in isolates from wild-types and *tlc1Δ* survivors after transformation with an empty vector (EV) or a plasmid expressing the RNA. The amount of TLC1 was normalized by the one of actin mRNA. B) Southern blot for all telomeres (CA-probe) from the survivors and wild-type used in A. DNA was prepared as described in Figure 9. "TLC1 +" and "-" indicates respectively the presence or absence of the exogenous telomerase RNA. The arrow at the bottom points to the population of short telomeres. C) TERRA levels measured in survivors and wild-types from A and B, in the presence and absence of exogenous TLC1. TERRA was first normalized by actin mRNA and the resulting values were divided by the average of TERRA levels from wild-types transformed with EV. The results are presented as mean + SEM (n=5/6). The p values were calculated by using an unpaired two-tailed Student's t test (*p<0.05; **p<0.01; ***p<0.001).

In the 15L telomere TRF blot, a pattern recurrent in survivors was visible: multiple bands of long telomeres within the same lane (see also Section 3.1.1). This occurs when cells with critically short telomeres simultaneously extend their TG tracts to different degrees or when freshly elongated telomeres mix with previously elongated telomeres.

To get a glimpse of the minimum length a telomere can reach before HDR-mediated extension, the Y' translocation products of telomere 1L from a similar experiment were sequenced (data not shown). Strikingly, the TG tract sitting between the 3' part of 1L subtelomere and the 5' region of the Y' element was ~ 40 bp long (Figure 4). This indicated that the short 1L telomere that strand invaded the internal TG repeats of a Y' telomere was 40 bp long or shorter, corroborating the idea that survivors, like senescent cells, engage HDR at extremely short telomeres^{45,110,111,119}.

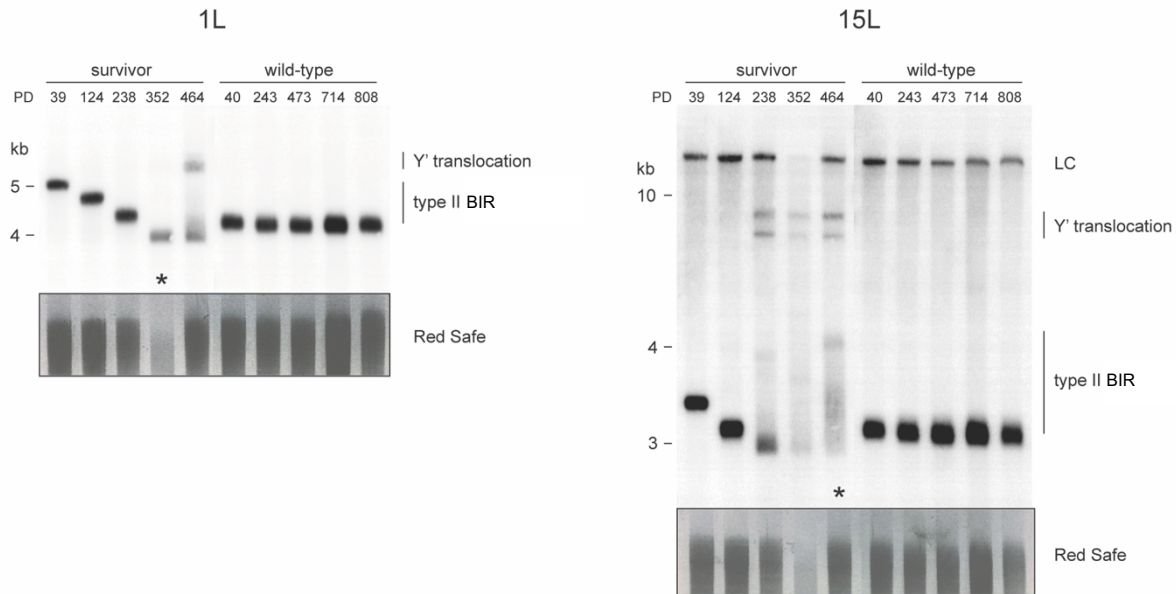


Figure 20. Survivors telomeres shorten gradually to abruptly extend. The Southern blots for telomere 1L and 15L were prepared by using the same subtelomere-specific probes as in Figure 10. DNA was obtained from a single survivor and wild-type clone propagated over multiple population doublings (PDs), digested with *Sall* (for telomere 1L) and *XhoI* (for telomere 15L) and separated by gel electrophoresis. The two types of recombination are indicated on the right of each blot and correspond to the two types of BIR illustrated in Figure 10. Y' translocation is the result of type I BIR and consists of the acquisition by telomere 1L and 15L of at least one Y' element. Type II BIR, instead, promotes telomere lengthening without Y' elements acquisition. The asterisk indicates the shortest telomere and the time point where the peak of TERRA expression was registered (Figure 23). The RedSafe staining worked as loading control along with the uppermost band in the blot for telomere 15L (LC, loading control).

To evaluate the real extent of elongation when telomeres acquire Y' elements, Southern blotting can be performed with genomic DNA digested by *PvuII*. Since this enzyme does not cut within Y' elements, it is possible to appreciate the Y' translocation products in their entirety, from the X element to the very end (Figure 21A). With this in mind, a survivor telomere 15L was monitored over multiple PDs by TRF analysis after *XhoI*- or *PvuII*-mediated DNA digestion.

When employing *XhoI*, the Southern blot showed Y' translocation throughout the entire experiment, as demonstrated by the persisting banding at 5.5 kb (Figure 21B). This indicated that upon the survivor emergence from senescence, the short 15L telomere acquired at least one Y' element. When *PvuII* was used, more details regarding the Y' elements acquisition and perseverance were revealed. The intense band formed at ~ 9.9 kb (restreak 1) suggested that a single short Y' element, presumably followed by a ~ 300 bp long TG tract, was acquired during the survivor formation (Figure 21C). On the other hand, bigger bands indicated acquisition of

either long/short Y' elements plus a long telomere or long Y' elements alone. Shorter bands implied translocation of truncated Y' elements.

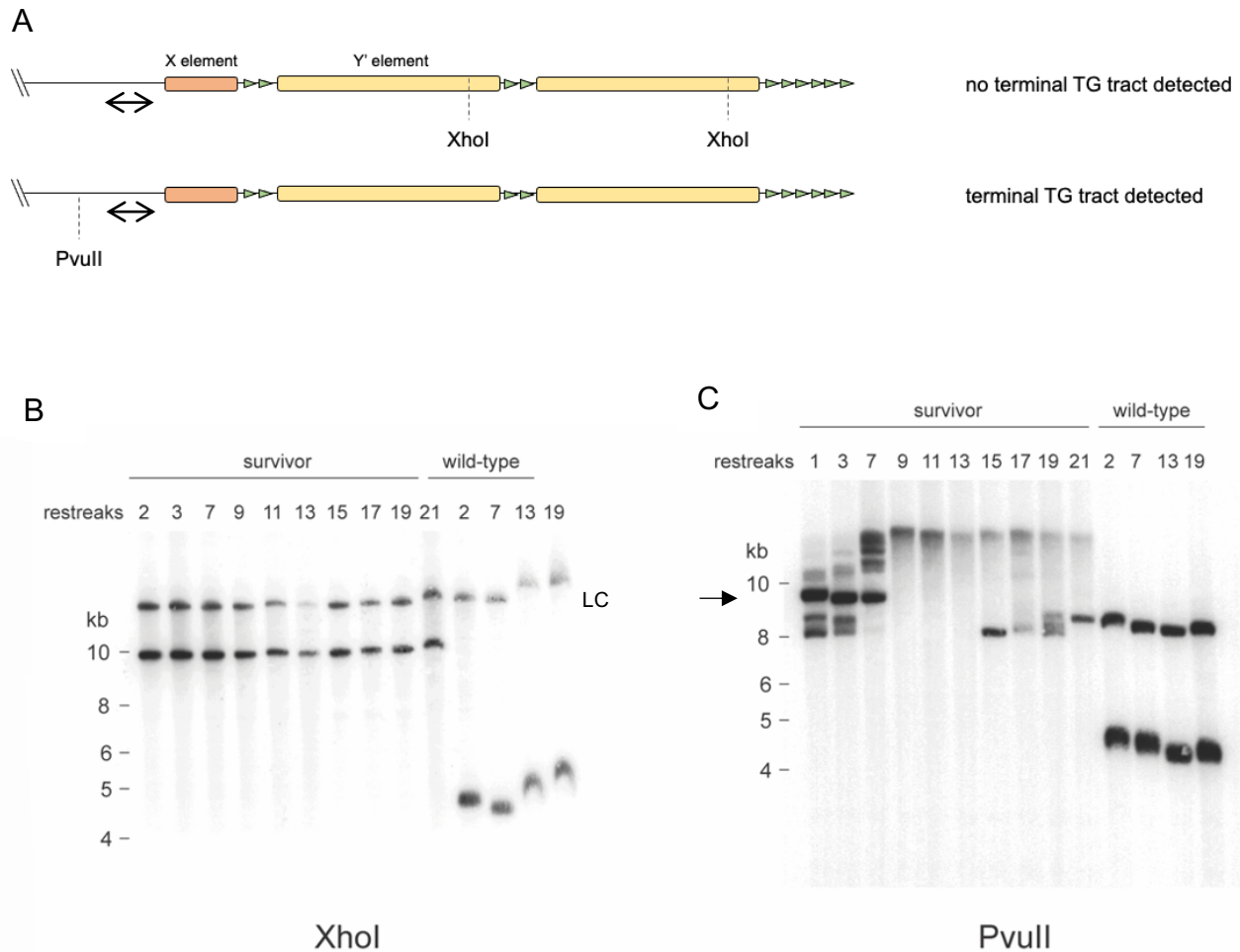


Figure 21. Telomere shortening can be visualized also after Y' translocation. A) Schematic of the cutting site of XhoI and PvuII on Y' telomeres. Since PvuII does not cut within Y' elements, terminal TG-repeats loss can be visualized on Southern blots. The double arrowheads indicate the site where the 15L subteloemere-specific probe binds. B) Southern blot for telomere 15L with XhoI-digested DNA from a single *tlc1Δ* survivor and wild-type clone restreaked on solid medium for multiple generations. "LC" stands for loading control. C) The same DNA was digested with PvuII and used for another 15L-specific Southern blot. The arrow indicates the point when the shortest telomere accumulates and recombines.

As expected, the Y'-containing telomere 15L shortened for three restreaks before being anew extended (Figure 21C). The new HDR event occurred to different extents and added more than ~ 5.6 kb long terminal DNA, presumably after exhausting the telomeric part downstream of the Y' element. Interestingly, the longest BIR product was the dominant form and kept shortening with no further lengthening, thus suggesting that a long telomere was inserted. Unfortunately, with this experimental setup, it is impossible to discriminate whether the HDR reaction comprised the acquisition of the long telomere alone or in combination with extra upstream Y' elements.

After eight restreaks from the elongation event (restreak 15, Figure 21C), an abrupt shortening was observed in parallel to the gradual telomere erosion. This was probably due to telomeric rapid deletion (TRD), a phenomenon occurring during the telomere shortening of type II survivors¹¹¹. Extension took place after two additional restreaks.

Similar to these TRF patterns, other survivors showed progressive shortening of telomere 1L and 15L followed by type I and II BIR. It was very common to observe that type I BIR becomes the major means of TMM in ALT-survivors cultured for several population doublings (Figure 22). This is probably due to the increased availability of Y' elements.

In some cases, a mixed population of cells adopting Y' translocation and type II BIR was visible since the very beginning of the clonal expansion (15L in Figure 22B and 1L in Figure 22C). This further sustained the concept that either HDR pathway is equally probable not only during type II survivors maintenance but also during their formation¹¹⁰. When type II BIR was adopted during emergence of survivors, the initial telomere length was rarely the same across the four survivors tested (Figure 20 and 22). Some presented telomeres in the range of wild-type length (telomere 1L at PD 39 and telomere 1L at PD 11 in Figure 22A and C, respectively), or even shorter (telomere 15L at PD 39 in Figure 22B), and some had extremely long telomeres (e.g., telomere 1L at PD 39 in Figure 20). The same was observed when short telomeres in established type II survivors were extended: the degree of elongation varied very often among survivors. This argues that telomere lengthening via HDR is a stochastic event during both survivors generation and maintenance.

Overall, these data propose a model where telomeres shorten in ALT-survivors regardless of the presence of Y' elements. When a critically short telomere forms, BIR takes place to re-extend it.

3.2.6.2 TERRA expression gradually increases as telomeres shorten

TERRA levels were monitored throughout the clonal propagation, at points where 1L and 15L telomere length varied. In all survivors tested, the transcript expression presented an inverse correlation with telomere length: TERRA levels gradually increased as telomeres shortened peaking at the shortest telomere (Figure 23). This enhancement was significant and ranged between a ~ 2 and a 40 fold increase over long telomeres (Figure 23E). Once lengthening had occurred, TERRA levels declined to a degree similar to the initial long telomeres. This strongly suggested that repression of TERRA expression is increasingly alleviated in response to telomere erosion and re-established when telomeres extend.

It was frequently observed that in order for TERRA expression to be measured at its maximum, a specific number of cells was required to accumulate the shortest telomere. This was evident when mixed populations occurred. In a mixed population like the one of the survivor in Figure 20 at PD 238, cells already harbored the shortest telomere 15L but additional ~ 110 PDs were required to detect the highest level of the transcript (Figure 23A). This was because the fraction of cells bearing the shortest terminus in the population was presumably smaller than the one at PD 352.

The same concept can be applied to explain why TERRA levels diminished upon HDR in a population still containing cells with the shortest telomere. In this case, part of the cell fraction highly expressing TERRA was replaced by cells that elongated their shortest telomere and downregulated the lncRNA. As a result, the total amount detected turned out to be decreased.

Overall, this shows that the total amount of TERRA measured corresponds to the sum of RNA quantities derived from different fractions of a composite cell population. When the bulk of cells presents the shortest telomere, a remarkable enhancement of TERRA can be detected.

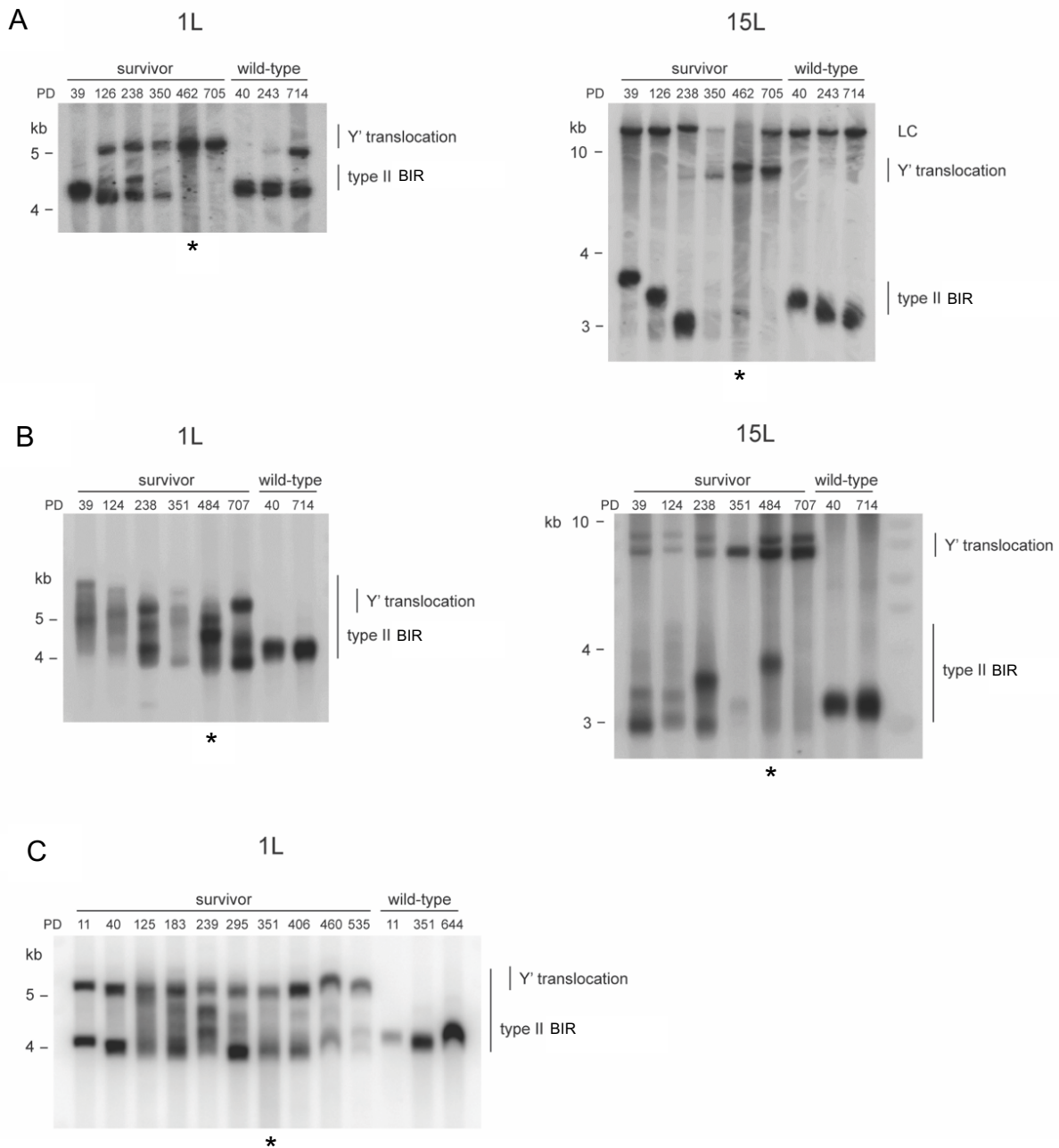


Figure 22. Different survivors display a similar shortening-lengthening profile. A, B and C represent the Southern blots for telomere 1L and 15L from three different *tlc1Δ* survivors propagated in liquid culture over multiple population doublings (PDs). DNA was digested with *Sall* and *XhoI* to study telomere 1L and 15L, respectively. Y' translocation indicates type I BIR-dependent acquisition of at least one Y' element on telomere 1L and 15L. On the other hand, type II BIR indicates lengthening events without acquisition of Y' elements. For more details see Figure 10. The asterisks indicate the shortest telomere and the time point where the peak of TERRA expression was registered (Figure 23). "LC" stands for loading control.

When comparing TERRA levels in survivors with wild-type cells at different time points of the clonal propagation, it was evident that, in the presence of long telomeres, post-senescent TERRA levels did not always exceed the ones of telomerase-positive cells. Therefore, the hypothesis that TERRA upregulation arises from the presence of short telomeres in ALT-survivors was further confirmed.

Taken together, these data show that ALT-survivors too adopt a telomere length-dependent regulation of TERRA with the transcript accumulating at the shortest telomere. Since this increase might reflect an enhanced abundance of telomeric RNA-DNA hybrids, it is possible that ALT-survivors, like senescent cells, activate HDR at short telomeres in response to R-loops-dependent genome instability⁶².

3.3. Post-crisis senescence: replicative potential does fluctuate in ALT-survivors

Given the similarities between ALT-survivors and senescent cells in terms of telomere maintenance, TERRA regulation and checkpoint activation, it was tempting to think that likewise survivors experience a loss of replicative potential during telomere erosion and regain it upon HDR. Previous studies have proposed that fluctuations in cells viability after senescence are a characteristic of type I survivors and only rarely of type II survivors, whose growth rate is normally stable and similar to wild-types^{24,108,111,187}. In these studies, however, a senescence phenotype in type II survivors might have been undetectable due to the following reasons: 1) viability assays were performed only for shortly-propagated survivors, whose telomeres were presumably too long to induce senescence; 2) growth kinetics were monitored on solid medium, insensitive to little viability variations; 3) propagation in liquid was not monoclonal thus allowing the outgrowth of non-senescent cells over the senescing ones.

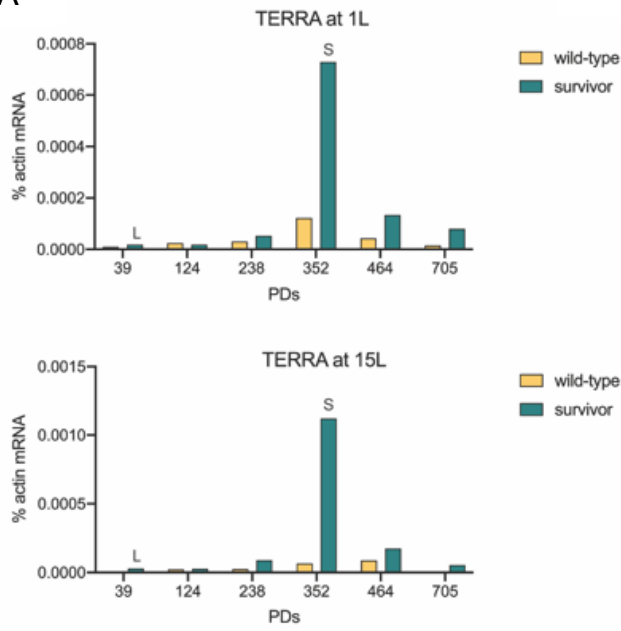
In order to identify a senescence phenotype in post-crisis cells, single clones of established type II survivors were isolated on solid medium and propagated in liquid via daily dilutions over several population doublings. The replicative potential of these cells was calculated from the optical density of each culture measured every 24 hours.

Strikingly, the majority of ALT-survivors displayed a progressive loss of proliferative potential that was then gradually reacquired (Figure 24A and data not shown). The extent and the occurrence time of these fluctuations varied among survivors. The reduction of replicative potential ranged between ~ 16% and an ~ 83% whereas the occurrence time of the lowest potential point varied between 68 PDs (population doublings) and 210 PDs. This variability suggested the presence of an underlying stochastic mechanism, such as telomere lengthening and shortening.

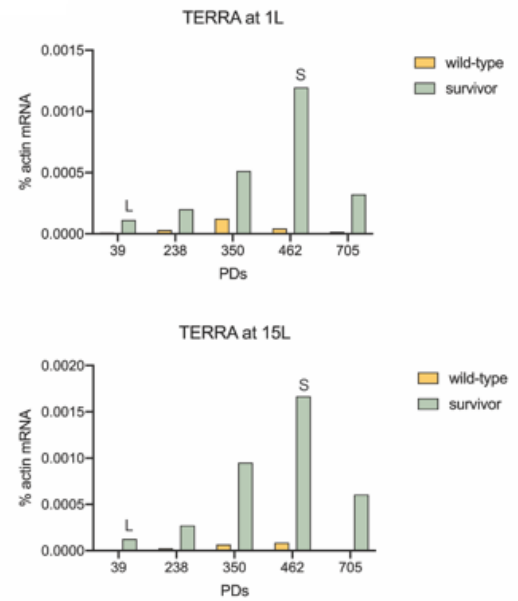
To validate this possibility, telomeres 1L and 15L from a single survivor were monitored in conjunction with TERRA expression during the clonal expansion. In line with the expectations, the replicative potential loss correlated well with the shortening of telomere 1L and 15L, reaching the lowest point when cells accumulated the shortest telomere length (Figure 24B). The following BIR events mediated telomere extension and rescued the proliferative capacity. In agreement with the results previously described, TERRA abundance increased as telomeres shortened in “senescing” survivors and decreased again once lengthening took place (Figure 24C).

This is the first report of type II survivors displaying a senescence-like phenotype driven by telomeres shortening. Due to its occurrence after telomeres crisis in senescing cells, this phenomenon will be referred to as “post-crisis senescence” (PCS).

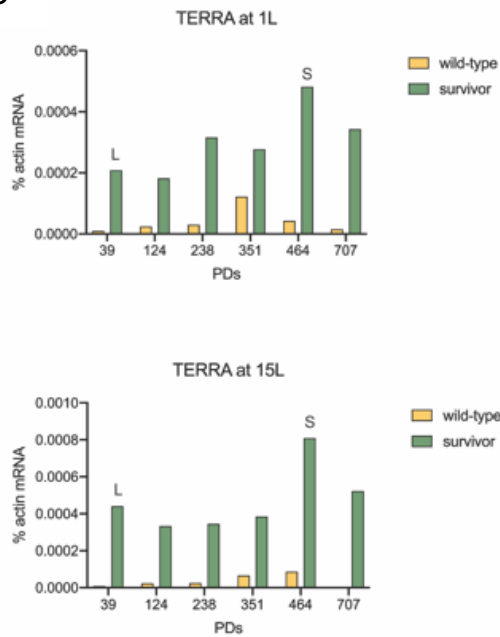
A



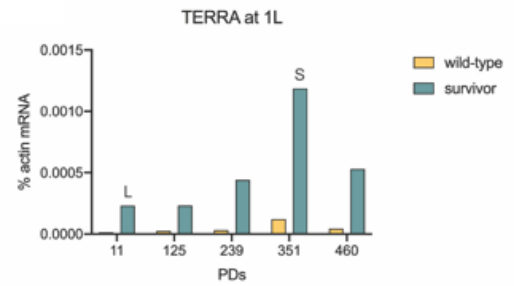
B



C



D



E

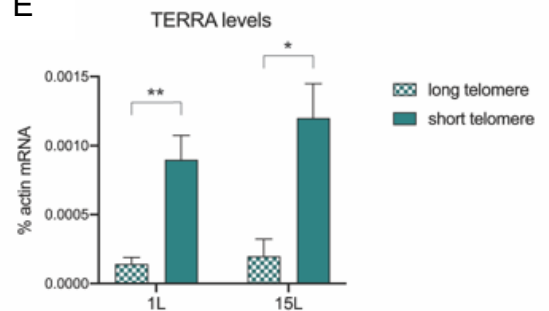


Figure 23. TERRA is regulated in a telomere length-dependent manner in survivors. A-D) TERRA levels from telomere 1L and 15L were monitored in single *tlc1Δ* survivor clones propagated in liquid culture over multiple population doublings (PDs). The telomere length variation was studied by the Southern blots presented in the previous figures. A corresponds to the same survivor of Figure 20, whereas B, C and D are the survivors of Figure 22A, B and C, respectively. TERRA levels were normalized by the actin mRNA. “L” indicates the point when long telomeres were observed whereas “S” corresponds to when the short telomeres accumulated in the Southern blots of Figure 20 and 20. E) The levels of TERRA from long and short telomeres (L and S, respectively, in A-D) were compared. The results are presented as mean + SEM (n=3/4). The p values were calculated by using an unpaired two-tailed Student’s t test (*p<0.05; **p<0.01).

As shown by the Southern blot for 1L and 15L, and by previous results, monoclonal propagations experience formation of mixed populations starting from early population doublings (Figure 22B and C and Figure 24B). This might have important consequences for the intensity of changes of the replicative capacity. Indeed, the survivors presenting long telomeres are supposed to alleviate the senescence effect of those with short telomeres. If this divergence worsens, the impact of senescing cells will be completely outcompeted by the non-senescing ones, thus resulting in a steady growth rate. This is highly likely what occurred at the end of the propagation of some survivor cultures, where little proliferative potential variation was observed (e.g., survivor D in Figure 24A). For the same reason, some survivors might have completely failed to senesce within the range of time investigated here (data not shown).

Overall, these and previous data depict a model where ALT-survivors senesce in response to telomere shortening, presumably by checkpoint activation. TERRA and TERRA-DNA hybrids accumulation seems not to participate in the checkpoint activation but might be equally involved in PCS, as reported for senescent cells.

3.3.1 PCS rate is modulated by R-loops

Senescent cells lose progressively their replicative potential in a manner influenced by RNA-DNA hybrids abundance¹¹⁹. When hybrids accumulate, the onset of senescence is delayed, whereas when they are reduced, the senescence rate is accelerated. Active recombination is required for this modulation as deletion of Rad52 abrogates it¹¹⁹.

In order to see if post-crisis senescence was affected by the amount of RNA-DNA hybrids, R-loops levels were modified in single clones of established ALT-survivors and their replicative potential variations were followed as described before. To observe the effect of reduced R-loops abundance on PCS, each clone was transformed either with an RNH1-overexpressing plasmid or with an empty vector before liquid propagation.

A system to define the senescence rate and compare it between the two conditions was based on the number of population doublings required for local minima, the lowest replicative potential values in a neighborhood of 4 adjacent values, to occur (Figure 25A). As shown by the Southern blot of telomere 1L and 15L during PCS, these points coincide with the shortest telomeres (Figure 24B and C). Therefore, measuring the amount of cell divisions needed to reach a minimum provides a good estimation of the senescence rate as it equals the amount of cell divisions required to accumulate the shortest telomere (Figure 25B).

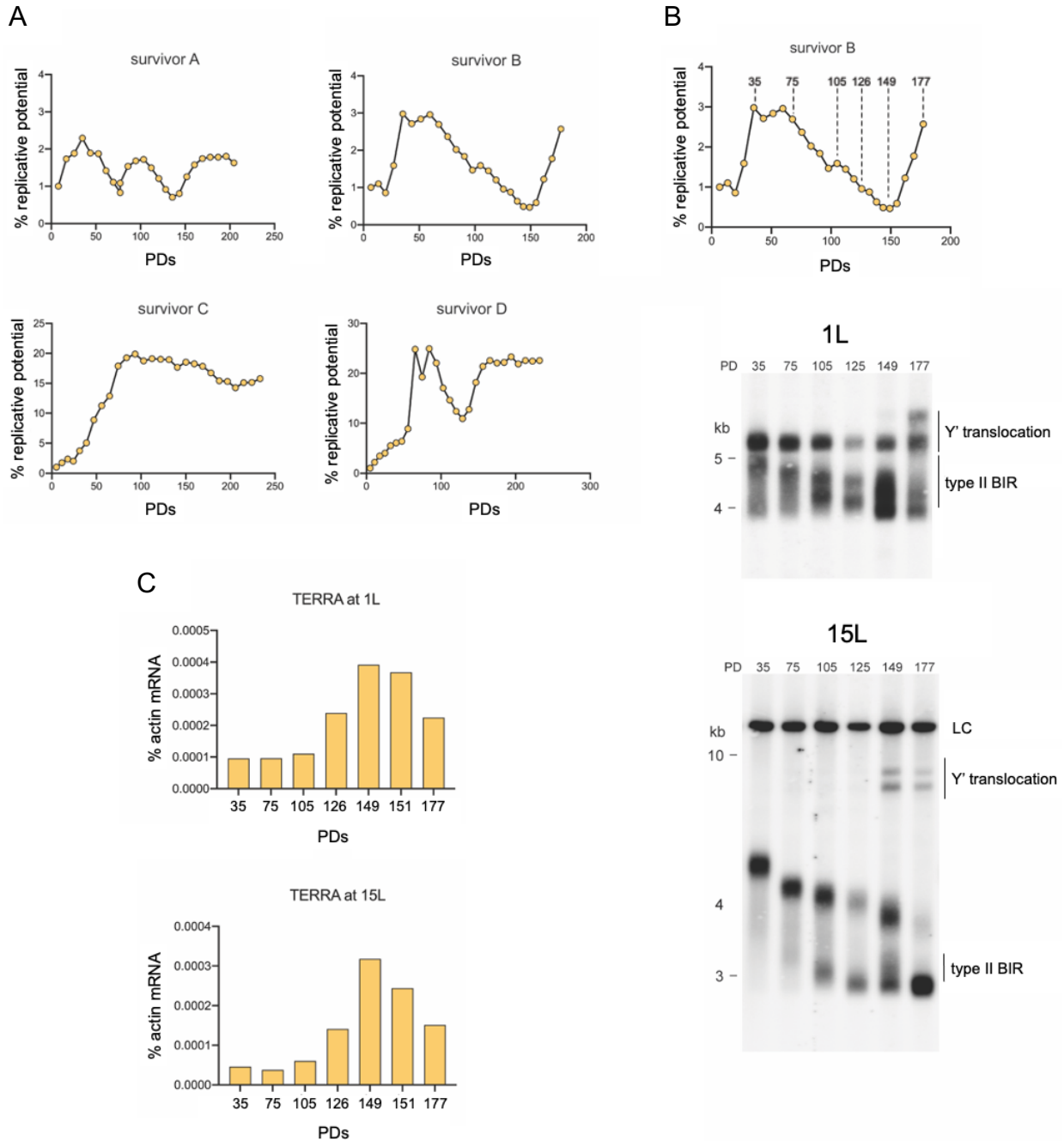


Figure 24. Post-crisis senescence: how survivors lose their replicative potential in response to telomere erosion. A) Single clones from *est2Δ* survivors were cultured in liquid and the replicative potential was calculated from daily measurements of the optical density. The percentage value was obtained by setting the first optical density value to 1 and by dividing the following values by it. Here, four representatives from the experiment in Figure 25 are shown. They correspond to the survivors transformed with the empty vector (EV). PDs indicate population doublings. B) 1L and 15L telomere length was monitored by Southern blot in survivor B at the different population doublings indicated. DNA was digested with *Sall* and *XhoI* to study telomere 1L and 15L, respectively. C) TERRA levels were measured in survivor B at the same time points when DNA was extracted for Southern blotting (B). The amount of TERRA is expressed as percentage of the actin mRNA.

Similar to senescent cells, the majority of type II survivors presented an accelerated senescence when overexpressing RNH1, compared to the isogenic EV controls (Figure 25C and data not shown). This was demonstrated by the significant reduction of time required for cells to reach the first local minima, which dropped from an average of ~ 140 PDs to ~ 115 PDs (Figure 25D). Southern blot and TERRA analysis for telomere 1L and 15L confirmed that the local minimum corresponded to the point when cells accumulated the shortest telomeres, also when overexpressing RNH1 (Figure 26).

Surprisingly, HDR took place to elongate the telomeres in the absence of R-loops in a manner similar to unperturbed conditions (Figure 26A). This was in line with the ability of survivors to restore their replicative potential after the reduction at the local minimum (Figure 26B). A similar scenario was observed in *S. pombe* survivors, which experienced a second crisis upon R-loops removal and recovered by lowering the amount of Rap1 at telomeres¹⁸⁸.

Overall, these data suggest that R-loops in established type II survivors counteract senescence. Since this is believed to be prompted in senescing cells by stimulation of Rad52-dependent HDR between sister chromatids in senescing cells, it is possible that the same mechanism is adopted in post-senescent survivor cells¹¹⁹. In contrast, the HDR that gives rise to the long telomeres for the restoration of the replicative potential seems to be R-loops-independent and might rely on a different telomeric structure like in *S. pombe* survivors.

To test if accumulation of R-loops reversed the phenotype observed upon RNH1 overexpression, type II survivors proliferative ability was monitored in the absence of Rnh201. In pre-survivors senescing cells, deletion of RNH201 causes a delay in senescence, even stronger than what has been described for *rnh1Δ rnh201Δ* strains (data not shown)¹¹⁹. Here, type II survivors were generated in a *tlc1Δ rnh201Δ* or *est2Δ rnh201Δ* background and single clones were transformed with either an EV (final genotype: *tlc1Δ/est2Δ rnh201Δ*) or an Rnh201-expressing plasmid (final genotype: *tlc1Δ/est2Δ*) before liquid culturing. *tlc1Δ/est2Δ rnh201Δ* survivors were not compared directly with *tlc1Δ/est2Δ* survivors because they were generated independently and the potential presence of telomeres with different initial telomere lengths might have biased the senescence profile.

Like before, clonal propagation was conducted for several population doublings and the senescence rate was estimated in terms of occurrence time of local minima. As expected, most of type II survivors displayed a slower senescence kinetics in the absence of Rnh201 compared to the isogenic *tlc1Δ/est2Δ* strains, as justified by the increased number of PDs required to reach the first local minima (Figure 27). The delay was of approximately 20 PDs (Figure 27B). This result further corroborated the idea of RNA-DNA hybrids having implications in telomere maintenance during PCS.

Both upon RNH1 overexpression and RNH201 deletion, the time required to reach the local minima varied a lot among survivors, emphasizing their heterogeneity in maintaining telomeres. Taken together, these results affirm that the dynamics of post-crisis senescence, similar to pre-survivors senescence, is shaped by the amount of RNA-DNA hybrids.

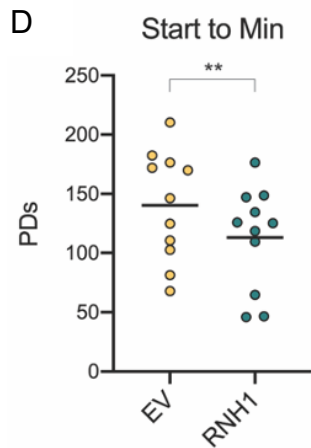
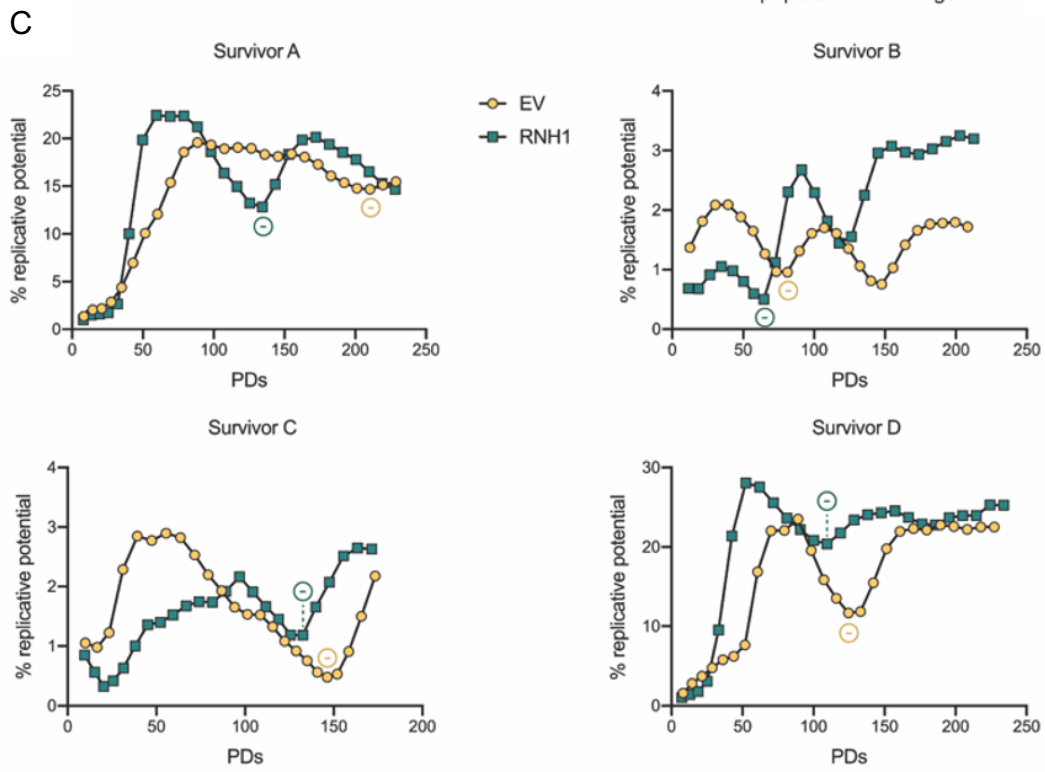
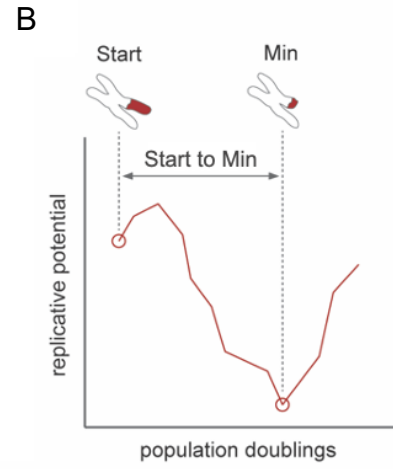
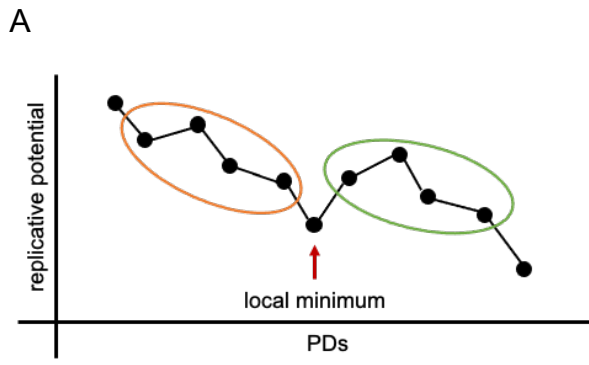


Figure 25. Removal of RNA-DNA hybrids accelerates post-crisis senescence. A) Schematic of how to calculate a local minimum, which is the lowest replicative potential value occurring in a neighborhood of four points (encircled in green and orange). PDs stands for population doublings. B) Schematic representing the correlation between the reduction of replicative potential and telomere shortening. "Start" indicates the beginning of the measurement of replicative potential while "Min" represents a local minimum. C) Single clones of *est2Δ* survivors were transformed with an empty vector (EV) or a plasmid overexpressing RNaseH1 (RNH1). These strains were grown in parallel and the replicative potential was calculated and monitored as described in Figure 24. The replicative potential values of cells with the empty vector and overexpressing RNH1 were obtained by dividing the optical density values by the first one of EV cells. Here, four representatives are shown. The circles with "-" indicate local minima. D) The amount of time between the Start point of each culture and a local minimum (Min) is a good estimation of the senescence rate. Here, these time periods, measured in PDs, were plotted for cells transformed with EV or overexpressing RNH1. The results are presented as scattered around the mean (n=11). The p value was calculated by using a paired one-tailed Student's t test (**p<0.01).

3.3.2 RNA-DNA hybrids counteract telomere shortening in ALT-survivors

In order to understand the mechanism underlying the RNA-DNA hybrids-dependent modulation of PCS, telomere 1L dynamics was monitored in more detail as it shortened in survivors in the presence and absence of R-loops. Different isolates of the same type II survivor, whose 1L telomere length was known to be ~ 400 bp, were transformed with an EV or an RNH1-overexpressing plasmid and cultured by daily dilution over ~ 70 PDs. The 1L telomere length kinetics was monitored by Southern blot and Telo-PCR.

The outcome from both assays was the same. Upon R-loops removal, telomere 1L shortened at a rate of 3.5 bp/PD, faster than the one of 2.8 bp/PD recorded in the EV control (Figure 28A, C and D). This held true also when examining the shortening profile, which appeared to be steeper in the presence of RNH1 overexpression (Figure 28B and E). Although the initial telomere length was slightly shorter in RNH1 overexpressing-cells, it is believed to be only a minor contributor to the phenotype observed.

In line with the observation that the length of telomere 1L decreased more rapidly in the absence of RNA-DNA hybrids, it underwent HDR at an earlier time point compared to unperturbed conditions (Figure 28D). As observed before, R-loops removal did not impair telomere lengthening, as demonstrated by the occurrence of type I and type II BIR products in RNH1-overexpressing survivors (Figure 28D).

Overall, these data suggest that RNA-DNA hybrids protect telomeres from shortening in type II survivors, thus providing an explanation for the hybrids influence on PCS. Although the exact mechanism remains elusive, it is highly likely that, like in senescent cells, hybrids counterbalance telomere shortening by promoting telomeric HDR¹⁸⁹. Furthermore, growing evidence regarding the role of R-loops in protecting DNA from resection adds another plausible layer of regulation by which hybrids might shelter telomeres^{189–191,192}.

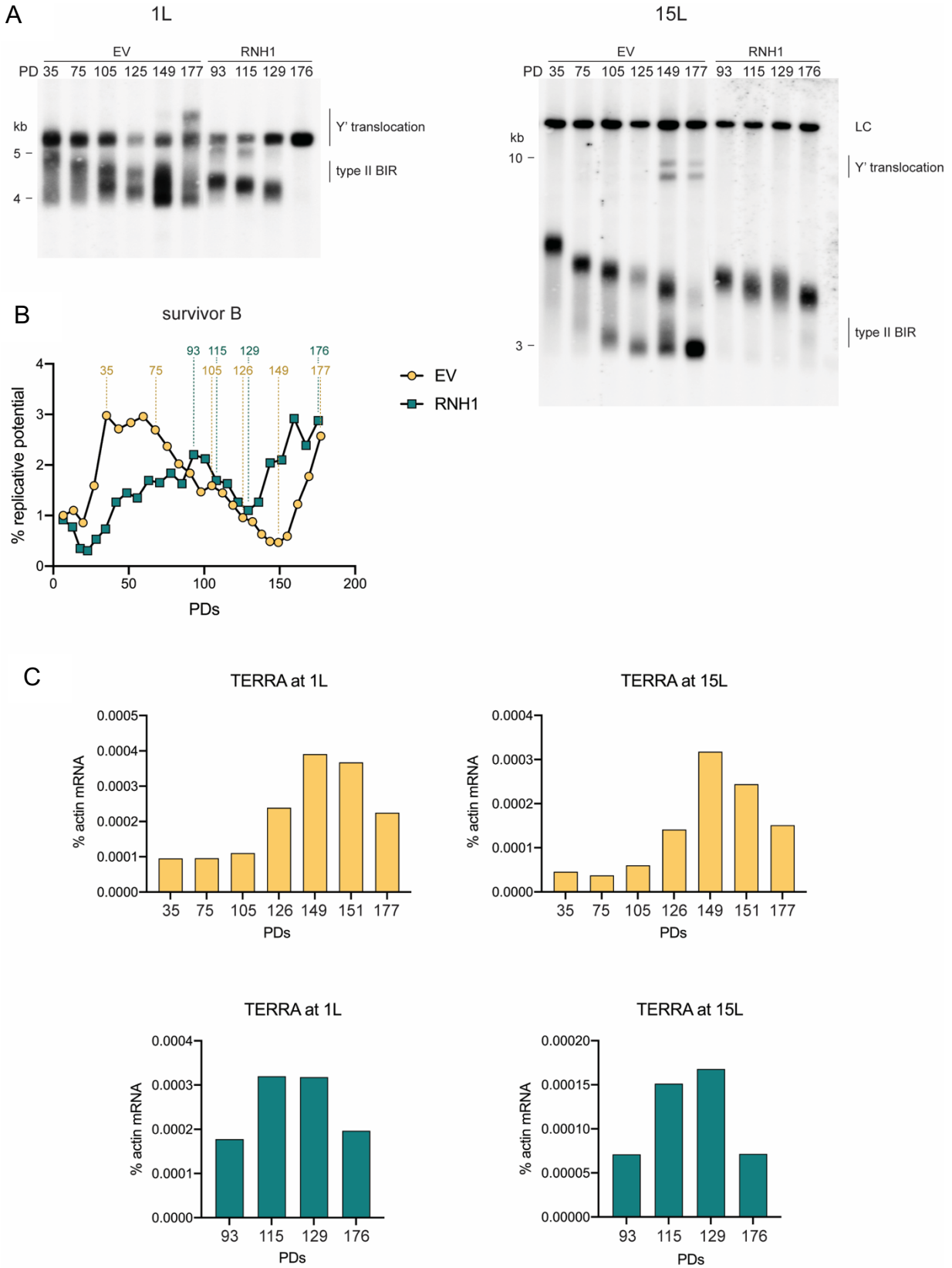


Figure 26. Telomere shorten and recombine during PCS in the presence and absence of RNA-DNA hybrids. A and B) The Southern blot, as represented in Figure 24, was carried out for telomere 1L and 15L from survivor B in Figure 25 at different time points of the clonal propagation. Telomeres were monitored in cells transformed with an empty vector (EV) or an RNH1-overexpressing plasmid (RNH1). The different time points are the ones reported in panel B. PDs stands for population doublings. C) TERRA levels were measured in the same survivor transformed with EV or the RNH1 plasmid at the same time points when DNA was collected for Southern blotting (A).

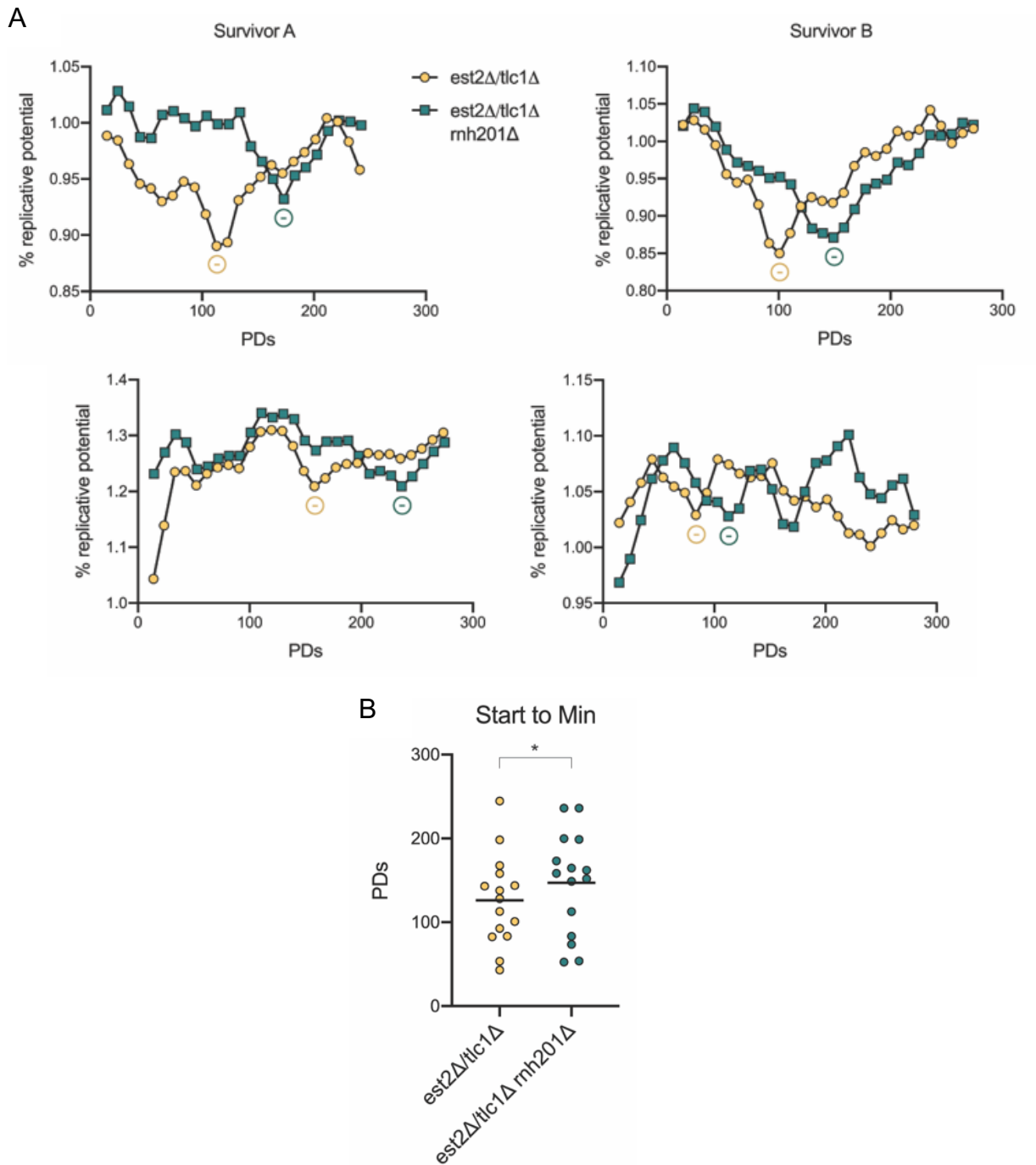


Figure 27. Increase of RNA-DNA hybrids delays post-crisis senescence. A) *est2Δ rnh201Δ* or *tlc1Δ rnh201Δ* survivors were transformed with an empty vector (final genotype: *est2Δ/tlc1Δ rnh201Δ*) or with an Rnh201-expressing plasmid (final genotype: *est2Δ/tlc1Δ*). Single clones of the transformants were propagated in liquid culture. The replicative potential was calculated from daily measurements of the optical density. The percentage value was obtained by setting the first optical density value from *est2Δ/tlc1Δ rnh201Δ* to 1 and by dividing all the other values by it. Circles with “-” indicate local minima, which were defined according to the same criteria of Figure 25. PDs indicate population doublings. Here, four representatives are shown. B) Similar to Figure 25D, the rate of senescence was defined as the amount of PDs from the Start point to a local minimum. The results are presented as scattered around the mean (n=15). The p value was calculated by using a paired one-tailed Student’s t test (*p<0.05).

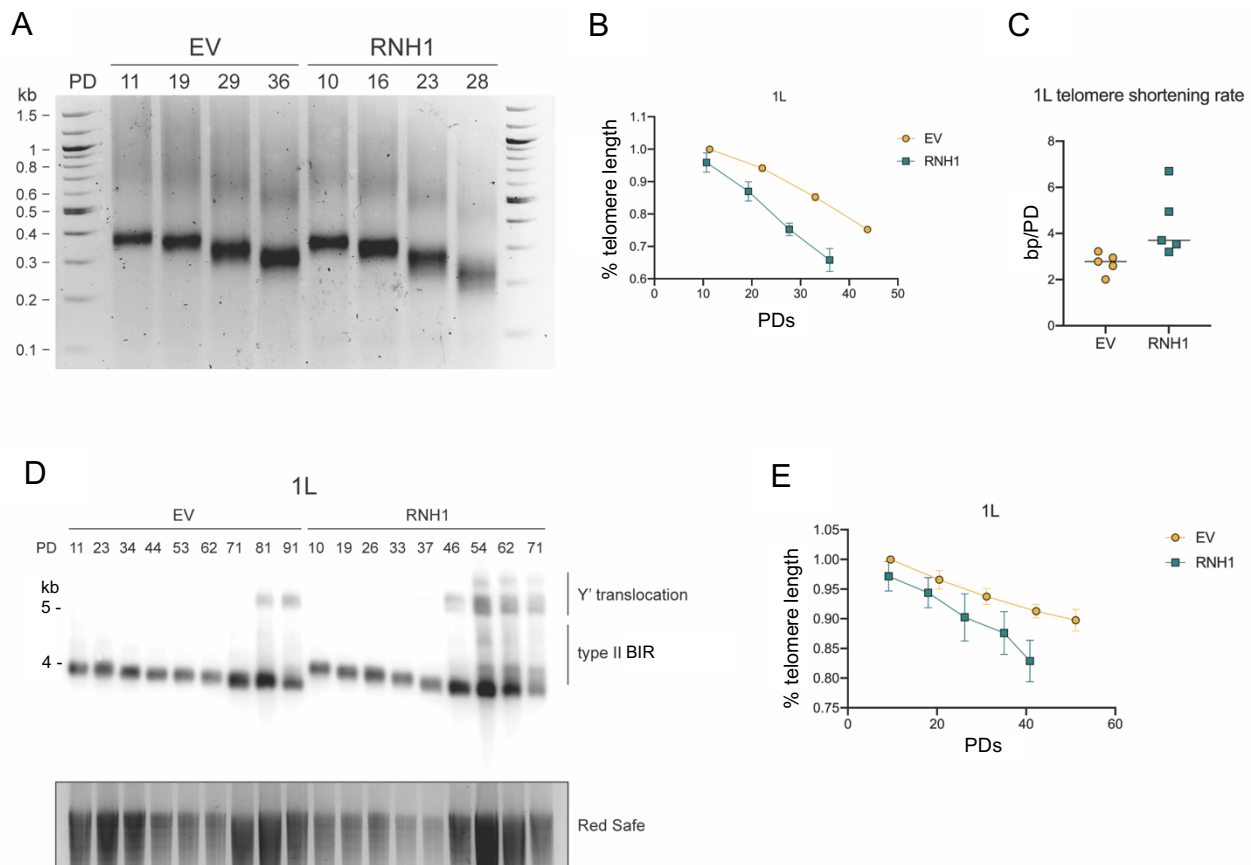


Figure 28. Telomere shortening is increased upon RNA-DNA hybrids removal in survivors. A) Telo-PCR to monitor 1L telomere shortening. A single survivor clone was transformed with an empty vector (EV) or an RNH1-overexpressing plasmid (RNH1) and propagated in liquid culture. The initial 1L telomere length was known to be ~ 400 bp. The telomere length variation was examined at the indicated population doublings (PDs). B) Plot showing the decrease of 1L telomere length, as defined by Telo-PCR, in five independent isolates from the survivor described in A. The percentage of telomere length was calculated by scaling all the length values to the first one of the EV cells. C) The shortening rate is calculated according to the Telo-PCR profiles and is represented as the number of base pairs lost in a single population doubling (bp/PD). The mean is shown. D) Representative Southern blot of telomere 1L from the same survivor used for the Telo-PCR experiments. DNA was digested with *Sall* and a 1L subtelomere-specific probe was used. The recombination products are shown on the side. E) 1L telomere lengths from five isolates of the survivor in A and D were derived by Southern blotting and plotted. The values in B and E are represented as mean + SEM.

4. Discussion

Alternative lengthening of telomeres provides a means to overcome telomere erosion-driven senescence in the absence of telomerase. Although it is clear that HDR is responsible for the lengthening process, the exact molecular details of the recombinational reaction are still elusive. TERRA and TERRA RNA-DNA hybrids accumulate in ALT cells, where they trigger HDR at telomeres, and manipulation of their abundance can have detrimental consequences for this TMM^{127,132,134,140}. However, it is yet to be determined whether TERRA upregulation is an essential requirement for the ALT phenotype.

In this work, the involvement of TERRA in ALT is explored and renewed with insights about the transcript regulation and function in protecting the chromosome ends in *Saccharomyces cerevisiae* ALT-survivors. In particular, the parallels between survivors and senescent cells alter our concept of post-senescence survival, which appears to be the continuation of processes already active during senescence rather than a newly established system.

Collectively, the data gathered in this study offer a model where telomere maintenance in ALT is similar to the one of senescent cells. TERRA is regulated in a cell cycle- and telomere length-dependent manner and counteracts telomere erosion. In this respect, by taking part in the regulation of telomere length, it modulates a novel ALT phenotype: post-crisis senescence.

These findings not only contribute to the general knowledge of telomere conservation beyond senescence, but open also new possibilities for therapeutics planning, having TERRA as a target or diagnostic tool.

4.1. TERRA expression is upregulated in ALT-survivors

TERRA overexpression in ALT is widely reported in humans^{132–134,137}. In yeast, a glimpse of the transcript importance in post-senescent survivors is provided by the work of Yu et al. with *S. cerevisiae* and Hu et al. with *S. pombe*^{169,188}. However, only the latter depicts an increase of the transcript and related RNA-DNA hybrids in survivors compared to wild-type cells.

In general, very little information is available regarding the source of TERRA upregulation in ALT. Studies on human cells revealed that a decreased transcriptional repression due to less telomeric heterochromatinization accounts for the high TERRA levels^{132,133}. Consistent with it, a reduced concentration of methylated TERRA CpG island promoters along with diminished H3K9me3 was detected at ALT chromosome ends in two independent studies^{132,133}. Furthermore, active telomeric transcription, as indicated by CHIP for pS2- and pS5-RNA pol II, was found in ALT cells and only barely observed in telomerase-positive cells¹³². TERRA stability was comparable between ALT cells and telomerase-positive cells, thereby ruling out the involvement of an impaired turnover in the upregulation¹³³.

As for the modulation of TERRA levels in ALT, the study from Flynn et al. proposes that the cell cycle regulation of the transcript present in telomerase-positive cells is abrogated in ALT, presumably due to loss of ATRX¹³⁵. Conversely, no direct support exists for a telomere length-dependent regulation. A first insight in this sense might be found in the work from Episkopou et al., where extension of short telomeres via telomerase reduces TERRA levels¹³³. However, the authors represent a model in which the overall increase of TERRA results from the general

decompaction of telomeres, regardless of their length. This is different from what previously reported about a telomere length-dependent control in telomerase-positive cells¹⁵⁰.

4.1.1 Low binding of Rat1 and Sir2

In the present study, type II survivors upregulated TERRA in a fashion reminiscent of their human counterpart¹³³. However, in contrast with what has been reported for human ALT, the underlying mechanism seems to be the impaired degradation of the transcript rather than higher transcription (Figure 13 and 14). More importantly, TERRA increase over wild-type cells derives from the presence of extremely short telomeres in survivors (Figure 19), which accumulate the lncRNA (Figure 20, 22 and 23).

Presumably, this subpopulation of telomeres accounts for the upregulation because of diminished binding of Rat1 (Figure 14) and Sir2 (Figure 15), two negative regulators of TERRA. A similar scenario has been proposed by Graf et al. for senescent cells, where the erosion of TG repeats diminished the space for Rif1/2, and therefore Rat1, binding⁶². However, in that work, no or little reduction of Sir2 enrichment was observed upon telomere shortening.

Three different possibilities can explain the lower Rat1 and Sir2 ChIP signal (Figure 29). The first one is that the concentration of the protein bound at telomeres (number of proteins/number of bp) is unchanged between survivors and wild-type cells (Figure 29A). In this case, the total number of immunoprecipitated proteins would be reduced in survivors due to the presence of short telomeres, which present a lower amount of binding sites for Rat1 and Sir2. The second possibility implies that short telomeres bind less proteins not only because of missing nucleotides but also because of a diminished concentration (Figure 29B). This would have a stronger effect on the protein shortage at eroded telomeres compared to the first possibility. Finally, according to the third possibility, a general reduction of the telomere-bound protein concentration would account for the lower ChIP signal in survivors, regardless of the telomere length (Figure 29C). Like in the other cases, short telomeres contribute to the generally reduced amount of telomere-bound proteins.

Different telomere and subtelomere states characterize the three scenarios. In the first one, despite a lower binding of Sir2 at short telomeres, the protein might still be able to spread and establish TPE also in the subtelomeric region (Figure 30A). This might explain why the reduction of Sir2 enrichment in survivors does not derepress telomeric transcription, as indicated by the unchanged ChIP profile of RNA pol II (Figure 13). Assuming that less Rat1 proteins bind the short telomeres, TERRA levels would be enhanced due to weakened degradation.

During senescence, the Sir proteins are lost only from the subtelomeres and not from the telomeres⁸³. This is dependent from Sas2-mediated acetylation of subtelomeric histones. If the same mechanism of subtelomeric euchromatinization applies to survivor telomeres, short telomeres might present reduced amounts of Sir2 also at the subtelomeric region (Figure 30B). This would be consistent with the increased reduction of the protein enrichment (almost 50%) compared to Rat1 (almost 40%), whose binding decrease is supposed to depend mostly from telomere loss and not from subtelomeric changes (Figure 14 and 15). Alternatively, it is also possible that Sir2 is lost from subtelomeres because its low occupancy at the TG repeats is insufficient to allow its efficient propagation.

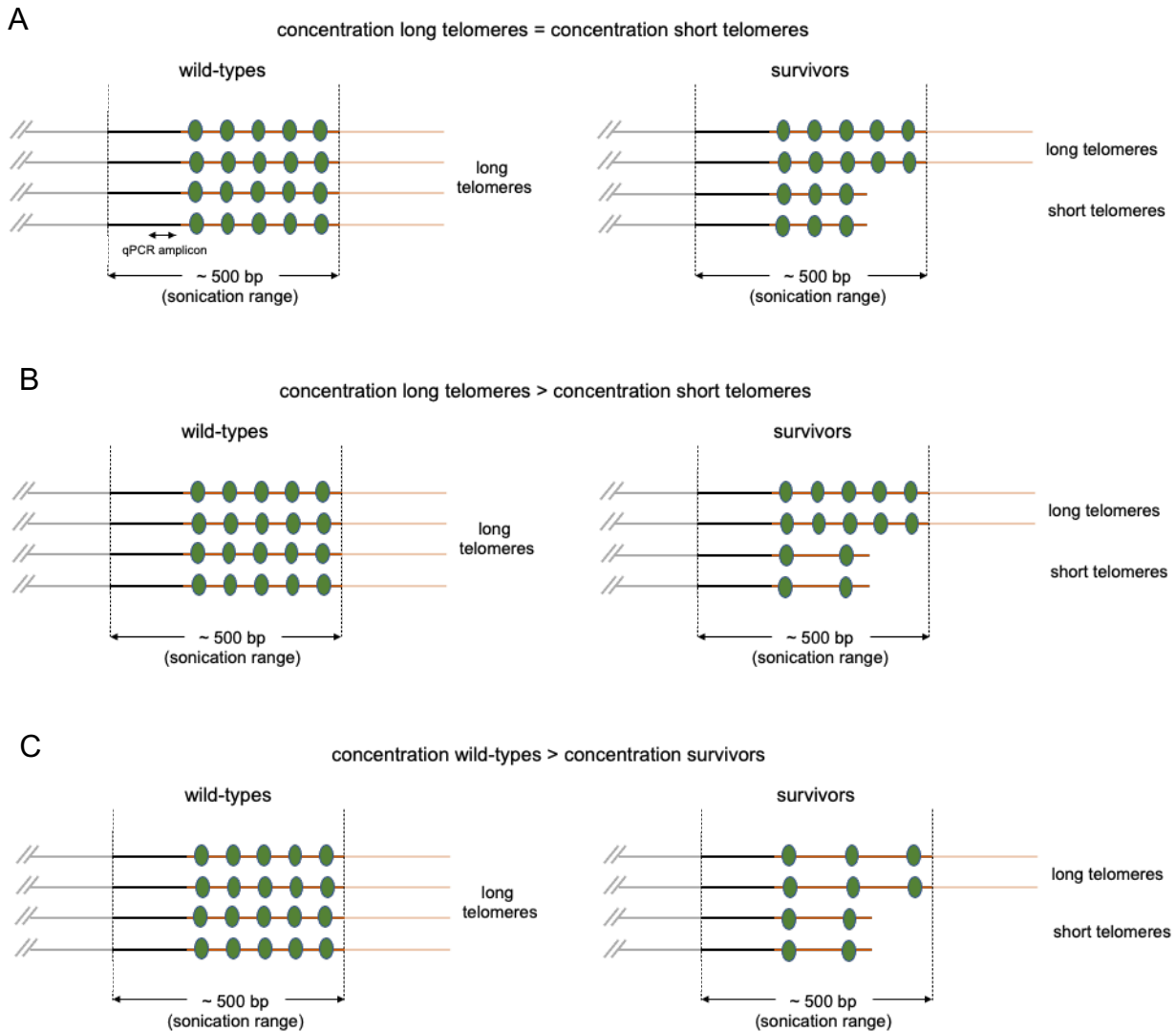


Figure 29. Models to explain the low binding of Rat1 and Sir2. A) In the first scenario proposed, the concentration of Rat1 and Sir2 (simplified as green ovals), intended as the number of proteins / amount of base pairs, bound to telomeres (orange segments) is not changed between wild-types (left panel) and survivors (right panel). This implies that long and short telomeres bind the same amount of proteins / bp. However, the total amount of proteins bound to telomeres is diminished in survivors because short telomeres are present. This is due to loss of the telomere sequence along with the bound proteins. The sonication range of ~ 500 bp represents the range of lengths of the sonication fragments, from virtually 0 bp to 500 bp. The qPCR reaction is supposed to detect only those fragments that contain the subtelomeric part (black segment) recognized by the primers (double arrowhead) and that fall within the 500 bp range. Long telomeres will not be detected in their entirety as only the subtelomere-proximal region will be amplified. B) In the second scenario proposed, the concentration of Rat1 and Sir2 bound to telomeres is diminished only at short telomeres in survivors. The concentration is unchanged at long telomeres in wild-types and survivors. In this case, the overall number of bound proteins is reduced in survivors not only because of the telomere loss of short telomeres but also because of the lower concentration. C) In the third scenario, the concentration of bound proteins is reduced in survivors independently from the telomere length. Short telomeres still contribute to the overall reduction of bound telomeres in survivors.

Another possibility to explain the reduction of Sir2 at the subtelomere is via dissolution of telomere looping (Figure 30C). Telomere looping might play a role in establishing subtelomeric heterochromatin and it decreases at short telomeres^{86,93,193,194}. Therefore, it is plausible that subtelomeres in survivors might lose Sir2 upon telomere shortening in response to looping attenuation. The effect would impact not only the lncRNA transcription but also degradation, as the number of TERRA-Rat1 contacts is expected to diminish.

The other two scenarios before presented propose different concentrations of telomeres-bound proteins between survivors and wild-types (Figure 29B and C). This can be proved by considering the total amount of Rat1 and Sir2 produced.

In order to have the same amount of proteins/number of bp, survivors are expected to increase the synthesis of their proteins to compensate for the extremely long telomeres. This would be particularly relevant for the Sir proteins, given their limiting quantity⁸³. However, as shown by Western blotting, survivors presented similar translation profiles of Rat1 and Sir2 compared to wild-type cells (Figure 14 and 15), suggesting a “dilution” of the proteins on survivors telomeres. This effect can be widespread on all chromosome ends (Figure 29C) or restricted to a specific telomeres subpopulation. Perhaps, due to the higher probability of long telomeres to be bound by proteins, the subset of telomeres with a lower protein concentration might be the one with a smaller extension (Figure 29B).

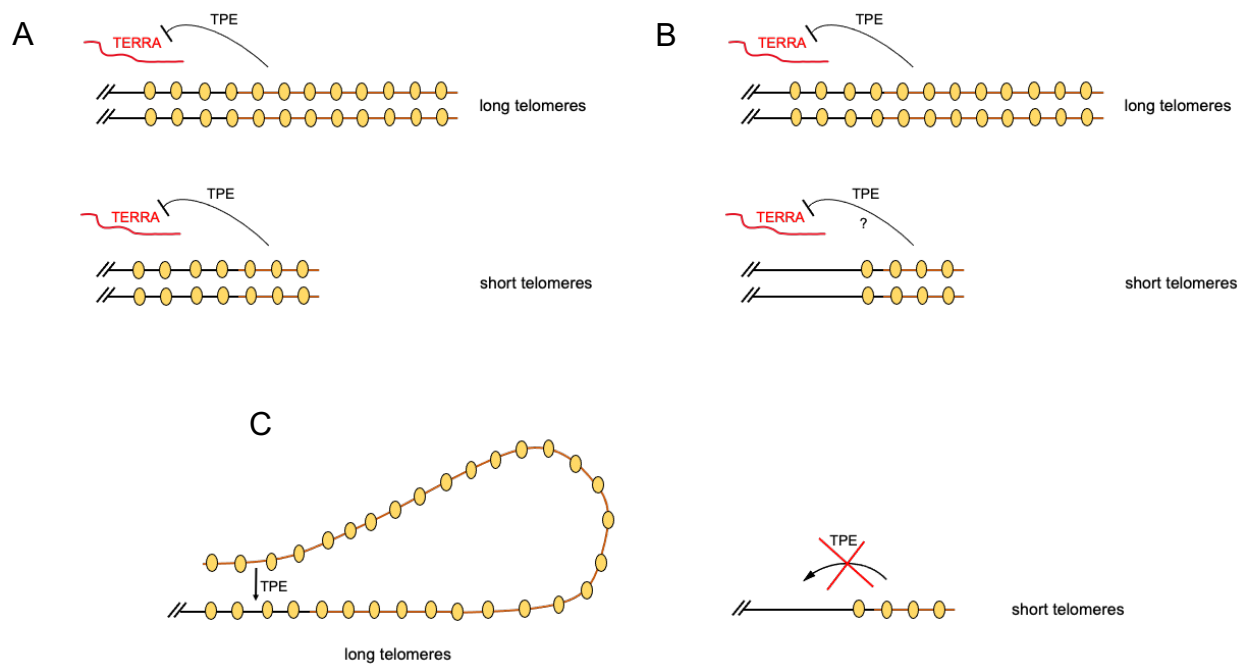


Figure 30. Models to explain the different states of long and short telomeres. A) In this scenario, long and short telomeres (orange segments) are equally able to propagate heterochromatin into the subtelomere (black segment) and repress TERRA transcription via telomere position effect (TPE). Each yellow oval represents a Sir2 protein. B) In this scenario, the reduced amount of Sir2 at the subtelomeres of short telomeres might not be sufficient to establish proper TPE and TERRA repression might be alleviated. C) Telomere looping might promote Sir2 propagation in the subtelomere of long telomeres (left). This would favor TPE and negatively affect TERRA transcription. At short telomeres (right), the reduced ability to fold back might hamper Sir2 propagation and attenuate TPE.

Y' elements present a typical euchromatic state, with low levels of Sir3 and hyperacetylation⁸⁵. Furthermore, transcription is enhanced compared to the heterochromatic X elements. Given the propensity of telomere looping to occur at heterochromatic regions, it is very likely that Y' telomeres, especially those with extended arrays of Y' elements, are less prone to fold back⁸⁶. This might have a negative influence on TPE propagation. Consistent with these observations, the acquisition of Y' elements at the X-only telomeres 1L and 15L in survivors might provide a valid justification to the lower Sir2, and perhaps Rat1, binding, regardless of the scenarios before listed.

A reduced concentration of TERRA negative regulators on all telomeres would infer a general favorable state for the transcript synthesis and stability. Supporting this idea, the work from Episkopou et al. demonstrates that both long and short telomeres in ALT are decondensed, presumably in response to ATRX loss and/or a lower binding of heterochromatinization factors¹³³. The presence of sequence variants, typical of ALT telomeres, are suggested to prompt the low affinity^{133,195}.

In summary, despite the different possibilities to elucidate why ALT-survivors bind less Rat1 and Sir2 at their telomeres, it is generally acceptable that the presence of short telomeres might constitute a valid explanation to it. This would be particularly true for Rat1, whose reduction is marginal. Conversely, Sir2 binding reduction may be a broader phenomenon.

If survivors upregulate TERRA because of deficient turnover at short telomeres, they might adopt the same mechanism of regulation described in senescent cells⁶². This would imply that the transcript accumulation does not derive from genetic changes, like mutations, specifically related to the survivors status but rather by the adoption of telomeres configurations that favor it.

Unfortunately, the present study does not allow to discriminate among the different scenarios proposed. To directly resolve the problem, it could be beneficial to monitor the enrichment of Rat1 and Sir2 as telomeres shorten in survivors or see if the ChIP signal increases after telomerase reintroduction. Complementarily, a microscopy-based approach could be used to see if the ratio of protein-telomere colocalizations/telomere length observed in wild-type cells is maintained in survivors. If yes, it can be assumed that the same concentration of telomere-bound proteins is present in wild-types and survivors. If the ratio is reduced, the proteins will result to be diluted on survivors telomeres.

4.1.2 Are there really no changes in transcription?

Several evidences indicate that transcription is increased at ALT telomeres. Also, in some of the hypotheses here formulated, enhanced transcription would seem to be one of the mechanisms underlying TERRA upregulation. However, the ChIP for RNA pol II, which very likely depicts the loading state of the enzyme at TERRA promoters, and pS2-RNA pol II, which frames transcription elongation, showed no increased signal in survivors compared to wild-types (Figure 13). This result, nonetheless, can be reinterpreted to favor the possibility of increased TERRA production also in yeast survivors.

A clue for this reconsideration can be found in the work from Graf et al., where telomeres shortening in senescent cells causes a reduction of pS2-RNA pol II enrichment at telomeres, without affecting the unphosphorylated version (Figure 31A). If this is caused by telomere erosion and loss of the bound proteins rather than a decrease of the protein concentration at

telomeres (Figure 31B), the same pattern would be expected for survivors harboring short telomeres. Hence, the scenario would resemble the one before postulated for Rat1 and Sir2 low binding (Figure 29A).

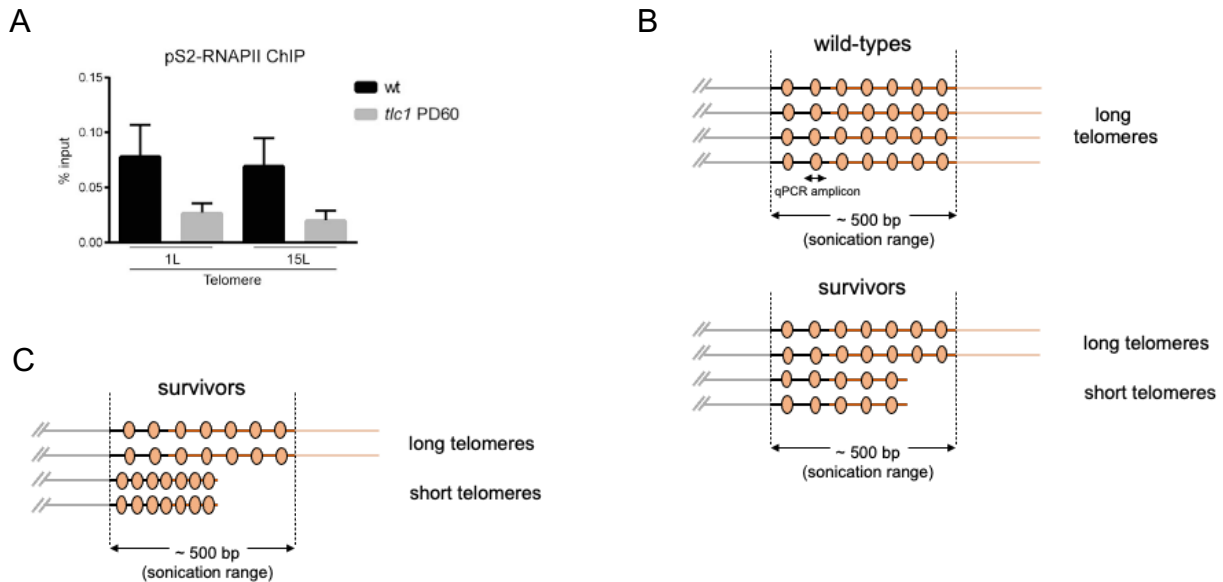


Figure 31. Models to explain the potential accumulation of pS2-RNA pol II at short telomeres. A) Enrichment of pS2-RNA pol II at short telomeres in *tlc1Δ* senescent cells and long telomeres in wild-types, as represented in Graf et al⁶². PD60 indicates population doubling 60. B) In this scenario, wild-type cells (top) and survivors (bottom) present the same concentration of pS2-RNA pol II (orange ovals) at long and short telomeres (orange segments). However, the presence of short telomeres in survivors reduces the overall amount of enzyme bound to telomeres. This might explain the reduction observed in senescent cells in A. C) In survivors, this reduction was not detected by ChIP. Therefore, short telomeres might compensate for the telomere loss-related reduced binding of pS2-RNA pol II by increasing its concentration.

No reduction of pS2-RNA pol II at telomeres was observed in survivors compared to wild-type cells. Therefore, it is possible that short telomeres in survivors present a higher concentration of the enzyme, thus compensating for the telomere erosion-dependent protein loss (Figure 31C). This would argue that an increased amount of pS2-RNA pol II binds to survivors short telomeres, perhaps indicative of a more processive elongation step, with reduced pausing.

Furthermore, the unchanged ChIP profile of unphosphorylated RNA pol II indicates an equal amount of the enzyme at TERRA promoters of wild-types and survivors. Applying this concept to short telomeres would infer that the more processive transcription elongation would require an equally processive loading at promoters.

These assumptions fit with the model of a more open chromatin at short telomeres in ALT (Figure 30B and C) and might suggest that TERRA high levels derive not only from impaired degradation at eroded telomeres but also increased transcription¹³³.

Other possibilities might explain the potential accumulation of pS2-RNA pol II at short telomeres and one of them does not necessarily imply increased transcription. According to it, RNA pol II might simply be more frequently “caught” at short telomeres because it slows down to allow termination^{196,197}.

4.1.3 TERRA cell cycle regulation might reveal enhanced transcription at ALT telomeres

The results here presented depict a model where TERRA upregulation in ALT-survivors derives from impaired degradation, and potentially enhanced transcription, at short telomeres.

Further proof for the potential involvement of transcription might be found in the way TERRA levels vary throughout the cell cycle in survivors and wild-type cells (Figure 18). In telomerase-positive cells, TERRA is very low in G1 and peaks in early S-phase to diminish again during replication⁶². According to the results illustrated by Graf et al., TERRA is transcribed within a limited time period of S-phase. After this brief production, transcription ceases and the accumulation of Rat1 at telomeres in middle and late S-phase determines the transcript degradation. No transcription takes place in G1 and G2.

The fact that survivors present a significant increase of TERRA over wild-types already in G1 might suggest two non-mutually exclusive options: 1) TERRA is transcribed in G1 in survivors and 2) TERRA degradation is so low in survivors that the transcript persists through mitosis until the new G1 phase. In case TERRA transcription does not take place in G1 but occurs at a normal, wild-type-like rate in early S-phase, the transcript levels during this stage would equal the sum of survivors G1 TERRA levels plus wild-types early S-phase TERRA levels (Figure 32):

$$\text{early S TERRA}_{\text{surv}} = \text{G1 TERRA}_{\text{surv}} + \text{early S TERRA}_{\text{wt}}$$

However, since the transcript amount in early S-phase was higher than the summed quantities, it is possible that an additional factor, perhaps enhanced transcription, might take part to TERRA upregulation in survivors. This was particularly evident at 15L TERRA.

Impaired recruitment of Rat1 cannot account for the enhancement over wild-types during early S-phase as wild-type telomeres present no enrichment of the protein at this time⁶². If transcription is elevated in survivors, it is possible that it occurs also in other cell cycle phases, in which it is normally repressed. This might be due to a general Sir2 loss-dependent euchromatinization. In case the overexpression persists during mitosis, survivors might use TERRA for MiDAS, one of the ALT pathways described in humans¹⁹⁸.

Overall, the observations presented so far suggest that TERRA upregulation might be the result of impaired degradation and increased transcription. It is tempting to think that enhanced transcription, like deficient turnover, are a prerogative of short telomeres. Indeed, if the accumulation of pS2-RNA pol II regarded the entire telomere population, more protein would have been immunoprecipitated in survivors compared to wild-type cells.

In addition to the proposed Rat1-dependent deficient degradation, TERRA perseverance in survivors might be caused by an ALT-specific signature of RNA modifications. This might include not only increased polyadenylation at the 3' terminus but also generation of stabilizing modifications and/or removal of destabilizing modified ribonucleotides^{63,199,200}.

To inquire more specifically the source of high TERRA in survivors, one could address the degradation efficiency by measuring the half-life of the lncRNA. After depletion of RNA pol II via a degron system, TERRA could be measured in a time course in both survivors and wild-type cells. If the transcript persists for a longer time in survivors, its degradation might be hampered.

Conversely, to validate enhanced transcription as a source of TERRA upregulation, *rat1-1* survivors and wild-types (or survivors and wild-types bearing a *Rat1* degron) can be generated and monitored for TERRA levels. In case TERRA abundance in survivors is still higher than wild-type cells upon *Rat1* depletion, transcription might be augmented.

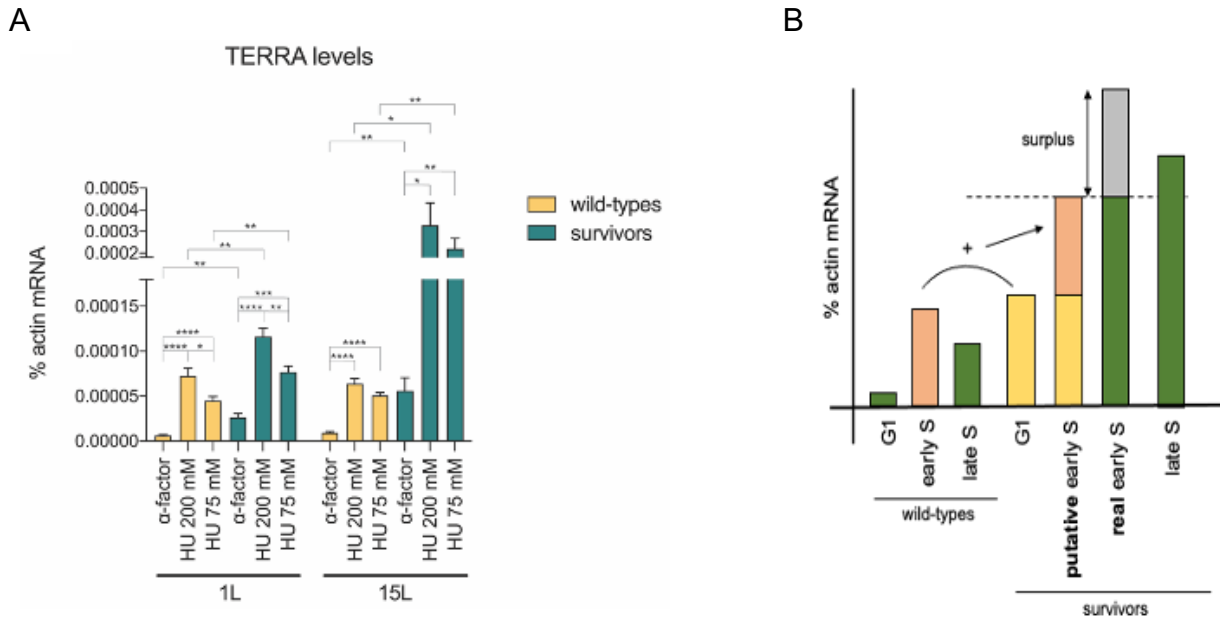


Figure 32. TERRA cell cycle regulation might reveal enhanced transcription in survivors. A) TERRA regulation in wild-type cells and survivors as reported in Figure 18. Survivors present the same regulatory mechanism of wild-type cells. However, the transcript levels are higher in survivors than in wild-types in every cell cycle phase. B) Assuming that the amount of TERRA in survivors early S-phase derives from the RNA persistence from G1 (TERRA amount in yellow) and a wild-type like transcription (TERRA amount in orange), the amount of TERRA in survivors early S phase would equal the sum of TERRA in survivors G1 (yellow) + TERRA in wild-types early S-phase (orange) (putative early S-phase TERRA). However, a surplus is observed over the summed quantities (grey rectangle in real early S-phase TERRA), indicating that additional TERRA production is involved. This is particularly evident in TERRA transcribed from telomere 15L.

4.1.4 Short telomeres account for the majority of TERRA

In different studies, TERRA has been shown to accumulate at short telomeres^{62,150}. In yeast, senescent cells upregulate the lncRNA by recruiting less *Rat1*, with little changes in the occupancy of the chromatin deacetylase *Sir2*⁶². In humans, instead, telomere length-dependent regulation of TERRA seems to rely more on chromatin variation and transcription, rather than changes in the transcript stability¹⁵⁰. This applies to both telomerase-positive cells and to some extent to ALT cells^{133,150}.

In yeast survivors, TERRA appears to be regulated in a similar manner to senescent cells. Telomere shortening triggers the RNA accumulation and telomerase-mediated extension abrogates it (Figure 19, 20, 22 and 23). According to these data, the following model can be proposed. Increase of TERRA and TERRA R-loops at short telomeres in senescent cells triggers replication stress and HDR that promote telomere lengthening and survivors formation. At this

point, long telomeres re-establish Rat1 and Sir2 binding, shutting down TERRA expression. As telomeres progressively shorten, the number of binding sites for TERRA negative regulators diminishes, causing a gradual increase of the lncRNA. When almost no TG repeats are left, the accumulation of TERRA and RNA-DNA hybrids is so enhanced that HDR takes place again, providing new extension. TERRA repression is reconstituted.

Consistent with this setup, freshly generated survivors would be anticipated to present only long telomeres and low levels of TERRA, which is the opposite of what observed. Three different scenarios might describe the relationship between telomere length and TERRA abundance: 1) TERRA is upregulated in survivors regardless of the telomere length; 2) TERRA is upregulated preferentially at short telomeres; 3) TERRA is upregulated exclusively at short telomeres. The results from the telomerase re-introduction experiment and the TERRA measurement in the monoclonal propagation argue against an equal probability of long and short telomeres to upregulate TERRA. Indeed, the majority of long telomeres presented transcript amounts similar to that of wild-type cells and telomerase expression lowered the RNA abundance to wild-type levels in most cases. However, since some long telomeres displayed increased amounts of TERRA over wild-types and TLC1 expression failed in certain cases to completely abolish the upregulation, it cannot be ruled out that extended telomeres participate in survivors TERRA upregulation (Figure 19, 20, 22 and 23). If this held true, the second scenario would seem more realistic than the other two.

The idea of long telomeres participating in TERRA overexpression would be in line with the general decondensed state of chromatin at human ALT telomeres and the extended reduction of Sir2 at survivors chromosome ends¹³³. However, it might be restricted only to a specific class of long telomeres. Perhaps, the one in which Y' elements acquisition disrupts TPE, and potentially degradation, by establishing an euchromatic environment^{85,146,153}. These telomeres might be the one detected by junction PCR, where Y' translocation did not interfere with the high levels of TERRA over wild-types (Figure 11).

To fit this with the Y' translocation causing a marked decline of TERRA during monoclonal propagation, it is possible that newly generated Y' telomeres find means alternative to TPE to suppress the transcript. This would be consistent with Y'-TERRA transcription being repressed in a Sir proteins-independent but Rif1-dependent manner¹⁴⁶. However, as suggested by the yet increased TERRA levels over wild-types, this suppressing mechanism might be less efficient than the one active at wild-type telomeres (Figure 22A and 23B, PD 705).

Beside these scenarios, where long telomeres actively participate to TERRA accumulation, it might be that upregulation is simply caused by TERRA increasing at short telomeres and persisting in the next cell divisions, when telomeres are elongated. According to this view, the nascent RNA from long telomeres would be immediately degraded without contributing to the overall TERRA enhancement over wild-type cells. Reinforced stability, perhaps by RNA modifications, would be essential for this perseverance.

In summary, the data here presented point out that TERRA increase in survivors derives mainly from short telomeres. Pre-HDR long telomeres suppress TERRA presumably via active degradation. When short telomeres accumulate, degradation impairment, and potentially transcription, significantly augments the transcript, which might persist throughout future generations with extended telomeres. Post-HDR long telomeres reconstitute degradation of TERRA, lowering its amounts. However, due to the permanence of RNA molecules from short

telomeres and/or a less efficient suppression at newly formed Y' telomeres, the reduction is not sufficient to reach wild-type levels.

4.2 Post-crisis senescence: between R-loops and adaptation

In telomerase-negative cells, senescence derives from loss of telomere proteins, which inhibit checkpoint activation, and replication stress. RNA-DNA hybrids promote replication stress at short telomeres, where they accumulate due to less binding of RNase H2⁶². At the same time, they alleviate senescence by counteracting telomere shortening in a HDR-dependent manner¹¹⁹. In survivors, RNA-DNA hybrids abundance might be increased, not only at telomeres but also elsewhere in the genome, as indicated by the Rnh201 ChIP (Figure 16). At telomeres, Rnh201 occupancy seems to be further reduced than at other loci tested. This could be due to short telomeres, which might bind even less enzyme in response to the binding sites erosion.

Given that ALT-survivors present in general a wild-type-like replicative potential and senesce occasionally, it is possible that DDR is generally repressed in post-senescent cells. However, checkpoint activation was detected in survivors, in the form of cell cycle arrest in G2, Rnr3 overexpression and Mrc1 phosphorylation (Figure 17). Since survivors present short telomeres, which are more prone to activate DDR, it is likely that checkpoint was induced by this subpopulation of telomeres. The potential accumulation of RNA-DNA hybrids, which triggers replication stress, at this class of telomeres further supports this idea^{62,201,202}.

To test if RNA-DNA hybrids were responsible for the checkpoint activation, RNH1 overexpression was induced in survivors and wild-type cells. Surprisingly, removal of R-loops did not alleviate DDR. This indicates that RNA-DNA hybrids might not be the source of the checkpoint-activating DNA damage in survivors and DDR derives probably from other causes, like telomere attrition.

Checkpoint adaptation is a frequent phenomenon during senescence that consists of cell division progression in presence of unrepaired DNA damage²⁰³. It accounts for almost 50% of senescence-related genome instability and might potentially participate to survivors formation²⁰³.

A possible way to explain the persistence of checkpoint activation upon RNH1 overexpression is by adaptation of survivors to R-loops-induced DNA damage. Indeed, if RNA-DNA hybrids accumulation does not trigger the checkpoint, RNH1 overexpression would have no effect on it. This idea might be sustained by the widespread increase of R-loops in survivors, as suggested by the general low occupancy of RNase H2: perhaps, RNA-DNA hybrids are so frequent, that cells adapted to tolerate and use them.

Adaptation to dysfunctional telomeres has been reported for *cdc13-1* survivors, where growth in absence of telomere capping is possible by mutations in the Mec1-dependent checkpoint branch²⁰⁴. Interestingly, in these strains, DNA damage is still recognized and potentially repaired but no checkpoint is activated due to the mutations. This form of adaptation may apply to R-loops-induced DNA damage as well. However, since checkpoint per se is not impaired in post-senescent cells, the related proteins are expected to be still functional. Furthermore, given the low mutation profile of survivors (data not shown) and the requirement of the checkpoint proteins Mec1 and Tel1 for ALT establishment, post-senescent cells might use an alternative means to adapt¹¹⁴. Presumably, this mechanism might not be mediated by the canonical checkpoint adaptation proteins Cdc5 and Tid1, as they both are dispensable for survivors formation²⁰³.

4.2.1 R-loops are required for sister chromatid HDR but not extensive recombinational events

According to the data above described, post-crisis senescence would be driven by the progressive loss of checkpoint inhibitors, independently from R-loops-associated replication stress. Nevertheless, RNA-DNA hybrids influence senescence indirectly by defining the pace of this loss, as shown by the counteracting effect on telomere shortening (Figure 28) and the R-loops abundance-dependent variations of senescence rate (Figure 25 and 27). Additional factors are expected to be involved in the regulation of survivors senescence, as indicated by the insensitivity of checkpoint activation to RNH1 overexpression. They might include secondary structures and/or recombination intermediates that regulate telomere length, and thus senescence, both positively and negatively. Some of these secondary structures could include, for example, extremely long ssDNA overhangs and G4 quadruplexes. They are able to induce the G2/M checkpoint and derive from extensive resection, which occurs at short telomeres and is important for survivors generation^{115,116}.

Among the recombination intermediates that might positively regulate telomere length and alleviate checkpoint is the one triggering type I and II BIR at critically short telomeres (Figure 28). This structure originates independently from R-loops, as shown by the appearance of recombination products upon RNH1 overexpression, and allows senescent survivors to regain viability (Figure 26). The independence of telomere elongation from R-loops further supports the assumption that RNA-DNA hybrids in survivors are not sensed as DNA damage that activates the checkpoint and requires repair.

As telomeres erode in pre-survivor cells, accumulation of RNA-DNA hybrids counteracts the shortening, averting fast senescence¹¹⁹. This depends on the R-loops ability to induce replication stress at telomeres and consequent Rad52-dependent HDR (discussed in more detail in section 1.2.3)^{119,120}. The lengthening reaction is proposed to consist of unequal sister chromatid exchange and/or inter-telomeric recombination, as justified by the appearance of divergent telomeric sequences^{45,114,119}.

In established survivors, the TMM active before telomeres reach a critically short length might present the same features. This is strongly supported by the observation that the abundance of RNA-DNA hybrids defines the senescence rate and R-loops prevent telomere erosion. Therefore, established survivors seem to adopt two different TMMs, one R-loops-dependent, which prevents telomere shortening and fast senescence, and one R-loops-independent, which triggers extensive lengthening at critically short telomeres. Beside R-loops, the two types of HDR might have other different requirements. In pre-survivor cells, telomere lengthening during survivor precursors formation is supposed to be limited and driven by Rad51/52 whereas maturation relies on Rad52/59-mediated pronounced extension (Figure 7)¹¹². Perhaps, the same mechanisms apply in established survivors: the recombination events preventing telomere shortening might be constrained and mediated by Rad51/52 while extensive lengthening requires Rad52/59. Additional factors, like Mus81, Mrc1 and Pif1, which are involved in averting fast senescence but are dispensable for the extensive lengthening underlying ALT-survivors formation, might also be distinctly required in the two TMMs^{205–208}.

The work from Yu et al. showed that removal of TERRA RNA-DNA hybrids abrogates type II survivors formation, thereby suggesting that the extensive lengthening at this moment relies on

a different mechanism than the one adopted in established survivors¹⁶⁹. One possible interpretation is that type II BIR depends on RNA-DNA hybrids only transiently, before the emergence of survivors. Plausibly, when adaptation to R-loops-dependent damage allows survivors to arise, telomere lengthening may occur also in absence of R-loops. In human ALT cells, TERRA RNA-DNA hybrids prevent the appearance of telomere free ends (TFEs), a sign of telomere shortening, indicating that TERRA might counteract telomere attrition in a manner similar to what observed during post-crisis senescence¹³². However, it is still unknown whether telomere recombination in humans can take place in absence of TERRA R-loops. A clue suggestive of R-loops-independent HDR would be that, despite significantly reduced, sister chromatid recombination is not completely abrogated in RNH1-overexpressing ALT human cells (see below for more details)¹³². Similarly, BIR can be still detected, although to a lower extent, in ALT human cells in which TERRA transcription is suppressed¹⁴⁰.

Overall, these observations suggest that R-loops-independent mechanisms of telomere lengthening might exist in ALT. As discussed below, ALT comprises several types of HDR, therefore it is tempting to think that the presence of R-loops might regulate the choice of adopting one over another.

4.2.2 Double effect of R-loops

In human ALT, TERRA RNA-DNA hybrids are required in a specific amount controlled by RNase H1. When the abundance of R-loops increases, replication stress in the form of pSer33-RPA accumulates at telomeres^{127,132}. Also the amount of C-circles, a sign of replication stress, augments^{128,132}. A proof of the hybrids impeding specifically replication at leading strands is the accumulation of C-rich ssDNA upon R-loops increase¹³². The effect of the hindered replication is revealed by the enhancement of TFEs, especially at leading strands. This might be due to fork stalling and collapse at the site of RNA-DNA hybrids or induction of DSBs. In either case, the final result is telomere loss. A similar scenario is observed when the helicase FANCM is removed. Because of its function in removing R-loops and alleviating TERRA R-loops-associated replication stress, FANCM depletion causes increased amount of pSer33-RPA and 53BP1, another replication stress indicator, at telomeres¹²⁷. Interestingly, removal of FANCM not only induces accumulation of C-rich ssDNA but also diminishes the amount of G-rich ssDNA. This might be due to the negative effect of R-loops on DNA resection^{189,190,192,191,209}. A similar effect is visible for Mph1, the yeast homolog of FANCM, which suppresses RNA-DNA hybrids at telomeres and the related DNA damage, as indicated by the reduction of Rad52 foci¹⁷⁷. In this case, the hybrids-associated stress is proposed to derive from the enzyme-mediated toxic recombination intermediates.

On the other hand, R-loops removal slightly alleviates telomere instability but promotes telomere loss¹³². This is believed to occur because of impaired recombination in absence of RNA-DNA hybrids, as shown by the reduction of double telomeric signals (DTSS). Similarly, repression of TERRA transcription attenuates DNA damage at telomeres, negatively affecting BITS¹⁴⁰.

Overall, these data suggest that R-loops have a double effect on ALT telomere stability. While their presence is required for BIR to take place and counteract telomere erosion, their accumulation is deleterious because of increased replication stress and potential DSBs formation. A similar scenario can be assumed to happen when hybrids control telomere resection¹⁹¹. R-loops accumulation at telomeres might inhibit both the MRX complex and Exo1, similar to what

observed at DSBs sites^{190,209}. If RNA-DNA hybrids removal causes increased telomere resection and ssDNA accumulation, checkpoint and DDR would be activated. This might be aggravated by the higher propension of ssDNA to break, leading to telomere loss. Therefore, despite R-loops removal is beneficial to relieve replication stress, it might be still responsible for genome instability. At short telomeres, the effect might be augmented. Here, the reduced binding of Cdc13 fails to counteract RPA. Moreover, since these telomeres are replicated at an earlier stage and resection might overlap with replication more frequently, replication stress might be triggered by collisions of the replisome with the resection machinery^{10,210}.

Taken together, these data might explain why R-loops removal in survivors did not alleviate checkpoint activation. When the hybrids are reduced, replication stress at telomeres is attenuated. However, reduced HDR induces telomere loss and senescence. On the other hand, increased resection might be detrimental in terms of telomere loss but beneficial for telomere recombination, as strand invasion might be facilitated.

These observations, along with the idea of survivors adapting to RNA-DNA hybrids-dependent instability, sustain the general and controlled requirement of RNA-DNA hybrids in ALT.

4.2.3 How TERRA RNA-DNA hybrids induce BIR in ALT

Yeast survivors and ALT human cells might adopt similar mechanisms to extend their telomeres. In both cases, TERRA RNA-DNA hybrids might be an important trigger.

In humans and yeast, ALT is mainly dependent on Rad52. In yeast, the protein facilitates the replacement of RPA with Rad51, thereby allowing the formation of the nucleoprotein filament involved in recombination²¹¹. In addition to this, Rad52 takes part in other repair activities, independently from Rad51. These processes require the protein single strand annealing ability reinforced by Rad59²¹¹. In humans, Rad52 seems to have kept the single strand annealing property of the yeast protein, whereas the Rad51 loading function has been inherited by BRCA2²²¹. Among the repair processes mediated by Rad52 independently from Rad51 is MiDAS, which is also important for telomere synthesis in ALT.

The common assumption is that replication stress at telomeres causes HDR-dependent telomeres lengthening. This might occur either directly by recombination between two telomeres sequences or in response to DSBs generation at the site of stress³⁶. RNA-DNA hybrids might induce this stress in both cases²¹².

In detail, replication stalling on the leading strand, where the R-loops form, might lead the newly synthesized strand to invade either the sister chromatid (sister chromatid recombination, SCR) or a different telomere molecule (inter-telomeric recombination) (Figure 33A). Sister chromatid recombination is promoted by Rad52 single strand annealing capacity and does not require Rad51²¹¹. It is reported that this form of repair prevents fast senescence presumably by allowing unequal and equal alignments between the invading strand and the donor²¹¹. Nevertheless, the appearance of fast senescence also in *rad51*Δ cells implies that Rad51-dependent HDR might take part as well²¹¹.

Interestingly, the ability of Rad52 to promote single strand annealing is essential for type II survivors, consistent with the requirement for Rad59 to generate this class of cells²¹¹. Type I survivors do not need it and might originate, instead, by long range recombination events

promoted by Rad51. Consistent with this view, type II survivors would seem to derive from a prolongation or intensification of the HDR events already taking place during senescence.

The source of this exacerbation might simply be the enhanced occurrence of short telomeres at the end of senescence. These telomeres might present so increased levels of RNA-DNA hybrids that normal SCR, or other repair activities, would take longer to resolve. As for the leading strand before mentioned, the persistence of R-loops would lead the molecule to undergo different cycles of lengthening, perhaps by iterative recombination, before the stress is relieved. This is sustained by the observation that Rad52 and recombination intermediates increase at short telomeres and that lengthening during survivors formation and maintenance is a one-step process^{101,103,111,213}.

After strand invasion and D-loop formation, the invading strand is lengthened by Pol δ , as normally proposed for a BIR reaction^{36,117}. The reaction is assisted by the BTR complex (BLM, Top3 α and Rmi1/2) (Figure 33B)²¹⁴. When the synthesis is complete, the fill-in procedure might be driven by Pol α -mediated priming events, either during the course of Pol δ -dependent synthesis or at the end. Rad52 might be involved in BIR as a starting point for the annealing between two ssDNAs or for Rad51-mediated strand invasion. However, as demonstrated by the worsened senescence profile of *est2 Δ rad52 Δ* cells compared to *est2 Δ pol32 Δ* cells, Rad52 is likely to have additional functions than prompting BIR²¹¹.

When replication stress at telomeres cannot be attenuated, like for example in case of particularly high levels of R-loops, the perseverance of replication and recombination intermediates leads to two potential fates¹²⁸. The first one is characterized by fork collapse and telomeric C-circles formation whereas the second one comprises resolution of the intermediates, with telomeres crossovers but no telomere addition (Figure 33C and D)^{128,214,215}.

Telomeric circles are a hallmark of human ALT¹²⁴. Their presence is reported in both survivor types where they display a different composition²¹⁶. In type I survivors, circles recognized by either a Y'-probe or a telomeric probe were detected, whereas type II survivors presented only TG-rich circles²¹⁶.

It is commonly accepted that telomeric circles are not only the bioproduct of replication stress but they can also be used as template for telomere synthesis^{114,217}. This is supposed to occur via a rolling circle mechanism, in which a telomere strand invades the circle and multiple rounds of synthesis extend it. It is tempting to think that short telomeres of senescent cells use this pathway to massively lengthen their telomeres in a limited time period, like the one of a single G2/M phase. Equally possible is that, once formed, survivors keep employing it for future extension events, also characterized by abrupt telomere addition (Figure 20 and 22).

The exact structure of telomeric circles is unknown but they have been reported to comprise tracts of both dsDNA and ssDNA. Given the presence of ssDNA, Rad52 might facilitate the invasion reaction by single strand annealing or by mediating Rad51-dependent recombination.

In case of resolution of recombination/replication intermediates, the SMX resolvase complex, including Slx1/4 and Mus81, cleaves the DNA intermediates resulting in not extended telomeres^{128,214,215}. This pathway counterbalances the canonical BITS promoted by the BTR complex and might be responsible for ALT maintenance upon Rad52 depletion^{121,214,215}.

In the absence of TERRA R-loops, HDR can still promote telomere elongation in established survivors (Figure 26 and 28). In this case, the lack of R-loops is expected not to trigger replication stress and the linked template switch reaction. However, it is possible that R-loops removal is not

completely detrimental for recombination. As speculated before, RNA-DNA hybrids attenuation might trigger extensive resection at telomeres, which might have a double beneficial effect on recombination: 1) replication stress might be triggered by collisions between the replisome and the resection machinery; 2) extended ssDNA overhangs, which are highly recombinogenic, are generated (Figure 34). In either case, recombination would consist of Rad52-Rad59-mediated single strand annealing or Rad51-promoted homology search. Since these reactions might equally occur in presence of R-loops, it is possible that the products from R-loops-dependent and -independent recombination are indistinguishable from one another. This fits well with the observation that recombination in established survivors produced generally similar outcomes in the absence and presence of R-loops (Figure 26 and 28).

Overall, these observations suggest that ALT relies on different lengthening mechanisms and RNA-DNA hybrids appear to have a central role in triggering and sustaining them. However, R-loops-independent HDR reactions are equally possible. The source and their physiological relevance are yet to be determined.

4.2.4 R-loops to promote a telomere-telomere interplay

In yeast, the strand invasion site during ALT might determine whether type I or type II BIR takes place. In case strand invasion occurs at a telomeric sequence that is not contiguous to a Y' element, type II BIR is promoted. When it happens at the internal TG tracts before a Y' element, type I BIR is more likely to follow.

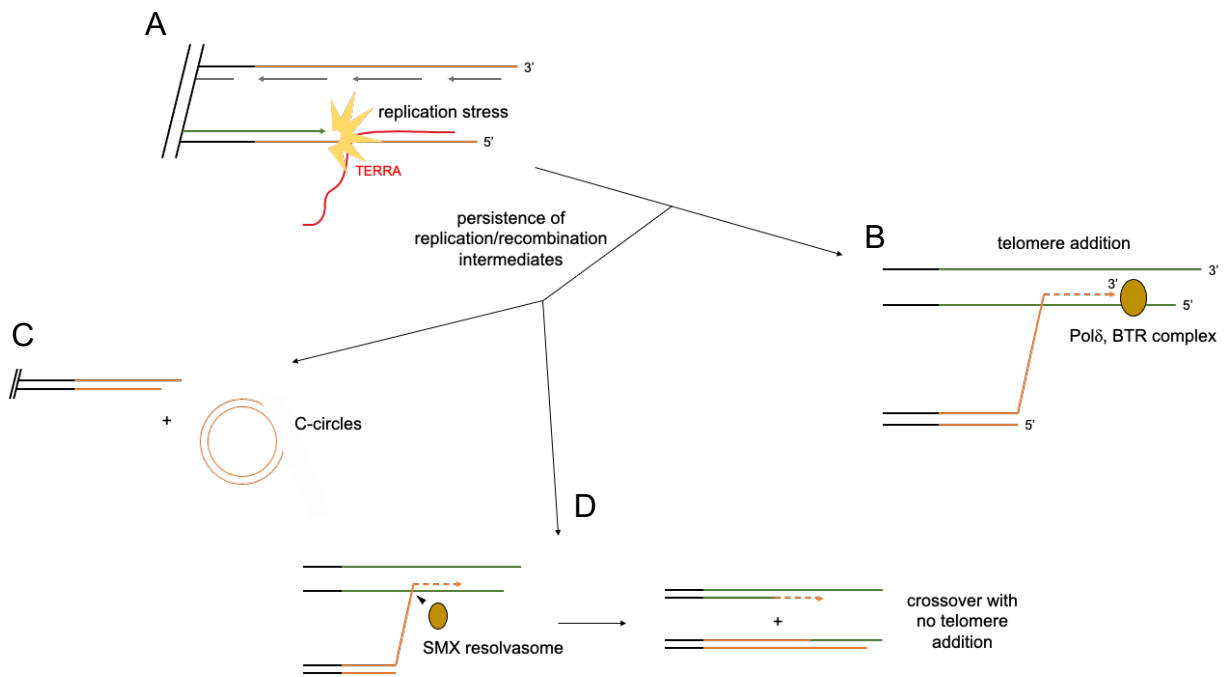


Figure 33. TERRA RNA-DNA hybrids-caused replication stress triggers BIR in ALT. A) Replication stress accumulates on the leading strand of telomeres (green arrow) when RNA-DNA hybrids are not removed. B) To resolve replication stress, inter-telomeric recombination with new telomere addition is promoted by Pol δ and the BTR complex. C) When replication/recombination intermediates persist, they can induce the formation of telomeric circles or be resolved by the SMX resolvosome (D). In this latter case, the result is a crossover without telomere addition.

RNA-DNA hybrids might have a role in telomeres recombination not only by causing replication stress and starting the reaction but also by generating a structure favorable for strand invasion. In this case, TERRA RNA-DNA hybrids might assemble a protein platform that assists recombination and/or induce a recombination-prone conformation of the double helix¹⁷⁴. In support of the former scenario, a recent work in humans has demonstrated the interaction between TERRA and BRCA1¹⁴⁹. Since BRCA1 promotes Rad51 nucleoprotein formation and increases its recombinase ability, it is very likely that the interaction with the lncRNA supports recombination at telomeres²¹⁸. However, TERRA has also been seen to interact with factors responsible for telomere heterochromatinization, a potential inhibitor of recombination^{133,141,166}. Perhaps, the transcript dynamically interacts with these proteins and in the event of HDR, heterochromatin factors are less present.

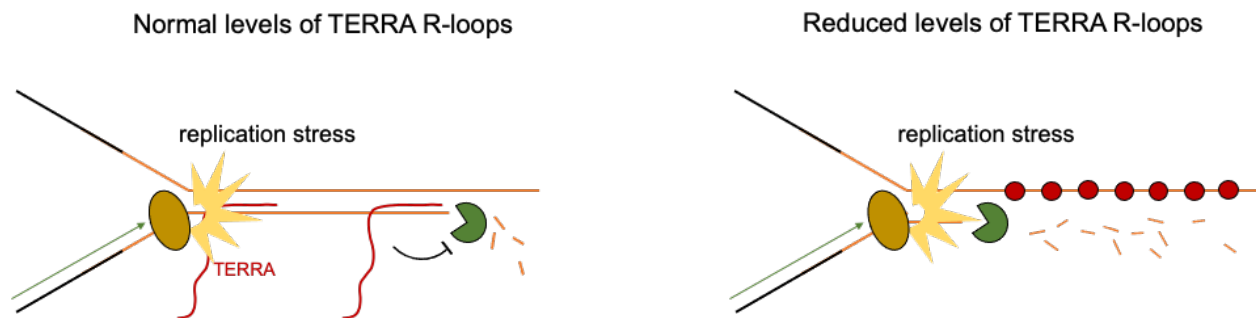


Figure 34. Schematic to illustrate how R-loops removal might trigger replicative stress and extensive resection at telomeres. When RNA-DNA hybrids form at telomeres (left panel), they might impede the activity of the resection machinery (section in green). At the same time, they induce replicative stress as the replisome (dark yellow oval) approaches the chromosome ends. When RNA-DNA hybrids are removed (right panel), like for example upon RNH1 overexpression, resection is not hampered and continues until colliding with the replisome. This might cause replicative stress. Simultaneously, long ssDNA overhangs generate, favoring telomeric recombination. The red ovals represent Rad51 proteins.

The R-loop structure may retain the ability to evolve into a D-loop during recombination. This would necessitate a coordination between RNA-DNA hybrids negative regulators, especially helicases such as SETX and/or FANCM, and Rad51^{127,219}. It is also possible that topological changes arising from transcription and/or replication, along with the direct effect of topoisomerases, play a role²²⁰.

As indicated by the formation of Y'-containing and Y'-free telomeric circles, replication stress followed by circles formation seems to be equally probable at Y' telomeres and X-only telomeres. Given the role of RNA-DNA hybrids in promoting replication stress, it is likely that genotoxic R-loops form at both telomere types. However, the euchromatic constitution of Y' elements, along with their elevated transcription, might render these regions a preferable target for

recombination⁸⁵. This might help explain why Y' translocation is a frequent event in telomere recombination.

TERRA R-loops can form in *trans* in a Rad51-mediated manner¹⁷⁴. This property can be used from one telomere expressing the RNA to influence the homeostasis of another telomere. At telomeric circles, TERRA from one telomere might be induced by Rad51 to form hybrids and favor telomere recombination via rolling circle. If the telomere producing TERRA is the shortest one, the hybrids at its TG repeats and on the circle would provide means for both recombination start and progress, respectively.

In the present study, it was frequently observed that TERRA upregulation as telomeres shortened occurred at the same time at telomere 1L and 15L, even when telomeres presented different initial lengths (Figure 20, 22 and 23). In order for this to occur, telomeres are supposed to shorten at different rates, with the extended one shortening faster and the short one shortening slower. To allow such interplay between telomeres, TERRA and its ability to form hybrids in *trans* might be involved. According to the same principle, TERRA overexpressed from a short telomere might form recombinogenic hybrids at other telomeres to facilitate the short telomere extension via inter-telomeres recombination. For the same purpose, overexpressed TERRA might trigger the RNA upregulation at other chromosome termini.

This TERRA-mediated interplay between different telomeres is suggested also by other works. The Blasco lab recently described that suppression of TERRA transcription from a single telomere provoked a widespread telomere loss and deprotection effect in human ALT cells²²¹. One possibility to interpret this result is that TERRA transcribed from one telomere can regulate the state of other telomeres, very likely by forming hybrids in *trans*. The long-range effect of TERRA has been described also in mice cells, where the transcript affects gene expression at non-telomeric loci, and yeast, where TERRA is exported into the cytoplasm in response to oxidative stress^{163,164}.

Taken together, these observations reveal that TERRA with its ability to form R-loops might be important for establishing a signaling network among telomeres and beyond. In ALT, this phenomenon might be further exacerbated to facilitate telomere recombination.

5. Conclusion

In this study, *Saccharomyces cerevisiae* post-senescent survivors were employed to address TERRA regulation and its influence on the alternative lengthening mechanism of telomere maintenance. The data obtained trace an interesting parallelism between ALT survivors and pre-survivors senescent cells. Both types of telomerase-negative cells shorten their telomeres in a gradual manner. This phenomenon is accompanied by progressive loss of replicative potential and TERRA increase (Figure 35). Consistent with it, the lncRNA reaches the maximum of its expression when cells accumulate the shortest telomere. Like in senescent cells, ALT-survivors seem to upregulate the transcript mainly due to impaired Rat1-dependent degradation. However, enhanced transcription cannot be excluded. Similarly, RNA-DNA hybrids might accumulate at the shortest telomere in response to less binding of RNase H2.

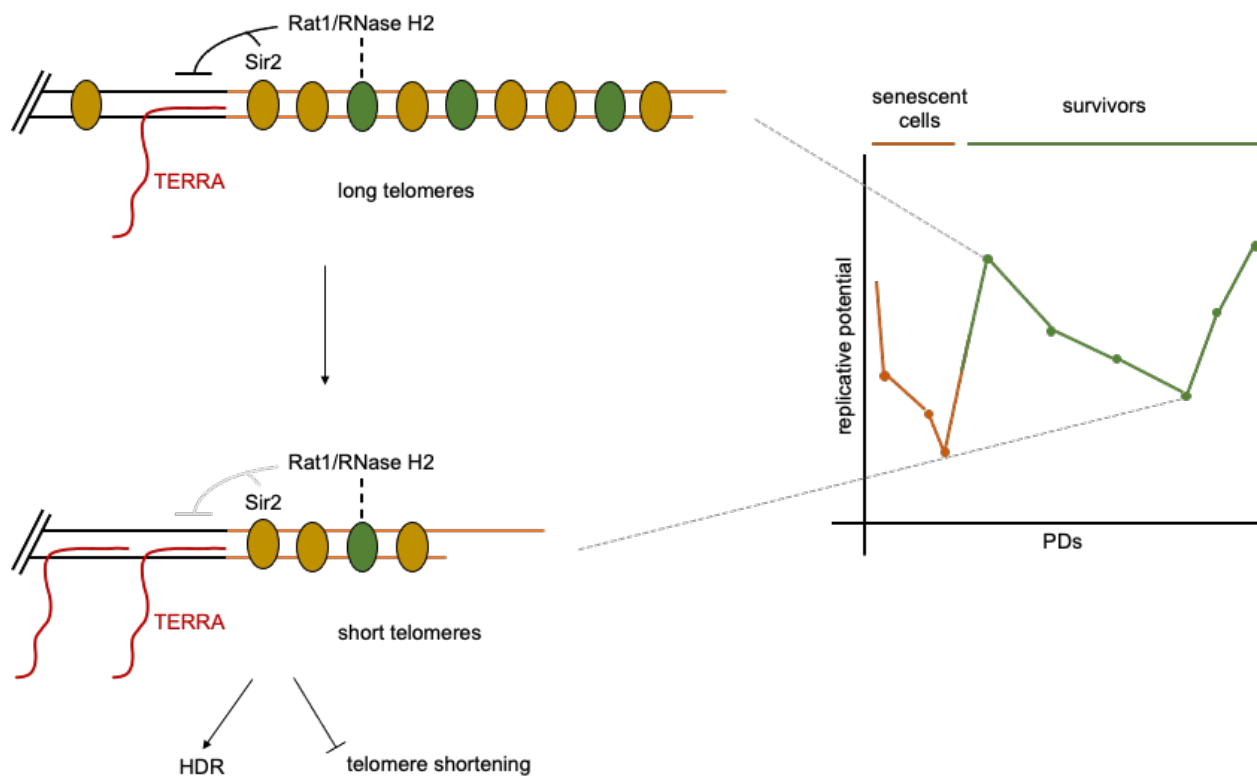


Figure 35. Model to correlate telomere shortening with TERRA upregulation during post-crisis senescence. After survivors formation, long telomeres present increased amounts of Rat1, Rnh201 and Sir2. These factors impact negatively on TERRA expression. As telomeres shorten senescence is triggered and TERRA expression is enhanced due to lower binding of the negative regulators. TERRA R-loops counteract telomere shortening and senescence. When critically short telomeres accumulate, telomere HDR promotes extension, re-establishing the negative regulation on TERRA expression.

In senescent cells, the accumulation of RNA-DNA hybrids at short telomeres is proposed to trigger HDR and allow survivors formation. In type II survivors, despite the same reaction is equally possible, an alternative and R-loops-independent means has been observed to mediate extensive

recombination. This mechanism differs from the one counteracting telomere shortening, which relies on RNA-DNA hybrids.

Overall, given the similarities existing between telomere maintenance in senescent cells and survivors, it might be possible that ALT is a reaction physiologically occurring when short telomeres accumulate, with no gross genetic changes required. While senescent cells need DDR to respond to telomere instability and enable survivors formation, established ALT cells might adapt to stress. This would allow them to proliferate infinitely despite the genomic instability.

If future studies uncover a post-crisis senescence phenotype in ALT human cancer cells, TERRA detection and manipulation will be important diagnostic and therapeutic means, respectively. In particular, TERRA measurements during tumor progression might reveal when cancer cells are at their lowest replicative potential and probably more vulnerable for treatment. The presence of heterogeneous populations with cells presenting different telomere lengths might represent an obstacle to such application. However, as demonstrated in this study, TERRA upregulation at critically short telomeres in senescing survivors is detectable also in mixed populations.

As for the therapeutic applications, inhibition of TERRA transcription and/or suppression of TERRA RNA-DNA hybrids might be an important tool to accelerate telomere shortening and reduce the tumor life span¹¹. This type of treatment will probably be parallel to the one counteracting resistance when TERRA R-loops-independent TMMs emerge.

5. Materials and Methods

5.1. Materials

5.1.1 Yeast strains

Name	Features	Description	Source
yDB13	Wild-type A	<i>MATα</i> ; <i>his3Δ1</i> ; <i>leu2Δ0</i> ; <i>ura3Δ0</i> ; <i>met15Δ0</i> ; <i>bar1::KAN + pBL189-URA3</i>	Diego Bonetti
yDB15	Wild-type B	<i>MATα</i> ; <i>his3Δ1</i> ; <i>leu2Δ0</i> ; <i>ura3Δ0</i> ; <i>met15Δ0</i> ; <i>bar1::KAN + pBL189-URA3</i>	Diego Bonetti
yDB05	Survivor A	<i>MATα</i> ; <i>his3Δ1</i> ; <i>leu2Δ0</i> ; <i>ura3Δ0</i> ; <i>met15Δ0</i> ; <i>bar1::KAN</i> ; <i>tlc1::HIS3</i>	Diego Bonetti
yDB06	Survivor B	<i>MATα</i> ; <i>his3Δ1</i> ; <i>leu2Δ0</i> ; <i>ura3Δ0</i> ; <i>met15Δ0</i> ; <i>bar1::KAN</i> ; <i>tlc1::HIS3</i>	Diego Bonetti
yDB07	Survivor C	<i>MATα</i> ; <i>his3Δ1</i> ; <i>leu2Δ0</i> ; <i>ura3Δ0</i> ; <i>met15Δ0</i> ; <i>bar1::KAN</i> ; <i>tlc1::HIS3</i>	Diego Bonetti
yDB08	Survivor D	<i>MATα</i> ; <i>his3Δ1</i> ; <i>leu2Δ0</i> ; <i>ura3Δ0</i> ; <i>met15Δ0</i> ; <i>bar1::KAN</i> ; <i>tlc1::HIS3</i>	Diego Bonetti
ySM269	Wild-type (Rat1 no-TAP)	<i>MATα</i> ; <i>his3Δ1</i> ; <i>leu2Δ0</i> ; <i>ura3Δ0</i> ; <i>met15Δ0</i>	Present study
ySM270	Wild-type (Rat1 no-TAP)	<i>MATα</i> ; <i>his3Δ1</i> ; <i>leu2Δ0</i> ; <i>ura3Δ0</i> ; <i>met15Δ0</i>	Present study
yBL7	Wild-type	<i>MATα</i> ; <i>his3Δ1</i> ; <i>leu2Δ0</i> ; <i>ura3Δ0</i> ; <i>met15Δ0</i>	Brian Luke
ySM 272	Wild-type (Rat1-TAP)	<i>MATα</i> ; <i>his3Δ1</i> ; <i>leu2Δ0</i> ; <i>ura3Δ0</i> ; <i>met15Δ0</i> ; <i>rat1-TAP::HIS3</i>	Present study
ySM273	Wild-type (Rat1-TAP)	<i>MATα</i> ; <i>his3Δ1</i> ; <i>leu2Δ0</i> ; <i>ura3Δ0</i> ; <i>met15Δ0</i> ; <i>rat1-TAP::HIS3</i>	Present study
ySM281	Survivor (Rat1 no-TAP)	<i>MATα</i> ; <i>his3Δ1</i> ; <i>leu2Δ0</i> ; <i>ura3Δ0</i> ; <i>met15Δ0</i> ; <i>tlc1::NAT</i>	Present study
ySM282	Survivor (Rat1 no-TAP)	<i>MATα</i> ; <i>his3Δ1</i> ; <i>leu2Δ0</i> ; <i>ura3Δ0</i> ; <i>met15Δ0</i> ; <i>tlc1::NAT</i>	Present study
ySM283	Survivor (Rat1 no-TAP)	<i>MATα</i> ; <i>his3Δ1</i> ; <i>leu2Δ0</i> ; <i>ura3Δ0</i> ; <i>met15Δ0</i> ; <i>tlc1::NAT</i>	Present study
ySM284	Survivor (Rat1-TAP)	<i>MATα</i> ; <i>his3Δ1</i> ; <i>leu2Δ0</i> ; <i>ura3Δ0</i> ; <i>met15Δ0</i> ; <i>tlc1::NAT</i> ; <i>rat1-TAP::HIS3</i>	Present study
ySM285	Survivor (Rat1-TAP)	<i>MATα</i> ; <i>his3Δ1</i> ; <i>leu2Δ0</i> ; <i>ura3Δ0</i> ; <i>met15Δ0</i> ; <i>tlc1::NAT</i> ; <i>rat1-TAP::HIS3</i>	Present study

ySM286	Survivor (Rat1-TAP)	<i>MATα; his3Δ1; leu2Δ0; ura3Δ0; met15Δ0; tlc1::NAT; rat1-TAP::HIS3</i>	Present study
ySM321	Survivor (Rnh201 no-TAP)	<i>his3Δ1; leu2Δ0; ura3Δ0; met15Δ0; est2::NAT</i>	Present study
ySM322	Survivor (Rnh201 no-TAP)	<i>his3Δ1; leu2Δ0; ura3Δ0; met15Δ0; est2::NAT</i>	Present study
ySM326	Survivor (Rnh201-TAP)	<i>his3Δ1; leu2Δ0; ura3Δ0; met15Δ0; est2::NAT; rnh201-TAP::HIS</i>	Present study
ySM329	Survivor (Rnh201-TAP)	<i>his3Δ1; leu2Δ0; ura3Δ0; met15Δ0; est2::NAT; rnh201-TAP::HIS</i>	Present study
ySM338	Wild-type (Rnh201-TAP)	<i>his3Δ1; leu2Δ0; ura3Δ0; met15Δ0; rnh201-TAP::HIS</i>	Present study
ySM342	Wild-type (Rnh201-TAP)	<i>his3Δ1; leu2Δ0; ura3Δ0; met15Δ0; rnh201-TAP::HIS</i>	Present study
ySM345	Wild-type (Rnh201 no-TAP)	<i>his3Δ1; leu2Δ0; ura3Δ0; met15Δ0;</i>	Present study
ySM346	Wild-type (Rnh201 no-TAP)	<i>his3Δ1; leu2Δ0; ura3Δ0; met15Δ0;</i>	Present study
ySM81-86	Survivor to be transformed with pBL211 (EV) or pBL352 (RNH1)	<i>MATα; his3Δ1; leu2Δ0; ura3Δ0; met15Δ0; tlc1::HIS</i>	Tina Wagner
yVP345	Survivor (<i>rnh201Δ</i>) to be transformed with pBL97 (EV) or pBL401 (RNH201)	<i>MATα; his3Δ1; leu2Δ0; ura3Δ0; met15Δ0; tlc1::NAT; rnh201::HYG</i>	Vanessa Pires
yVP347	Survivor (<i>rnh201Δ</i>) to be transformed with pBL97 (EV) or pBL401 (RNH201)	<i>MATα; his3Δ1; leu2Δ0; ura3Δ0; met15Δ0; tlc1::NAT; rnh201::HYG</i>	Vanessa Pires
ySM518-530	Survivor (<i>rnh201Δ</i>) to be transformed with pBL97 (EV) or pBL401 (RNH201)	<i>his3Δ1; leu2Δ0; ura3Δ0; met15Δ0; est2::HYG; rnh201::NAT</i>	Present study
ySM123	yDB05 passaged in liquid culture: 1L telomere length is of ~ 400 bp)	<i>MATα; his3Δ1; leu2Δ0; ura3Δ0; met15Δ0; bar1::KAN; tlc1::HIS3</i>	Present study

5.1.2 Plasmids

Name	Description	Source
pSM2	pRS316; <i>TLC1</i> ; CEN; <i>URA3</i>	Kathy Friedman

pBB39	pRS426; <i>pGPD-RNH1-HA</i> ; 2 μ ; <i>URA3</i>	(Balk et al., 2013)
pBL97	pRS316; CEN; <i>URA3</i>	Matthias Peter
pBL211	pRS425; <i>pGal</i> ; 2 μ ; <i>LEU2</i>	Matthias Peter
pBL352	pRS425; <i>pGal-RNH1-HA</i> ; 2 μ ; <i>LEU2</i>	Brian Luke
pBL189	pRS426; <i>pGPD</i> ; 2 μ ; <i>URA3</i>	(Balk et al., 2013)
pBL401	pRS316; <i>RNH201</i> ; CEN; <i>URA3</i>	Brian Luke

5.1.3 Oligonucleotides

Name	Sequence	Purpose
oSM1	GAAGCGGATGGTAATGAGAC	Fw – 1L probe for Southern blot
oSM2	AGATGTATGATGCTGGGGAG	Rv – 1L probe for Southern blot; Junction PCR: 1L tel
oSM3	TCTTGATGTGTCTTCACAAG	Fw – 15L probe for Southern blot
oSM4	ATTCTCACCATCAAAGAAG	Rv – 15L probe for Southern blot
oSM5	CTATCTGCTTAGTCGAGGAGAAC	Fw – Junction PCR: Y' elements
oSM9	ATGCTGCCATGGATTCAACC	Rv – Junction PCR: 15L tel
oLK49	GGCTTGGAGGAGACGTACATG	Fw – RT-qPCR: 6 Y' tel
oLK50	CTCGCTGTCACTCCTTACCCG	Rv – RT-qPCR: 6 Y' tel
oLK57	GGGTAACGAGTGGGGAGGTAA	Fw – RT-qPCR: 15L tel
oLK58	CAACACTACCCTAATCTAACCTGT	Rv – RT-qPCR: 15L tel
oBL207	CACCACACCCACACACCACCCACA	Reverse transcription
oBL240	AAGAGGCATACCTCCGCCTATC	Rv – Reverse transcription; RT-qPCR: Tlc1
oBL241	TTGGTGTGTTGATTACAGCT	Fw – RT-qPCR: Tlc1
oBL292	CCCAGGTATTGCCGAAAGAATGC	Fw – RT-qPCR: Actin
oBL293	TTTGTGGAAGGTAGTCAAAGAAGCC	Rv – RT-qPCR: Actin
oBL295	CGGTGGGTGAGTGGTAGTAAGTAGA	Fw – RT-qPCR: 1L tel
oBL296	ACCCTGTCCCATTCAACCATAC	Rv – RT-qPCR: 1L tel
oBL358	GCGGTACCAGGGTTAGATTAGGGCTG	Rv – Telo-PCR: 1L tel
oBL359	CGGGATCCGGGGGGGGGGGGGGGGGG	Fw – Telo-PCR: oligo-dG

5.1.4 Liquid media

YPD medium	
ddH ₂ O	900 ml
Peptone	17.6 g

Bacto Yeast Extract	8.8 g
Autoclave	20 min at 121°C
20% Glucose	100 ml (final: 2%)

SC medium

ddH ₂ O	900/800 ml
Yeast Nitrogen Base without Aminoacids	6.7 g
Yeast Synthetic Dropout Medium without Aminoacids	1.9/1.6 g
Autoclave	20 min at 121°C
20% Glucose	100 ml (final: 2%)
or	
20% Raffinose	100 ml (final: 2%)
+/-	+/-
20% Galactose	100 ml (final: 2%)

Sporulation medium

ddH ₂ O	990 ml
KAc	10 g (final: 1%)
5 mg/ml ZnAc	10 ml
NaCl	10 g
Autoclave	20 min at 121°C

LB medium

ddH ₂ O	to 1000 ml
Bacto Tryptone	10 g
Bacto Yeast Extract	5 g
NaCl	10 g
Autoclave	20 min at 121°C
100 mg/ml Carbenicillin (when present)	1 ml

5.1.5 Solid media

Agar plates

ddH ₂ O	to 1000 ml
Peptone	100 g
Bacto Yeast Extract	50 g
20% Glucose	100 ml (final: 2%)
Agar	100 g
Autoclave	20 min at 121°C
50 mg/ml KAN (G418) (when present)	5 ml
100 mg/ml HYG (when present)	3 ml
100 mg/ml NAT (when present)	1 ml

SC plates

ddH ₂ O	to 900 ml
Yeast Nitrogen Base without Aminoacids	6.7 g
Yeast Synthetic Dropout Medium without Aminoacids	1.9 g
Agar	100 g
Autoclave	20 min at 121°C
20% Glucose	100 ml (final: 2%)
50 mg/ml KAN (G418) (when present)	5 ml
100 mg/ml HYG (when present)	3 ml
100 mg/ml NAT (when present)	1 ml

Pre-sporulation plates

ddH ₂ O	750 ml
Bacto Yeast Extract	10 g
Standard Nutrient Broth	30 g
Autoclave	20 min at 121°C
20% Glucose	250 ml (final: 5%)

LB plates

ddH ₂ O	to 1000 ml
Bacto Tryptone	10 g
Bacto Yeast Extract	5 g
NaCl	10 g
Agar	15 g
Autoclave	20 min at 121°C
Ampicillin (when present)	100 mg

5.1.6 Buffers

	10X TE
TRIS (pH 7.5)	0.1 M
0.5 M EDTA (pH 8.0)	10 mM
Autoclave	20 min at 121°C

	10X TBE
Boric acid	0.89 M
Tris base	0.89 M
Na ₂ EDTA (pH 8.0)	20 mM

	10X PBS
KCl	30 mM
NaCl	1.37 M
KH ₂ PO ₄	20 mM
Na ₂ HPO ₄ x 2 H ₂ O	80 mM
pH adjusted to 7.4	
Autoclave	20 min at 121°C

	LiAc-Mix
LiAc	0.1 M
TE	1X

	PEG-Mix
PEG 400	40 % in LiAc Mix
Autoclave	20 min at 121°C

AE-buffer

NaAc (pH 5.3)	50 mM
EDTA	10 mM

FA Lysis Buffer -SOD

NaCl	140 mM
HEPES (pH 7.5)	50 mM
Triton X-100	1%
EDTA (pH 8.0)	1 mM

FA Lysis Buffer +SOD

NaCl	140 mM
HEPES (pH 7.5)	50 mM
Triton X-100	1%
EDTA (pH 8.0)	1 mM
Sodium deoxycholate	2.4 mM

FA Lysis Buffer 500

NaCl	0.5 M
HEPES (pH 7.5)	50 mM
Triton X-100	1%
EDTA (pH 8.0)	1 mM
Sodium deoxycholate	2.4 mM

Buffer III

LiCl	250 mM
Tris-HCl (pH 8.0)	10 mM
NP-40	1%
EDTA (pH 8.0)	1 mM
Sodium deoxycholate	24 mM

Elution Buffer

SDS	1%
Tris-HCl (pH 7.5)	50 mM
EDTA (pH 8.0)	10 mM

Solution 1

β -mercaptoethanol	1.09 M
NaOH	1.85 M

Solution 2

Trichloroacetic acid	50%
----------------------	-----

Solution 3

Acetone	100%
---------	------

Urea Buffer

Urea	8 M
Glycerol	5%
β -mercaptoethanol	143 mM
Tris-HCl (pH 6.8)	120 mM
SDS	8%
Bromophenol blue	

Running Buffer

Glycine	1.92 M
Tris-HCl	250 mM
SDS	0.1%

Transfer Buffer

Absolute ethanol	20%
5X Bio-Rad transfer buffer	20%

1X PBS-Tween

Tween-20	0.1%
PBS	1X

Blocking Buffer

Skim milk powder	5%
------------------	----

Denaturing Solution

NaOH	0.4 M
NaCl	0.6 M

Neutralizing Solution

Trizma base	1 M
NaCl	1.5 M
pH adjusted to 7.4 via HCl	

20X SSC

Sodium citrate tribasic dihydrate	0.3 M
NaCl	3 M
pH adjusted to 7.0 via HCl	

5.1.7 Reagents and additional materials

Primary antibodies

Name	Supplier
rabbit monoclonal PAP	Sigma-Aldrich
rabbit polyclonal α -pS2 RNA pol II	Abcam
mouse monoclonal α -Pgk1	Invitrogen
rabbit polyclonal α -Sir2	Santa Cruz

rabbit polyclonal α -Rnr3	Agrisera Antibodies
mouse monoclonal α -Myc tag	Cell Signaling/NEB

Secondary antibodies

Name	Supplier
goat α -rabbit (GAR) conjugated with HRP	Bio-Rad
goat α -mouse (GAM) conjugated with HRP	Bio-Rad

Enzymes

Name	Supplier
XhoI	NEB
Sall	NEB
PvuII	NEB
EcoRI	NEB
DNase I	QIAGEN
SuperScript III Reverse Transcriptase	Invitrogen
Lyticase	Sigma-Aldrich
RNase A	Thermo Scientific
Proteinase K	QIAGEN
Phusion Hot Start II DNA polymerase	Thermo Scientific
Terminal transferase	Thermo Scientific

Reaction mixes/buffers

Name	Supplier
2X Phusion High-Fidelity PCR Master Mix with HF buffer	NEB
2X Taq Mastermix	NEB
DyNAmo Flash SYBR-Green	Applied Biosystems
Cut Smart	NEB
First Strand buffer	Invitrogen
RDD buffer	QIAGEN
NEB 4 buffer	NEB

Others

Name	Supplier
Media reagents	Sigma-Aldrich
SC medium supplemented without aminoacids	MP Biomedicals
Agarose	Sigma-Aldrich
DMSO	Sigma-Aldrich
Yeastmarker Carrier DNA	Clontech
PEG 400	Sigma-Aldrich
Glycerol	Grüssing
α -factor	Zymo Research
Hydroxyurea	Sigma-Aldrich
D-Sorbitol	Sigma-Aldrich
β -mercaptoethanol	Sigma-Aldrich
Absolute ethanol	Sigma-Aldrich
Isopropanol	Sigma-Aldrich
RedSafe	iNtRON Biotechnology
SYBR Safe	Invitrogen
Trizma base	Sigma-Aldrich

PerfectHyb Plus hybridization buffer	Sigma-Aldrich
dATP [α - ³² P]	Perkin Elmer/ Hartmann Analytic
SDS 20%	AppliChem
DEPC H ₂ O	Sigma-Aldrich
Phenol	Sigma-Aldrich
Phenol:Chloroform:Isoamyl alcohol (25:24:1)	Sigma-Aldrich
dNTPs (25 mM for each dNTP)	NEB
DTT	Invitrogen
RNase OUT	Invitrogen
Formaldehyde 37%	AppliChem
Glycine	AppliChem/ Sigma-Aldrich
HEPES	AppliChem
Triton X-100	Sigma-Aldrich
LiCl	AppliChem
Sodium deoxycholate	Sigma-Aldrich
NP-40	AppliChem
cOmplete Mini EDTA-free Protease Inhibitor Cocktail Tablets	Roche
Bradford	AppliChem
nProtein (A or G) Sepharose 4 Fast Flow	GE Healthcare
IgG Sepharose 6 Fast Flow	GE Healthcare
BSA (20 mg/ml)	NEB
Trichloroacetic acid	Sigma-Aldrich
Urea	Sigma-Aldrich
Bromophenol blue	Sigma-Aldrich
Skim milk powder	Sigma-Aldrich
Tween-20	Sigma-Aldrich
SuperSignal West Dura Extended Duration Substrate	Thermo Scientific
SuperSignal West Pico Extended Duration Substrate	Thermo Scientific
Methyl methasulfonate	Sigma-Aldrich
SYTOX Green	Thermo Scientific

Ladders

Name	Supplier
100 bp DNA ladder	NEB
1 kb DNA ladder	NEB
Prestained Protein Marker, broad range	NEB

Additional materials

Name	Supplier
Neutral nylon membrane (Hybond-NX)	GE Healthcare
Positively charged nylon membrane	Roche
Hard-Shell 384-Well PCR plates	Bio-Rad
Microseal "B" PCR Adhesive Seal	Bio-Rad
FastPrep Lysing Matrix C tubes	MP Biomedicals
15 ml Bioruptor Pico Tubes	Diagenode
Sonication beads	Diagenode
Mini-PROTEAN TGX Precast Gels 4-15%	Bio-Rad
Mini-PROTEAN TGX Precast Gels 7.5%	Bio-Rad
Amersham Protran Premium Nitrocellulose Membrane	GE Healthcare

5.1.8 Commercial assays

Name	Supplier
QIAprep Spin Miniprep Kit	QIAGEN
QIAquick Gel Extraction Kit	QIAGEN
QIAquick PCR Purification Kit	QIAGEN
DECAprime II DNA Labeling Kit	Thermo Scientific
RNeasy MinElute Cleanup Kit	QIAGEN

5.1.9 Electronic instrumentation

Name	Supplier
Dissection Microscope MSM 400	Singer Instruments
Spectrophotometer Ultrospec 2100 pro	Biochrom

PowerPac Basic	Bio-Rad
ChemiDoc Touch Imaging System	Bio-Rad
NanoDrop 2000	Thermo Scientific
C1000 Touch Thermal Cycler	Bio-Rad
UV Stratalinker 2400	Stratagene
Hybridization oven OV3	Biometra
Typhoon FLA 9500	GE Healthcare
CFX384 Touch Real-Time PCR Detection System	Bio-Rad
BioRuptor Pico	Diagenode
BioRuptor water cooling system	Diagenode
FastPrep-25	MP Biomedicals
Trans-Blot Turbo Transfer System	Bio-Rad
BD FACSVers	Becton Dickinson

5.1.10 Software

Name	Supplier
SnapGene	GSL Biotech
Image Lab	Bio-Rad
Typhoon FLA 9500 Control Software	GE Healthcare
CFX Manager 3.1	Bio-Rad
Image J	NIH
Prism 7	GraphPad
FACSuite 1.0.5	Becton Dickinson

5.2. Methods

5.2.1 Yeast and bacteria manipulation

5.2.1.1 Yeast mating, sporulation and tetrad dissection

In order to generate diploid cells, haploid cells with different mating types (MAT α and MAT α) were streaked to single colonies on YPD plates and left growing for 2 days at the appropriate temperature. Once grown, two colonies, one from each mating type, were patched together on double-selection plates and incubated overnight at the appropriate temperature. Part of the

patch was then streaked to single colonies on double-selection plates to isolate diploid cells after 2 days of growth at required temperature.

In order to induce sporulation, diploid cells were streaked to single colonies on YPD or selective plates and left growing for 2 days at the appropriate temperature. After that, a single colony was patched on a pre-sporulation plate and incubated overnight at the appropriate temperature. Sporulation was induced by resuspending the entire patch in 3 ml sporulation medium, followed by incubation for the required time (usually 5-7 days) at 23°C. Tetrads formation was assessed under the microscope. When a relevant number of tetrads was observed, 10 µl sporulating cells were mixed with 10 µl lyticase and incubated for 20 min at room temperature. After mixing, 10 µl were transferred on YPD or selective plates and dissection took place by micromanipulation. The spores were left growing for 2-3 days at the appropriate temperature.

5.2.1.2 Yeast transformation

Overnight cultures were diluted to OD₆₀₀ 0.1 in 25 ml YPD or selective medium and grown to OD₆₀₀ 0.3-0.7 at the appropriate temperature. Cells were pelleted and resuspended in 5 ml LiAc-mix. After centrifugation, the pellet was resuspended in 250 µl LiAc-mix and 100 µl of the resulting mix were combined with 300-500 ng plasmid, or 7-10 µl PCR product, 10 µl Yeastmarker Carrier DNA and 700 µl PEG-mix. After mixing, the suspension was kept rotating for 30 min at room temperature and heat shock was induced for 15 min at 42°C. Following, the cells were pelleted and resuspended in 300 µl YPD medium and left growing for 30 min at the appropriate temperature. In case of exogenous DNA integration into the genome, cells were incubated up to 8 hrs. After that, 250 µl of the final suspension was plated on selective plates and grown for 2 days at the required temperature.

When competent cells needed to be stored at -80°C, 93 µl of the cells-LiAc suspension was mixed with 7 µl DMSO and kept at -80°C until needed.

5.2.1.3 Bacteria transformation

E. coli DH5α cells were thawed at room temperature and 50 µl were mixed with 100 ng plasmid. After 20 min on ice, cells were heat shocked for 1 min at 42°C and incubated on ice for additional 2 min, followed by resuspension in 300 µl LB medium. After 30 min of incubation at 37°C, cells were plated on selective plates and incubated overnight at 37°C.

5.2.2 TERRA analysis

5.2.2.1 RNA extraction and clean-ups

Cells from overnight cultures were grown to exponential phase in 15 ml of appropriate medium at the required temperature. After pelleting, cells were resuspended in 400 µl AE-buffer and mixed with 20 µl 20% SDS and 500 µl pre-equilibrated phenol. The resulting mix was incubated for 5 min at 65°C and subsequently on ice for 5 min. Following, the samples were centrifuged at 4°C for 3 min at 14000 rpm. The supernatant was mixed with 500 µl phenol-chloroform (1:1) and

incubated for 5 min at room temperature. After that, the samples were centrifuged as before and the supernatant combined with 40 μ l 3M NaAc and 1 ml 100% ethanol. The resulting mix was incubated for 30 min at -20°C . Subsequently, the samples were centrifuged as previously described and the pellet was washed with 1 ml 80% ethanol and resuspended in a solution composed of 86 μ l H_2O , 10 μ l RDD buffer and 4 μ l DNase I. Followed an incubation of 1 hr at 37°C . To further purify the RNA content, 50 μ g RNA were purified 3 consecutive times with the RNeasy kit. Incubation with 87 μ l H_2O , 10 μ l RDD buffer and 3 μ l DNase I at 37°C took place between each clean-up step. During the final step, RNA was eluted in 30 μ l H_2O .

5.2.2.2 Reverse transcription

3 μ g RNA were diluted in a final volume of 7 μ l and mixed with 0.4 μ l dNTPs (25 mM each stock), 1 μ l oligo oBL207 (10 μ M stock), 0.4 μ l oligo oBL293 (10 μ M stock) and 4.2 μ l H_2O . Following, the samples were first heated for 1 min at 90°C and then brought with a gradient of ca. $0.8^{\circ}\text{C}/\text{sec}$ to a temperature of 55°C . At this step, a mix composed of 1 μ l DTT (0.1M stock), 1 μ l SuperScript III Reverse Transcriptase, 1 μ l RNase OUT and 4 μ l First Strand buffer (5X stock) was added and samples were kept first for 1 hr at 65°C and then for 15 min at 70°C . The same reaction was performed in parallel in absence of reverse transcriptase (1 μ l H_2O was added instead) to generate the corresponding negative control. Once the cDNA was synthesized, 30 μ l H_2O were added to both the reverse transcriptase-containing samples and the controls.

5.2.2.3 RT-qPCR

1 μ l cDNA was combined with 1 μ l each primer (section 5.1.3), 2 μ l water, 5 μ l SYBR-Green. qPCR was carried out by denaturing DNA at 95°C for 10 min, followed by 40 cycles of 15 sec at 95°C , 1 min at 60°C to measure the signal amount. TERRA levels were normalized to actin by calculating $\Delta\text{Ct} = \text{Ct TERRA} - \text{Ct actin}$ for each sample.

5.2.3 Telomere analysis

5.2.3.1 Genomic DNA extraction

Cells were grown in 30 ml of the appropriate medium from OD_{600} : 0.2 to OD_{600} : 0.6-0.8 and pelleted. Cells were resuspended then in 1 ml of a 0.9 M sorbitol + 0.1 M EDTA pH 8 solution and pelleted again. After removing the supernatant, the pellet was resuspended in the same solution supplemented with β -mercaptoethanol (1:1000) and mixed with 20 μ l lyticase (2.5 mg/ml stock). Followed an incubation for 1 hr at 45°C . After checking the formation of spheroplasts, cells were pelleted, resuspended in 400 μ l 1X TE and mixed with 90 μ l of a 500 μ l 0.5 M EDTA pH 8, 200 μ l 1M Tris-base, 100 μ l 20% SDS and 100 μ l H_2O solution. The resulting mix was incubated then for 30 min at 65°C , followed by the addition of 80 μ l 5M KAc and immediate transfer on ice. After 1 hr on ice, the samples were centrifuged for 15 min at 4°C and the supernatant was added to 750 μ l cold 100% EtOH. Subsequently, the samples were inverted and left for 30 min at -20°C . Nucleic acids were spun down for 5 min at 4°C and the pellet was air dried at 37°C and resuspended in 500 μ l 1X TE. After full resuspension, RNA was digested by incubation with 2.5 μ l RNase A (10

mg/ml stock) for 30 min at 37°C. 500 µl Isopropanol were added and the samples were kept for 30 min at -20°C after inverting multiple times. Followed a centrifugation for 15 min at 4°C and air-drying of the pellet at 37°C. The resulting pellet was resuspended in 50 µl 1X TE and centrifuged once more for 10 min at 4°C. The salts pelleting at the bottom of the tube were discarded and the supernatant was kept.

5.2.3.2 Southern blot

Nearly 5 µg DNA were digested with 1.5 µl of the appropriate enzyme and 2.5 µl CutSmart for 5 hrs at 37°C. The restriction enzyme XhoI was applied when the Southern blot was used to detect either the whole telomere population or the single telomere 15L. Alternatively, the restriction enzyme Sall was used when visualizing the telomere 1L. After digestion, the samples were mixed with 5 µl loading dye (6X stock), loaded on a 0.8% agarose gel and run for 22 hrs at 50V. 5 µl of a 1 kb ladder was run along.

Following, the DNA contained in the gel was denatured and neutralized in a denaturing and neutralizing solution, respectively. Afterwards, the DNA was transferred to a neutral nitrocellulose membrane via vertical capillarity in the presence of 10X SSC for 3 nights. After the transfer, the DNA was cross-linked via UV light using the “auto cross-link” mode of the Stratalinker and pre-hybridized overnight at 55°C in 20 ml PerfectHyb hybridization buffer. The following day, a ³²P-radiolabeled probe was directly added to the hybridization buffer and hybridization took place overnight at 55°C. Four rounds of washes were then performed, the first two with 25 ml of a pre-warmed solution containing 2X SSC and 0.1% SDS for 5 min and the last two with 25 ml of a pre-warmed 0.5X SSC and 0.1% SDS solution for 20 min. The membrane was then left air drying and a radio-sensitive film was applied on top to impress the radioactive signal. After 4 nights of exposure, the signal on the film was read with the IP filter of Typhoon FLA 9500.

5.2.3.3 Radioactive probe generation

In order to generate the CA-probe detecting the whole telomere population, a ca. 350 bp-long fragment of DNA was obtained by digesting the plasmid pBL423 with 3 µl EcoRI and 5 µl CutSmart for 1 hr at 37°C. After digestion, DNA was run on a 1.5% agarose gel and the ca. 350 bp-long band was extracted from the gel via the Gel Extraction Kit.

As for the probes specific for telomere 1L and 15L, a PCR reaction was performed as follows: 1 µl genomic DNA from a wild-type strain was combined with 2.5 µl of each oligo (5 µM stock) (section 5.1.3), 25 µl Phusion mix and 20 µl H₂O. The resulting mix was thermocycled with an annealing step of 30 sec at 58°C and 50°C for the 1L and 15L probe, respectively, and an elongation step of 1 min at 72°C. The PCR products were then loaded and run on a 1% agarose gel and the 591 bp-long and 662 bp-long bands, corresponding respectively to the 1L- and 15L-specific PCR products, were extracted as for the CA-probe.

To randomly radioactive label each probe, the DecaPrime II DNA Labeling Kit was used. 60 ng DNA were combined with 2.5 µl Decamers (10X stock) and brought to a volume of 14 µl with H₂O. The mix was boiled for 10 min at 95°C, cooled down on ice, spun and combined with 5 µl of a reaction buffer (5X stock) without ATP supplemented with 1 µl of the polymerase Klenow fragment and 5 µl dATP [α -³²P] (3000 Ci/mmol stock). Followed an incubation for 30 min at 37°C.

After that, the probes were boiled again for 10 min at 95°C, cooled down, briefly spun and kept on ice until usage.

5.2.3.4 Telo-PCR

1 µl genomic DNA at a concentration of 100 ng/µl was combined with 7.1 µl H₂O and 0.9 µl 10X NEB4 buffer. After incubation for 10 min at 96°C, 1 µl of a mix containing 4 U Terminal Transferase, 0.1 µl 10X NEB 4 buffer, 0.1 µl 10 mM dCTP and H₂O up to a final volume of 1 µl was added to the samples directly on the PCR machine. Followed an incubation for 30 min at 37°C, 10 min at 65°C and 5 min at 96°C. Samples were then brought back to 65°C and kept at this temperature. At this step, 21 µl H₂O were combined with 4 µl 10X PCR buffer, 4 µl dNTPs (2mM stock), 0.3 µl of a forward oligo (100 µM stock) (section 5.1.3), 0.3 µl of the G₁₈ reverse oligo oBL359 (100 µM stock) and heated at 65°C. Once heated, 0.5 µl Phusion Hot Start II DNA Polymerase was added and the resulting mix was combined with the samples directly on the PCR machine. Thermocycling took place then as follows: 3 min at 95°C, 45 cycles of 30 sec at 95°C, 15 sec at 63°C and 20 sec at 68°C. Subsequently, the samples were held for 5 min at 68°C and afterwards at 4°C. The resulting PCR products were separated then on a 1.8% agarose gel for 2.5 hrs at 100V and the telomere length established with the Image Lab software.

5.2.3.5 Junction PCR

1 µl DNA (approximately 250ng) was combined with 2.5 µl of each oligo (section 5.1.3), 20 µl water, 25 µl Phusion High-Fidelity PCR Master Mix with HF Buffer. PCR consisted of initial DNA denaturation at 98°C for 3min, followed by 35 cycles of 30 sec at 98°C, 30 sec at 58°C and 3 min at 72°C. After the last cycle, samples were incubated at 72°C for 5 min and kept at 12°C until loading. 2 µl from each reaction was mixed with 8 µl 6X Gel Loading Dye Blue and loaded onto a 0.8% agarose gel. Electrophoresis took place for 45 min at 100V. Bands localization was identified by the Gel Red program of the ChemiDoc Touch Imaging System (Bio-Rad).

5.2.4 Protein analysis

5.2.4.1 Protein extraction

2 OD₆₀₀ units of exponentially growing cells were pelleted and resuspended in 150 µl of a solution containing 1.85M NaOH, 1.09M β-mercaptoethanol. After incubation on ice for 10min, 150 µl of a 50% TCA solution were added and further incubation on ice took place for 10 min. After centrifuging at 4°C, pellets were resuspended in 1 ml acetone and centrifuged again at 4°C. Pellets were resuspended in 100 µl urea buffer (120 mM Tris-HCl pH 6.8, 5% glycerol, 8 M urea, 143 mM β-mercaptoethanol, 8% SDS, bromophenol blue indicator) and stored at -80°C.

5.2.4.2 Western blot

Samples were thawed at room temperature and incubated at 75°C for 5 min. After brief centrifugation at room temperature, 8 µl from each sample were loaded onto Mini Protean TGX

Pre-cast 4–15% gels. Separation took place for approximately 45 min at 150V. Gels were blotted on nitrocellulose membranes and transfer was performed by using the “high molecular weight” program of the Trans-BlotTurbo System. The membrane was blocked in a blocking solution containing 5% skim milk, 1X PBS, 0.1% Tween-20 at room temperature for 1 hr, followed by overnight incubation at 4°C with primary antibodies diluted in blocking solution. The antibodies used in this project are listed in section 5.1.7. After incubation with the primary antibody, the membrane was washed four times for 15 min with washing solution (1X PBS, 0.1% Tween-20) and incubated at room temperature for 1 hr with respective HRP-coupled secondary antibodies (listed in section 5.1.7) diluted in blocking solution. After washing three times for 15 min with washing solution, the membrane was incubated for 1 min with Super Signal West Pico or Dura Chemiluminescent Substrate and proteins were detected by the Chemiluminescence program of the ChemiDoc Touch Imaging System.

5.2.4.3 Chromatin immunoprecipitation (ChIP)

Exponentially growing cells were cross-linked with 1.2% formaldehyde at room temperature for 10 min, when detecting the enrichment of Rat1-TAP and Sir2, or 15 min, when detecting the enrichment of RNA polymerase II, RNA polymerase II phosphorylated on Ser2 and Rnh201-TAP. Followed quenching with 355 mM glycine (quenching for two replicates in the Rnh201-TAP ChIP was performed with 114 mM glycine) for 5 min and incubation on ice for at least 12 min. The samples were pelleted then at 4°C and washed twice with 20 ml cold 1X PBS. After centrifuging, the pellets were stored at -80°C.

The pellets were thawed on ice and resuspended in 400 µl cold FA lysis buffer –SOD supplemented with protease inhibitor. The samples were transferred then in lysing Matrix C tubes kept on ice and lysed with the FastPrep machine for 3 runs (each of 30 sec) at 4°C at level of 6.5 M/sec, with 1 min on ice between runs. After that, the extracts were recovered by adding 800 µl cold FA lysis buffer + SOD supplemented with protease inhibitor. After mixing, the extracts were centrifuged for 15 min at 4°C and the pellet was resuspended in 1.5 ml cold FA lysis buffer + SOD supplemented with protease inhibitor. 20 µl 20% SDS were added and 750 µl of the resulting mix were combined with 0.4 g beads kept on ice. Sonication took place for 5 cycles of 30 sec on/off at 4°C with Bioruptor Pico. The remaining volume of the mix was combined with 0.4 g beads kept on ice and sonicated in the same manner. The samples were centrifuged then for 15 min at 4°C and the supernatant, which constituted the ChIP extract, was stored at -80°C. Sonication efficiency was determined by evaluating the average length of the sheared DNA fragments. To accomplish this, 100 µl ChIP extract were combined with 100 µl elution buffer, decross-linked overnight at 65°C, subjected to digestion with 7.5 µl Proteinase K and 1 µl RNase A and run on a 1.5% agarose gel for 45 min at 100V.

When pulling down the protein of interest, the protein concentration within the ChIP extract was measured by Bradford and diluted to 1 mg/ml in 2 ml cold FA lysis buffer + SOD supplemented with protease inhibitor. From this mix, 50 µl were stored as 5% input at -20°C. The remaining volume was split in 2: one half was used to pull down the protein in presence of the antibody (+ Ab) and the other one as a negative control in absence of the antibody (- Ab). Both + and - Ab ChIP extracts were incubated with 30 µl of the appropriate Sepharose beads, previously washed and supplemented with 5% BSA, for 1 hr at 4°C on rotating wheel. After that, the samples were

centrifuged at 4°C and the supernatant separated from the beads. The proper amount of antibody (the antibodies are listed in section 5.1.7) was added to the supernatant and incubation for 1 hr at 4°C on rotating wheel took place. Subsequently, 50 µl of the appropriate Sepharose beads were added and the samples were incubated overnight at 4°C on rotating wheel. For TAP ChIPs, IgG sepharose beads were used, whereas for RNA polymerase II (both unphosphorylated and phosphorylated) and Sir2, Protein G beads were adopted.

The following day, beads were washed with 1 ml cold FA lysis buffer +SOD, 1 ml cold FA lysis buffer 500, 1 ml cold buffer III and 1 ml TE pH 8.0. At this point, the beads were eluted twice in 100 µl elution buffer, vortexed and incubated for 8 min at 65°C. After centrifugation, the eluate was combined with 7.5 µl Proteinase K (20 mg/ml stock) and incubated overnight at 65°C in order to be decross-linked. Meanwhile, the input DNA was thawed at room temperature, mixed with 150 µl elution buffer and 7.5 µl Proteinase K and incubated overnight at 65°C. Following, both the immunoprecipitate and the input samples were purified with the PCR purification kit, eluted in 50 µl elution buffer and the DNA amount measured by RT-qPCR, as previously described.

5.2.5 Flow cytometry

Cells were grown exponentially and ~ 0.2 OD₆₀₀ units were pelleted and resuspended in 70% EtOH. After an overnight incubation at 4°C, EtOH was removed and cells were washed with H₂O. Followed the resuspension in 500 µl 50 mM Tris-HCl pH 7.5 and incubation with 10 µl RNase A (10 mg/ml stock) for 3 hrs at 37°C. 25 µl Proteinase K (20 mg/ml stock) were added afterwards and the samples were incubated for 1 hr at 50°C. At this point, the samples were pelleted and resuspended in 500 µl 50 mM Tris-HCl pH 7.5. Followed sonication and introduction of the samples into FACS tubes. SYTOX Green was added and the DNA content was measured via BD FACSVerse.

5.2.6 Replicative potential analysis

5.2.6.1 Replicative potential measurement

Survivor cells were streaked for single colonies on solid selective medium or YPD. When colonies arose, they were individually inoculated in liquid selective medium or YPD and grown overnight at 30°C. The following day, the optical density (OD₆₀₀) of the cultures was measured and cells were passed into fresh liquid medium to obtain a final OD₆₀₀ of 0.01 and grown overnight. This procedure of daily dilutions and OD₆₀₀ was carried out every 24 hrs.

The replicative potential was determined by setting the first OD₆₀₀ value of cells transformed with an empty vector (EV in the experiment illustrated in Figure 25) or with the Rnh201-expressing plasmid (final genotype: *tlc1Δ/est2Δrnh201Δ* in the experiment depicted in Figure 27) as 1 and by dividing all the other OD₆₀₀ values, from the same day and the following days, by it. The resulting value indicates the percentage of proliferative ability (% replicative potential) that cells have in relation to the initial replicative potential.

When survivors were monitored for telomere length and TERRA levels during the clonal propagation, cells were isolated from the overnight cultures on different days and exponentially

grown. After collecting the pellet, the procedure to examine the two nucleic acids was the same as described above.

5.2.6.2 Post-crisis senescence rate measurement

The senescence rate in survivors was defined as the number of population doublings (PDs) required for telomeres to reach the smallest length. This was assumed to coincide with the lowest value of replicative potential, or local minimum, during the clonal propagation. In order to avoid biases given by stochastic fluctuations of the OD₆₀₀ measurement, the number of % replicative potential values was reduced by calculating the average of two consecutive values. Moreover, local minima were considered only if no other values in a neighborhood of four were inferior. The similarity between the proliferative potential profiles of the conditions tested, e.g., EV vs RNH1, was also used as a criterion to select the local minima.

7. Bibliography

1. McKnight, T. D. Plant Telomere Biology. *Plant Cell* **16**, 794–803 (2004).
2. McClintock, B. The Stability of Broken Ends of Chromosomes in Zea Mays. *Genetics* **26**, 234–82 (1941).
3. Meselson, B. Y. M. & Stahl, F. W. The Replication of DNA in Escherichia coli. *PNAS* **44**, 671–682 (1958).
4. Crick, F. & Watson, J. Molecular Structure of Nucleic Acids. *Nature* **171**, 737–738 (1953).
5. Okazaki, R., Okazaki, T., Sakabe, K., Sugimoto, K. & Sugino, A. Mechanism of DNA Chain Growth, I. Possible Discontinuity and Unusual Secondary Structure of Newly Synthesized Chains. *PNAS* **59**, 598–605 (1968).
6. Ogawa, T. & Okazaki, T. Discontinuous DNA Replication. *Ann. Rev. Biochem.* **49**, 421–457 (1980).
7. Watson, J. Origin of Concatemeric T7 DNA. *Nat. New Biol.* **239**, 197–201 (1972).
8. Olovnikov, A. M. A theory of marginotomy. The incomplete copying of template margin in enzymic synthesis of polynucleotides and biological significance of the phenomenon. *J. Theor. Biol.* **41**, 181–190 (1973).
9. Hayflick, L. & Moorhead, P. S. The serial cultivation of human diploid cell strains. *Exp. Cell Res.* **25**, 585–621 (1961).
10. Soudet, J., Jolivet, P. & Teixeira, M. T. Elucidation of the DNA end-replication problem in *saccharomyces cerevisiae*. *Mol. Cell* **53**, 954–964 (2014).
11. Wu, P., Takai, H. & De Lange, T. Telomeric 3' overhangs derive from resection by Exo1 and apollo and fill-in by POT1b-associated CST. *Cell* **150**, 39–52 (2012).
12. MacHattie, L. A., Ritchie, D. A., Thomas, C. A. & Richardson, C. C. Terminal repetition in permuted T2 bacteriophage DNA molecules. *J. Mol. Biol.* **23**, 355-IN12 (1967).
13. Ritchie, D. A., Thomas, C. A., MacHattie, L. A. & Wensink, P. C. Terminal repetition in non-permuted T3 and T7 bacteriophage DNA molecules. *J. Mol. Biol.* **23**, 365-IN15 (1967).
14. Shampay, J., Szostak, J. W. & Blackburn, E. H. DNA sequences of telomeres maintained in yeast. *Nature* **310**, 154–157 (1984).
15. Richards, E. J. & Ausubel, F. M. Isolation of a higher eukaryotic telomere from *Arabidopsis thaliana*. *Cell* **53**, 127–136 (1988).
16. Moyzis, R. K. *et al.* A highly conserved repetitive DNA sequence, (TTAGGG)(n), present at the telomeres of human chromosomes. *Proc. Natl. Acad. Sci. U. S. A.* **85**, 6622–6626 (1988).
17. Greider, C. W. & Blackburn, E. H. Identification of a specific telomere terminal transferase activity in tetrahymena extracts. *Cell* **43**, 405–413 (1985).
18. Bernardis, A., Michels, P. A. M., Lincke, C. R. & Borst, P. Growth of chromosome ends in multiplying trypanosomes. *Nature* **303**, 592–597 (1983).
19. Greider, C. W. & Blackburn, E. H. The telomere terminal transferase of tetrahymena is a ribonucleoprotein enzyme with two kinds of primer specificity. *Cell* **51**, 887–898 (1987).
20. Greider, C. W. & Blackburn, E. H. A telomeric sequence in the RNA of Tetrahymena telomerase required for telomere repeat synthesis. *Nature* **337**, 331–337 (1989).
21. Morin, G. B. The human telomere terminal transferase enzyme is a ribonucleoprotein that synthesizes TTAGGG repeats. *Cell* **59**, 521–529 (1989).

22. Counter, C. M., Hirte, H. W., Bacchetti, S. & Harley, C. B. Telomerase activity in human ovarian carcinoma. *Proc. Natl. Acad. Sci. U. S. A.* **91**, 2900–2904 (1994).
23. Penev, A. *et al.* Alternative splicing is a developmental switch for hTERT expression. *Mol. Cell* (2021) doi:10.1016/j.molcel.2021.03.033.
24. Lundblad, V. & Blackburn, E. H. An alternative pathway for yeast telomere maintenance rescues est1- senescence. *Cell* **73**, 347–360 (1993).
25. Bryan, T. M., Englezou, A., Dalla-Pozza, L., Dunham, M. A. & Reddel, R. R. Evidence for an alternative mechanism for maintaining telomere length in human tumors and tumor-derived cell lines. *Nat. Med.* **3**, 1271–1274 (1997).
26. Bryan, T. M., Englezou, A., Gupta, J., Bacchetti, S. & Reddel, R. R. Telomere elongation in immortal human cells without detectable telomerase activity. *EMBO J.* **14**, 4240–4248 (1995).
27. Wellinger, R. J. & Zakian, V. A. Everything you ever wanted to know about *Saccharomyces cerevisiae* telomeres: Beginning to end. *Genetics* **191**, 1073–1105 (2012).
28. Wang, S. S. & Zakian, V. A. Sequencing of *Saccharomyces* telomeres cloned using T4 DNA polymerase reveals two domains. *Mol. Cell. Biol.* **10**, 4415–4419 (1990).
29. Bryan, T. M. G-quadruplexes at telomeres: Friend or foe? *Molecules* **25**, (2020).
30. Smith, J. S. *et al.* Rudimentary G-quadruplex-based telomere capping in *Saccharomyces cerevisiae*. *Nat. Struct. Mol. Biol.* **18**, 478–486 (2011).
31. Jurikova, K. *et al.* Role of folding kinetics of secondary structures in telomeric G-overhangs in the regulation of telomere maintenance in *Saccharomyces cerevisiae*. *J. Biol. Chem.* **295**, 8958–8971 (2020).
32. Biffi, G., Tannahill, D., McCafferty, J. & Balasubramanian, S. Quantitative visualization of DNA G-quadruplex structures in human cells. *Nat. Chem.* **5**, 182–186 (2013).
33. Moye, A. L. *et al.* Telomeric G-quadruplexes are a substrate and site of localization for human telomerase. *Nat. Commun.* **6**, 7643 (2015).
34. Gauthier, L. R. *et al.* Rad51 and DNA-PKcs are involved in the generation of specific telomere aberrations induced by the quadruplex ligand 360A that impair mitotic cell progression and lead to cell death. *Cell. Mol. Life Sci.* **69**, 629–640 (2012).
35. Amato, R. *et al.* G-quadruplex stabilization fuels the ALT pathway in ALT-positive osteosarcoma cells. *Genes (Basel)*. **11**, (2020).
36. Dilley, R. L. *et al.* Break-induced telomere synthesis underlies alternative telomere maintenance. *Nature* **539**, 54–58 (2016).
37. Zhang, M. *et al.* Mammalian CST averts replication failure by preventing G-quadruplex accumulation. *Nucleic Acids Res.* **47**, 5243–5259 (2019).
38. De Magis, A. *et al.* DNA damage and genome instability by G-quadruplex ligands are mediated by R loops in human cancer cells. *Proc. Natl. Acad. Sci. U. S. A.* **116**, 816–825 (2019).
39. Kwapisz, M. & Morillon, A. Subtelomeric Transcription and its Regulation. *J. Mol. Biol.* **432**, 4199–4219 (2020).
40. Kupiec, M. Biology of telomeres: Lessons from budding yeast. *FEMS Microbiol. Rev.* **38**, 144–171 (2014).
41. Gilson, E., Roberge, M., Giraldo, R., Rhodes, D. & Gasser, S. M. Distortion of the DNA double helix by RAP1 at silencers and multiple telomeric binding sites. *J. Mol. Biol.* **231**,

- 293–310 (1993).
42. Williams, T. L., Levy, D. L., Maki-Yonekura, S., Yonekura, K. & Blackburn, E. H. Characterization of the yeast telomere nucleoprotein core: Rap1 binds independently to each recognition site. *J. Biol. Chem.* **285**, 35814–35824 (2010).
 43. König, P., Giraldo, R., Chapman, L. & Rhodes, D. The crystal structure of the DNA-binding domain of yeast RAP1 in complex with telomeric DNA. *Cell* **85**, 125–136 (1996).
 44. Marcand, S., Gilson, E. & Shore, D. A protein-counting mechanism for telomere length regulation in yeast. *Science (80-.)*. **275**, 986–990 (1997).
 45. Teixeira, M. T., Arneric, M., Sperisen, P. & Lingner, J. Telomere length homeostasis is achieved via a switch between telomerase- extendible and -nonextendible states. *Cell* **117**, 323–335 (2004).
 46. Negrini, S., Ribaud, V., Bianchi, A. & Shore, D. DNA breaks are masked by multiple Rap1 binding in yeast: Implications for telomere capping and telomerase regulation. *Genes Dev.* **21**, 292–302 (2007).
 47. Kyrion, G., Liu, K., Liu, C. & Lustig, A. J. RAP1 and telomere structure regulate telomere position effects in *Saccharomyces cerevisiae*. *Genes Dev.* **7**, 1146–1159 (1993).
 48. Shi, T. *et al.* Rif1 and Rif2 shape telomere function and architecture through multivalent Rap1 interactions. *Cell* **153**, 1340 (2013).
 49. Platt, J. M. *et al.* Rap1 relocalization contributes to the chromatin-mediated gene expression profile and pace of cell senescence. *Genes Dev.* **27**, 1406–1420 (2013).
 50. Azad, G. K. & Tomar, R. S. The multifunctional transcription factor Rap1: A regulator of yeast physiology. *Frontiers in Bioscience - Landmark* vol. 21 918–930 (2016).
 51. Kaizer, H., Connelly, C. J., Bettridge, K., Viggiani, C. & Greider, C. W. Regulation of telomere length requires a conserved N-terminal domain of Rif2 in *Saccharomyces cerevisiae*. *Genetics* **201**, 573–586 (2015).
 52. Wotton, D. & Shore, D. A novel Rap1p-interacting factor, Rif2p, cooperates with Rif1p to regulate telomere length in *Saccharomyces cerevisiae*. *Genes Dev.* **11**, 748–760 (1997).
 53. Levy, D. L. & Blackburn, E. H. Counting of Rif1p and Rif2p on *Saccharomyces cerevisiae* Telomeres Regulates Telomere Length. *Mol. Cell. Biol.* **24**, 10857–10867 (2004).
 54. Ribeyre, C. & Shore, D. Anticheckpoint pathways at telomeres in yeast. *Nat. Struct. Mol. Biol.* **19**, 307–313 (2012).
 55. Bonetti, D. *et al.* DNA binding modes influence Rap1 activity in the regulation of telomere length and MRX functions at DNA ends. *Nucleic Acids Res.* **48**, 2424–2441 (2020).
 56. Hirano, Y., Fukunaga, K. & Sugimoto, K. Rif1 and Rif2 Inhibit Localization of Tel1 to DNA Ends. *Mol. Cell* **33**, 312–322 (2009).
 57. Fontana, G. A., Reinert, J. K., Thomä, N. H. & Rass, U. Shepherding DNA ends: Rif1 protects telomeres and chromosome breaks. *Microbial Cell* vol. 5 327–343 (2018).
 58. Longhese, M. P., Bonetti, D., Manfrini, N. & Clerici, M. Mechanisms and regulation of DNA end resection. *EMBO Journal* vol. 29 2864–2874 (2010).
 59. Mattarocci, S. *et al.* Rif1 maintains telomeres and mediates DNA repair by encasing DNA ends. *Nat. Struct. Mol. Biol.* **24**, 588–595 (2017).
 60. Shubin, C. B. & Greider, C. W. The role of rif1 in telomere length regulation is separable from its role in origin firing. *Elife* **9**, 1–40 (2020).
 61. Mattarocci, S. *et al.* Rif1 Controls DNA replication timing in yeast through the PP1

- Phosphatase Glc7. *Cell Rep.* **7**, 62–69 (2014).
62. Graf, M. *et al.* Telomere Length Determines TERRA and R-Loop Regulation through the Cell Cycle. *Cell* **170**, 72-85.e14 (2017).
 63. Luke, B. *et al.* The Rat1p 5' to 3' Exonuclease Degrades Telomeric Repeat-Containing RNA and Promotes Telomere Elongation in *Saccharomyces cerevisiae*. *Mol. Cell* **32**, 465–477 (2008).
 64. Lockhart, A. *et al.* RNase H1 and H2 Are Differentially Regulated to Process RNA-DNA Hybrids. *Cell Rep.* **29**, 2890-2900.e5 (2019).
 65. Wu, Z. J. *et al.* CDC13 is predominant over STN1 and TEN1 in preventing chromosome end fusions. *Elife* **9**, 1–25 (2020).
 66. Mason, M. *et al.* Cdc13 OB2 dimerization required for productive stn1 binding and efficient telomere maintenance. *Structure* **21**, 109–120 (2013).
 67. Chen, H. *et al.* Structural Insights into Yeast Telomerase Recruitment to Telomeres. *Cell* **172**, 331-343.e13 (2018).
 68. Nugent, C. I., Hughes, T. R., Lue, N. F. & Lundblad, V. Cdc13p: A single-strand telomeric DNA-binding protein with a dual role in yeast telomere maintenance. *Science (80-.)*. **274**, 249–252 (1996).
 69. Faure, V., Coulon, S., Hardy, J. & Géli, V. The Telomeric Single-Stranded DNA-Binding Protein Cdc13 and Telomerase Bind through Different Mechanisms at the Lagging- and Leading-Strand Telomeres. *Mol. Cell* **38**, 842–852 (2010).
 70. Bonetti, D., Martina, M., Clerici, M., Lucchini, G. & Longhese, M. P. Multiple Pathways Regulate 3' Overhang Generation at *S. cerevisiae* Telomeres. *Mol. Cell* **35**, 70–81 (2009).
 71. Vodenicharov, M. D., Laterreur, N. & Wellinger, R. J. Telomere capping in non-dividing yeast cells requires Yku and Rap1. *EMBO J.* **29**, 3007–3019 (2010).
 72. Vodenicharov, M. D. & Wellinger, R. J. DNA Degradation at Unprotected Telomeres in Yeast Is Regulated by the CDK1 (Cdc28/Clb) Cell-Cycle Kinase. *Mol. Cell* **24**, 127–137 (2006).
 73. Biswas, H., Goto, G., Wang, W., Sung, P. & Sugimoto, K. Ddc2ATRIP promotes Mec1ATR activation at RPA-ssDNA tracts. *PLoS Genet.* **15**, e1008294 (2019).
 74. Deshpande, I. *et al.* Structural Basis of Mec1-Ddc2-RPA Assembly and Activation on Single-Stranded DNA at Sites of Damage. *Mol. Cell* **68**, 431-445.e5 (2017).
 75. Teixeira, M. T. *Saccharomyces cerevisiae* as a model to study replicative senescence triggered by telomere shortening. *Front. Oncol.* **3 APR**, 1–16 (2013).
 76. Chandra, A., Hughes, T. R., Nugent, C. I. & Lundblad, V. Cdc13 both positively and negatively regulates telomere replication. *Genes Dev.* **15**, 404–414 (2001).
 77. Qian, W. *et al.* Ten1p promotes the telomeric DNA-binding activity of Cdc13p: Implication for its function in telomere length regulation. *Cell Res.* **19**, 849–863 (2009).
 78. Bonetti, D., Clerici, M., Manfrini, N., Lucchini, G. & Longhese, M. P. The MRX complex plays multiple functions in resection of Yku- and Rif2-protected DNA ends. *PLoS One* **5**, 14142 (2010).
 79. Vodenicharov, M. D., Laterreur, N. & Wellinger, R. J. Telomere capping in non-dividing yeast cells requires Yku and Rap1. *EMBO J.* **29**, 3007–3019 (2010).
 80. Rusche, L. N., Kirchmaier, A. L. & Rine, J. The establishment, inheritance, and function of silenced chromatin in *Saccharomyces cerevisiae*. *Annu. Rev. Biochem.* **72**, 481–516

- (2003).
81. Mishra, K. & Shore, D. Yeast Ku protein plays a direct role in telomeric silencing and counteracts inhibition by Rif proteins. *Curr. Biol.* **9**, 1123–1126 (1999).
 82. Hsu, H. C. *et al.* Structural basis for allosteric stimulation of Sir2 activity by sir4 binding. *Genes Dev.* **27**, 64–73 (2013).
 83. Kozak, M. L. *et al.* Inactivation of the Sas2 histone acetyltransferase delays senescence driven by telomere dysfunction. *EMBO J.* **29**, 158–170 (2010).
 84. Altaf, M. *et al.* Interplay of Chromatin Modifiers on a Short Basic Patch of Histone H4 Tail Defines the Boundary of Telomeric Heterochromatin. *Mol. Cell* **28**, 1002–1014 (2007).
 85. Zhu, X. & Gustafsson, C. M. Distinct differences in chromatin structure at subtelomeric X and Y' elements in budding yeast. *PLoS One* **4**, (2009).
 86. Wagner, T. *et al.* Chromatin modifiers and recombination factors promote a telomere fold-back structure, that is lost during replicative senescence. *PLoS Genet.* **16**, e1008603 (2020).
 87. Tomaska, L., Nosek, J., Kar, A., Willcox, S. & Griffith, J. D. A New View of the T-Loop Junction: Implications for Self-Primed Telomere Extension, Expansion of Disease-Related Nucleotide Repeat Blocks, and Telomere Evolution. *Front. Genet.* **10**, 792 (2019).
 88. De Lange, T. How telomeres solve the end-protection problem. *Science (80-.).* **326**, 948–952 (2009).
 89. De Lange, T. T-loops and the origin of telomeres. *Nat. Rev. Mol. Cell Biol.* **5**, 323–329 (2004).
 90. Sarek, G. *et al.* CDK phosphorylation of TRF2 controls t-loop dynamics during the cell cycle. *Nature* **575**, 523–527 (2019).
 91. Verdun, R. E. & Karlseder, J. The DNA Damage Machinery and Homologous Recombination Pathway Act Consecutively to Protect Human Telomeres. *Cell* **127**, 709–720 (2006).
 92. Poschke, H. *et al.* Rif2 Promotes a Telomere Fold-Back Structure through Rpd3L Recruitment in Budding Yeast. *PLoS Genet.* **8**, 1002960 (2012).
 93. Kim, W. & Shay, J. W. Long-range telomere regulation of gene expression: Telomere looping and telomere position effect over long distances (TPE-OLD). *Differentiation* **99**, 1–9 (2018).
 94. Lansdorp, P. M. Telomeres, stem cells, and hematology. *Blood* vol. 111 1759–1765 (2008).
 95. Campisi, J. & D'Adda Di Fagagna, F. Cellular senescence: When bad things happen to good cells. *Nature Reviews Molecular Cell Biology* vol. 8 729–740 (2007).
 96. Lundblad, V. & Szostak, J. W. A mutant with a defect in telomere elongation leads to senescence in yeast. *Cell* **57**, 633–643 (1989).
 97. Enomoto, S., Glowczewski, L. & Berman, J. MEC3, MEC1, and DDC2 are essential components of a telomere checkpoint pathway required for cell cycle arrest during senescence in *Saccharomyces cerevisiae*. *Mol. Biol. Cell* **13**, 2626–2638 (2002).
 98. Neurohr, G. E., Terry, R. L., Van Werven, F. J., Holt, L. J. & Correspondence, A. A. Excessive Cell Growth Causes Cytoplasm Dilution And Contributes to Senescence. *Cell* **176**, (2019).
 99. Ritchie, K. B., Mallory, J. C. & Petes, T. D. Interactions of TLC1 (Which Encodes the RNA

- Subunit of Telomerase), TEL1 , and MEC1 in Regulating Telomere Length in the Yeast *Saccharomyces cerevisiae* . *Mol. Cell. Biol.* **19**, 6065–6075 (1999).
100. Chan, S. W. L., Chang, J., Prescott, J. & Blackburn, E. H. Altering telomere structure allows telomerase to act in yeast lacking ATM kinases. *Curr. Biol.* **11**, 1240–1250 (2001).
 101. Abdallah, P. *et al.* A two-step model for senescence triggered by a single critically short telomere. *Nat. Cell Biol.* **11**, 988–993 (2009).
 102. Fallet, E. *et al.* Length-dependent processing of telomeres in the absence of telomerase. *Nucleic Acids Res.* **42**, 3648–3665 (2014).
 103. Khadaroo, B. *et al.* The DNA damage response at eroded telomeres and tethering to the nuclear pore complex. *Nat. Cell Biol.* **11**, 980–987 (2009).
 104. Blastyák, A. *et al.* Yeast Rad5 Protein Required for Postreplication Repair Has a DNA Helicase Activity Specific for Replication Fork Regression. *Mol. Cell* **28**, 167–175 (2007).
 105. Malyavko, A. N., Parfenova, Y. Y., Zvereva, M. I. & Dontsova, O. A. Telomere length regulation in budding yeasts. *FEBS Lett.* **588**, 2530–2536 (2014).
 106. Dunham, M. A., Neumann, A. A., Fasching, C. L. & Reddel, R. R. Telomere maintenance by recombination in human cells. *Nat. Genet.* **26**, 447–450 (2000).
 107. Muntoni, A., Neumann, A. A., Hills, M. & Reddel, R. R. Telomere elongation involves intra-molecular DNA replication in cells utilizing alternative lengthening of telomeres. *Hum. Mol. Genet.* **18**, 1017–1027 (2009).
 108. Teng, S. C. & Zakian, V. A. Telomere-telomere recombination is an efficient bypass pathway for telomere maintenance in *Saccharomyces cerevisiae*. *Mol. Cell. Biol.* **19**, 8083–93 (1999).
 109. Dunn, B., Szauter, P., Pardue, M. Lou & Szostak, J. W. Transfer of yeast telomeres to linear plasmids by recombination. *Cell* **39**, 191–201 (1984).
 110. Churikov, D., Charifi, F., Simon, M. N. & Géli, V. Rad59-Facilitated Acquisition of Y' Elements by Short Telomeres Delays the Onset of Senescence. *PLoS Genet.* **10**, (2014).
 111. Teng, S. C., Chang, J., McCowan, B. & Zakian, V. a. Telomerase-independent lengthening of yeast telomeres occurs by an abrupt Rad50p-dependent, Rif-inhibited recombinational process. *Mol. Cell* **6**, 947–52 (2000).
 112. Kockler, Z. W., Comeron, J. M. & Malkova, A. A unified alternative telomere-lengthening pathway in yeast survivor cells. *Mol. Cell* **81**, 1–14 (2021).
 113. Straatman, K. R. & Louis, E. J. Localization of telomeres and telomere-associated proteins in telomerase-negative *Saccharomyces cerevisiae*. *Chromosom. Res.* **15**, 1033–1050 (2007).
 114. Claussin, C. & Chang, M. The many facets of homologous recombination at telomeres. *Microb. Cell* **2**, 308–321 (2015).
 115. Johnson, F. B. *et al.* The *Saccharomyces cerevisiae* WRN homolog Sgs1p participates in telomere maintenance in cells lacking telomerase. *EMBO J.* **20**, 905–913 (2001).
 116. Maringele, L. & Lydall, D. EXO1 Plays a Role in Generating Type I and Type II Survivors in Budding Yeast. *Genetics* **166**, 1641–1649 (2004).
 117. Lydeard, J. R., Jain, S., Yamaguchi, M. & Haber, J. E. Break-induced replication and telomerase-independent telomere maintenance require Pol32. *Nature* **448**, 820–823 (2007).
 118. Hu, Y. *et al.* Telomerase-Null Survivor Screening Identifies Novel Telomere

- Recombination Regulators. *PLoS Genet.* **9**, 1003208 (2013).
119. Balk, B. *et al.* Telomeric RNA-DNA hybrids affect telomere-length dynamics and senescence. *Nat. Struct. Mol. Biol.* **20**, 1199–1206 (2013).
 120. Maicher, A., Kastner, L., Dees, M. & Luke, B. Deregulated telomere transcription causes replication-dependent telomere shortening and promotes cellular senescence. *Nucleic Acids Res.* **40**, 6649–6659 (2012).
 121. Verma, P. *et al.* RAD52 and SLX4 act nonepistatically to ensure telomere stability during alternative telomere lengthening. *Genes Dev.* **33**, 221–235 (2019).
 122. Roumelioti, F. *et al.* Alternative lengthening of human telomeres is a conservative DNA replication process with features of break-induced replication. *EMBO Rep.* **17**, 1731–1737 (2016).
 123. Min, J., Wright, W. E. & Shay, J. W. Alternative Lengthening of Telomeres Mediated by Mitotic DNA Synthesis Engages Break-Induced Replication Processes. *Mol. Cell. Biol.* **37**, (2017).
 124. Zhang, J. M. & Zou, L. Alternative lengthening of telomeres: From molecular mechanisms to therapeutic outlooks. *Cell and Bioscience* vol. 10 1–9 (2020).
 125. Zhang, J. M., Yadav, T., Ouyang, J., Lan, L. & Zou, L. Alternative Lengthening of Telomeres through Two Distinct Break-Induced Replication Pathways. *Cell Rep.* **26**, 955-968.e3 (2019).
 126. Cho, N. W., Dilley, R. L., Lampson, M. A. & Greenberg, R. A. Interchromosomal homology searches drive directional ALT telomere movement and synapsis. *Cell* **159**, 108–121 (2014).
 127. Silva, B. *et al.* FANCM limits ALT activity by restricting telomeric replication stress induced by deregulated BLM and R-loops. *Nat. Commun.* **10**, 1–16 (2019).
 128. Zhang, T. *et al.* Strand break-induced replication fork collapse leads to C-circles, C-overhangs and telomeric recombination. *PLoS Genet.* **15**, e1007925 (2019).
 129. Cox, K. E., Maréchal, A. & Flynn, R. L. SMARCAL1 Resolves Replication Stress at ALT Telomeres. *Cell Rep.* **14**, 1032–1040 (2016).
 130. Lu, R. *et al.* The FANCM-BLM-TOP3A-RMI complex suppresses alternative lengthening of telomeres (ALT). *Nat. Commun.* **10**, 1–14 (2019).
 131. Poole, L. A. *et al.* SMARCAL1 maintains telomere integrity during DNA replication. *Proc. Natl. Acad. Sci. U. S. A.* **112**, 14864–14869 (2015).
 132. Arora, R. *et al.* RNaseH1 regulates TERRA-telomeric DNA hybrids and telomere maintenance in ALT tumour cells. *Nat. Commun.* **5**, 5220 (2014).
 133. Episkopou, H. *et al.* Alternative Lengthening of Telomeres is characterized by reduced compaction of telomeric chromatin. *Nucleic Acids Res.* **42**, 4391–4405 (2014).
 134. Lovejoy, C. A. *et al.* Loss of ATRX, genome instability, and an altered DNA damage response are hallmarks of the alternative lengthening of Telomeres pathway. *PLoS Genet.* **8**, 12–15 (2012).
 135. Flynn, R. L. *et al.* Alternative lengthening of telomeres renders cancer cells hypersensitive to ATR inhibitors. *Science (80-.)*. **347**, 273–277 (2015).
 136. Wang, Y. *et al.* G-quadruplex DNA drives genomic instability and represents a targetable molecular abnormality in ATRX-deficient malignant glioma. *Nat. Commun.* **10**, 1–14 (2019).

137. Azzalin, C. M., Reichenbach, P., Khoriauli, L., Giulotto, E. & Lingner, J. Telomeric Repeat Containing RNA and RNA Surveillance Factors at Mammalian Chromosome Ends. *Science (80-.)*. **318**, 798–801 (2007).
138. Schoeftner, S. & Blasco, M. A. Developmentally regulated transcription of mammalian telomeres by DNA-dependent RNA polymerase II. *Nat. Cell Biol.* **10**, 228–236 (2008).
139. Nergadze, S. G. *et al.* CpG-island promoters drive transcription of human telomeres. *RNA* **15**, 2186–2194 (2009).
140. Baiano-higia, O. Silva *et al.*, 2021. **6**, 169–184 (2021).
141. Porro, A. *et al.* Functional characterization of the TERRA transcriptome at damaged telomeres. *Nat. Commun.* **5**, 1–13 (2014).
142. Luke, B. & Lingner, J. TERRA: telomeric repeat-containing RNA. *EMBO J.* **28**, 2503–2510 (2009).
143. Azzalin, C. M. & Lingner, J. Telomeres: The silence is broken. *Cell Cycle* vol. 7 1161–1165 (2008).
144. Porro, A., Feuerhahn, S., Reichenbach, P. & Lingner, J. Molecular Dissection of Telomeric Repeat-Containing RNA Biogenesis Unveils the Presence of Distinct and Multiple Regulatory Pathways. *Mol. Cell. Biol.* **30**, 4808–4817 (2010).
145. Luke, B. & Lingner, J. TERRA: Telomeric repeat-containing RNA. *EMBO Journal* vol. 28 2503–2510 (2009).
146. Iglesias, N. *et al.* Subtelomeric repetitive elements determine TERRA regulation by Rap1/Rif and Rap1/Sir complexes in yeast. *EMBO Rep.* **12**, 587–593 (2011).
147. Rodrigues, J. & Lydall, D. Paf1 and Ctr9, core components of the PAF1 complex, maintain low levels of telomeric repeat containing RNA. *Nucleic Acids Res.* **46**, 621–634 (2018).
148. Novo, C. *et al.* The heterochromatic chromosome caps in great apes impact telomere metabolism. *Nucleic Acids Res.* **41**, 4792–4801 (2013).
149. Vohhodina, J. *et al.* BRCA1 binds TERRA RNA and suppresses R-Loop-based telomeric DNA damage. *Nat. Commun.* **12**, 3542 (2021).
150. Arnoult, N., Van Beneden, A. & Decottignies, A. Telomere length regulates TERRA levels through increased trimethylation of telomeric H3K9 and HP1 α . *Nat. Struct. Mol. Biol.* **19**, 948–956 (2012).
151. Deng, Z. *et al.* A role for CTCF and cohesin in subtelomere chromatin organization, TERRA transcription, and telomere end protection. *EMBO J.* **31**, 4165–4178 (2012).
152. Feretzaki, M., Nunes, P. R. & Lingner, J. Expression and differential regulation of human TERRA at several chromosome ends. *RNA* **25**, 1470–1480 (2019).
153. Gottschling, D. E., Aparicio, O. M., Billington, B. L. & Zakian, V. A. Position effect at *S. cerevisiae* telomeres: Reversible repression of Pol II transcription. *Cell* **63**, 751–762 (1990).
154. Lovejoy, C. A. *et al.* Loss of ATRX, genome instability, and an altered DNA damage response are hallmarks of the alternative lengthening of Telomeres pathway. *PLoS Genet.* **8**, 1002772 (2012).
155. Brosnan-Cashman, J. A. *et al.* ATRX loss induces multiple hallmarks of the alternative lengthening of telomeres (ALT) phenotype in human glioma cell lines in a cell line-specific manner. *PLoS One* **13**, e0204159 (2018).
156. Yehezkel, S., Segev, Y., Viegas-Péquignot, E., Skorecki, K. & Selig, S. Hypomethylation of

- subtelomeric regions in ICF syndrome is associated with abnormally short telomeres and enhanced transcription from telomeric regions. *Hum. Mol. Genet.* **17**, 2776–2789 (2008).
157. Moravec, M. *et al.* TERRA promotes telomerase-mediated telomere elongation in *Schizosaccharomyces pombe*. *EMBO Rep.* **17**, 1–14 (2016).
 158. Cusanelli, E., Romero, C. A. P. & Chartrand, P. Telomeric Noncoding RNA TERRA Is Induced by Telomere Shortening to Nucleate Telomerase Molecules at Short Telomeres. *Mol. Cell* **51**, 780–791 (2013).
 159. Greenwood, J. & Cooper, J. P. Non-coding telomeric and subtelomeric transcripts are differentially regulated by telomeric and heterochromatin assembly factors in fission yeast. *Nucleic Acids Res.* **40**, 2956–2963 (2012).
 160. Oh, B. K. *et al.* Increased amounts and stability of telomeric repeat-containing RNA (TERRA) following DNA damage induced by etoposide. *PLoS One* **14**, e0225302 (2019).
 161. Galigniana, N. M., Charó, N. L., Uranga, R., Cabanillas, A. M. & Piwien-Pilipuk, G. Oxidative stress induces transcription of telomeric repeat-containing RNA (TERRA) by engaging PKA signaling and cytoskeleton dynamics. *Biochim. Biophys. Acta - Mol. Cell Res.* **1867**, 118643 (2020).
 162. Diman, A. *et al.* Nuclear respiratory factor 1 and endurance exercise promote human telomere transcription. *Sci. Adv.* **2**, e1600031 (2016).
 163. Perez-Romero, C. A., Lalonde, M., Chartrand, P. & Cusanelli, E. Induction and relocalization of telomeric repeat-containing RNAs during diauxic shift in budding yeast. *Curr. Genet.* **64**, 1117–1127 (2018).
 164. Chu, H. P. *et al.* TERRA RNA Antagonizes ATRX and Protects Telomeres. *Cell* **170**, 86–101.e16 (2017).
 165. Bettin, N., Oss Pegorar, C. & Cusanelli, E. The Emerging Roles of TERRA in Telomere Maintenance and Genome Stability. *Cells* **8**, 246 (2019).
 166. Deng, Z., Norseen, J., Wiedmer, A., Riethman, H. & Lieberman, P. M. TERRA RNA Binding to TRF2 Facilitates Heterochromatin Formation and ORC Recruitment at Telomeres. *Mol. Cell* **35**, 403–413 (2009).
 167. Montero, J. J. *et al.* TERRA recruitment of polycomb to telomeres is essential for histone trimethylation marks at telomeric heterochromatin. *Nat. Commun.* **9**, 1–14 (2018).
 168. Redon, S., Reichenbach, P. & Lingner, J. The non-coding RNA TERRA is a natural ligand and direct inhibitor of human telomerase. *Nucleic Acids Res.* **38**, 5797–5806 (2010).
 169. Yu, T.-Y., Kao, Y. & Lin, J.-J. Telomeric transcripts stimulate telomere recombination to suppress senescence in cells lacking telomerase. *Proc. Natl. Acad. Sci.* **111**, 3377–3382 (2014).
 170. Pfeiffer, V. & Lingner, J. TERRA promotes telomere shortening through exonuclease 1-mediated resection of chromosome ends. *PLoS Genet.* **8**, (2012).
 171. Tutton, S. *et al.* Subtelomeric p53 binding prevents accumulation of DNA damage at human telomeres. *EMBO J.* **35**, 193–207 (2016).
 172. Aguilera, A. & García-Muse, T. R Loops: From Transcription Byproducts to Threats to Genome Stability. *Molecular Cell* vol. 46 115–124 (2012).
 173. Sagie, S. *et al.* Telomeres in ICF syndrome cells are vulnerable to DNA damage due to elevated DNA:RNA hybrids. *Nat. Commun.* **8**, 1–12 (2017).
 174. Feretzaki, M. *et al.* RAD51-dependent recruitment of TERRA lncRNA to telomeres

- through R-loops. *Nature* **587**, 303–308 (2020).
175. Lee, Y. W., Arora, R., Wischnewski, H. & Azzalin, C. M. TRF1 participates in chromosome end protection by averting TRF2-dependent telomeric R loops. *Nat. Struct. Mol. Biol.* **25**, 147–153 (2018).
 176. Toubiana, S. & Selig, S. DNA:RNA hybrids at telomeres – when it is better to be out of the (R) loop. *FEBS Journal* vol. 285 2552–2566 (2018).
 177. Lafuente-Barquero, J. *et al.* The Smc5/6 complex regulates the yeast Mph1 helicase at RNA-DNA hybrid-mediated DNA damage. *PLoS Genet.* **13**, e1007136 (2017).
 178. Boué, J. B. & Zakian, V. A. The yeast Pif1p DNA helicase preferentially unwinds RNA-DNA substrates. *Nucleic Acids Res.* **35**, 5809–5818 (2007).
 179. Arora, R. & Azzalin, C. M. Telomere elongation chooses TERRA ALTERNatives. *RNA Biol.* **12**, 938–941 (2015).
 180. Li, F. *et al.* ATRX loss induces telomere dysfunction and necessitates induction of alternative lengthening of telomeres during human cell immortalization . *EMBO J.* **38**, e96659 (2019).
 181. Nguyen, D. T. *et al.* The chromatin remodelling factor ATRX suppresses R-loops in transcribed telomeric repeats . *EMBO Rep.* **18**, 914–928 (2017).
 182. Apte, M. S. & Cooper, J. P. Life and cancer without telomerase: ALT and other strategies for making sure ends (don't) meet. *Critical Reviews in Biochemistry and Molecular Biology* vol. 52 57–73 (2017).
 183. Misino, S., Bonetti, D., Luke-Glaser, S. & Luke, B. Increased TERRA levels and RNase H sensitivity are conserved hallmarks of post-senescent survivors in budding yeast. *Differentiation* **100**, 37–45 (2018).
 184. Van Beneden, A., Arnoult, N. & Decottignies, A. Telomeric RNA expression: Length matters. *Frontiers in Oncology* vol. 3 JUL 178 (2013).
 185. Jain, D., Hebden, A. K., Nakamura, T. M., Miller, K. M. & Cooper, J. P. HAATI survivors replace canonical telomeres with blocks of generic heterochromatin. *Nature* **467**, 223–227 (2010).
 186. Fu, X. H. *et al.* Telomere recombination preferentially occurs at short telomeres in telomerase-null type II survivors. *PLoS One* **9**, (2014).
 187. Grandin, N. & Charbonneau, M. Telomerase- and Rad52-Independent Immortalization of Budding Yeast by an Inherited-Long-Telomere Pathway of Telomeric Repeat Amplification. *Mol. Cell. Biol.* **29**, 965–985 (2009).
 188. Hu, Y. *et al.* RNA-DNA hybrids support recombination-based telomere maintenance in fission yeast. *Genetics* **213**, 431–437 (2019).
 189. Ohle, C. *et al.* Transient RNA-DNA Hybrids Are Required for Efficient Double-Strand Break Repair. *Cell* **167**, 1001-1013.e7 (2016).
 190. Daley, J. M. *et al.* Specificity of end resection pathways for double-strand break regions containing ribonucleotides and base lesions. *Nat. Commun.* **11**, 1–12 (2020).
 191. Jimeno, S. *et al.* ADAR2-mediated RNA editing of DNA:RNA hybrids is required for DNA double strand break repair One sentence summary: DNA recombination requires RNA editing of DNA:RNA hybrids to ease their melting and facilitate DNA end resection. *bioRxiv* 2021.03.24.436729 (2021) doi:10.1101/2021.03.24.436729.
 192. Marnef, A. & Legube, G. R-loops as Janus-faced modulators of DNA repair. *Nat. Cell Biol.*

- 23**, 305–313 (2021).
193. Robin, J. D. *et al.* Telomere position effect: Regulation of gene expression with progressive telomere shortening over long distances. *Genes Dev.* **28**, 2464–2476 (2014).
 194. Kim, W. *et al.* Regulation of the Human Telomerase Gene TERT by Telomere Position Effect—Over Long Distances (TPE-OLD): Implications for Aging and Cancer. *PLoS Biol.* **14**, 1–25 (2016).
 195. Conomos, D. *et al.* Variant repeats are interspersed throughout the telomeres and recruit nuclear receptors in ALT cells. *J. Cell Biol.* **199**, 893–906 (2012).
 196. Mischo, H. E. & Proudfoot, N. J. Disengaging polymerase: Terminating RNA polymerase II transcription in budding yeast. *Biochimica et Biophysica Acta - Gene Regulatory Mechanisms* vol. 1829 174–185 (2013).
 197. Proudfoot, N. J. Transcriptional termination in mammals: Stopping the RNA polymerase II juggernaut. *Science* vol. 352 (2016).
 198. Min, J., Wright, W. E. & Shay, J. W. Alternative Lengthening of Telomeres Mediated by Mitotic DNA Synthesis Engages Break-Induced Replication Processes. *Mol. Cell. Biol.* **37**, MCB.00226-17 (2017).
 199. Lee, Y., Choe, J., Park, O. H. & Kim, Y. K. Molecular Mechanisms Driving mRNA Degradation by m6A Modification. *Trends in Genetics* vol. 36 177–188 (2020).
 200. Boo, S. H. & Kim, Y. K. The emerging role of RNA modifications in the regulation of mRNA stability. *Experimental and Molecular Medicine* vol. 52 400–408 (2020).
 201. Aguilera, A. & Gómez-González, B. Genome instability: A mechanistic view of its causes and consequences. *Nature Reviews Genetics* vol. 9 204–217 (2008).
 202. Hamperl, S. & Cimprich, K. A. Conflict Resolution in the Genome: How Transcription and Replication Make It Work. *Cell* vol. 167 1455–1467 (2016).
 203. Coutelier, H. *et al.* Adaptation to DNA damage checkpoint in senescent telomerase-negative cells promotes genome instability. *Genes Dev.* **32**, 1499–1513 (2018).
 204. Mersaoui, S. Y., Gravel, S., Karpov, V. & Wellinger, R. J. DNA damage checkpoint adaptation genes are required for division of cells harbouring eroded telomeres. *Microb. Cell* **2**, 394–405 (2015).
 205. Schwartz, E. K. *et al.* *Saccharomyces cerevisiae* Mus81-Mms4 prevents accelerated senescence in telomerase-deficient cells. *PLoS Genet.* **16**, (2020).
 206. Chen, Q., Ijpm, A. & Greider, C. W. Two Survivor Pathways That Allow Growth in the Absence of Telomerase Are Generated by Distinct Telomere Recombination Events. *Mol. Cell. Biol.* **21**, 1819–1827 (2001).
 207. Grandin, N. & Charbonneau, M. Mrc1, a non-essential DNA replication protein, is required for telomere end protection following loss of capping by Cdc13, Yku or telomerase. *Mol. Genet. Genomics* **277**, 685–699 (2007).
 208. Hu, Y. *et al.* Telomerase-Null Survivor Screening Identifies Novel Telomere Recombination Regulators. *PLoS Genet.* **9**, 1003208 (2013).
 209. Rawal, C. C. *et al.* Senataxin Ortholog Sen1 Limits DNA:RNA Hybrid Accumulation at DNA Double-Strand Breaks to Control End Resection and Repair Fidelity. *Cell Rep.* **31**, 107603 (2020).
 210. Bianchi, A. & Shore, D. Early Replication of Short Telomeres in Budding Yeast. *Cell* **128**, 1051–1062 (2007).

211. Claussin, C. & Chang, M. Multiple Rad52-Mediated Homology-Directed Repair Mechanisms Are Required to Prevent Telomere Attrition-Induced Senescence in *Saccharomyces cerevisiae*. *PLoS Genet.* **12**, 1006176 (2016).
212. Amon, J. D. & Koshland, D. RNase H enables efficient repair of R-loop induced DNA damage. *Elife* **5**, 1–20 (2016).
213. Lee, J. Y., Kozak, M., Martin, J. D., Pennock, E. & Johnson, F. B. Evidence that a RecQ helicase slows senescence by resolving recombining telomeres. *PLoS Biol.* **5**, 1334–1344 (2007).
214. Sobinoff, A. P. *et al.* BLM and SLX4 play opposing roles in recombination-dependent replication at human telomeres. *EMBO J.* e201796889 (2017) doi:10.15252/embj.201796889.
215. Mason-Osann, E. *et al.* RAD54 promotes alternative lengthening of telomeres by mediating branch migration. *EMBO Rep.* **21**, e49495 (2020).
216. Larrivé, M. & Wellinger, R. J. Telomerase- and capping-independent yeast survivors with alternate telomere states. *Nat. Cell Biol.* **8**, 741–7 (2006).
217. Lin, C. Y. *et al.* Extrachromosomal telomeric circles contribute to Rad52-, Rad50-, and polymerase δ -mediated telomere-telomere recombination in *Saccharomyces cerevisiae*. *Eukaryot. Cell* **4**, 327–336 (2005).
218. Zhao, W. *et al.* BRCA1-BARD1 promotes RAD51-mediated homologous DNA pairing. *Nature* **550**, 360–365 (2017).
219. Cohen, S. *et al.* Senataxin resolves RNA:DNA hybrids forming at DNA double-strand breaks to prevent translocations. *Nat. Commun.* **9**, 1–14 (2018).
220. Promonet, A. *et al.* Topoisomerase 1 prevents replication stress at R-loop-enriched transcription termination sites. *Nat. Commun.* **11**, 1–12 (2020).
221. Montero, J. J., López De Silanes, I., Granã, O. & Blasco, M. A. Telomeric RNAs are essential to maintain telomeres. *Nat. Commun.* **7**, 1–13 (2016).